ABSTRACT

JIANG, BI. Iridium Complexes with Cp* Ligand: Synthesis, Characterization and Application in Catalysis. (Under the direction of Dr. Elon Ison.)

Herein we describe the selective oxidations of primary and secondary alcohols catalyzed by iridium complexes using molecular oxygen as oxidant. A series of iridium(I) and iridium(III) complexes have been synthesized and their catalytic reactivities in aerobic alcohol oxidation reactions have been investigated. $[Cp^*IrCl(\mu\text{-}Cl)]_2$, **1** has higher catalytic reactivity than the other complexes. The role of molecular oxygen in this reaction was also investigated by comparing reaction under air and nitrogen. We have established that molecular oxygen is important to catalytic turn over. The scope of reactivity using $[Cp^*IrCl(\mu\text{-}Cl)]_2$ for oxidation reactions of different primary and secondary alcohols has been examined. Both primary and secondary alcohols have about 90% conversion. It was also established that there is a clear electronic dependence on the reactivity and the reaction favors electron-donating substituents. The mechanism of this reaction was investigated and oxygen stoichiometry was measured by O_2 up-take experiment. An intermediate of this reaction $[(Cp^*IrCl)_2(\mu\text{-}H)(\mu\text{-}Cl)]$, **2** was isolated and characterized. Several experiments have been taken to investigate presence of **2** in the catalytic cycle. A proposed mechanism is given and a rate law is derived based on experimental results.

A series of water-soluble iridium (III) complexes, bearing Cp*(1, 2, 3, 4, 5-pentamethylcyclopentadiene) ligand, have been synthesized. Their reactivities in the aerobic oxidation of primary and secondary alcohols in aqueous solution have been investigated and

their pH dependences in water solution have been studied too. An Ir-H intermediate was generated during the reaction. A mechanism was proposed for the reaction of $[(Cp^*Ir)_2(\mu\text{-}Cl)_3]BF_4$ and cyclopentanol. Those water-soluble iridium complexes were also utilized in the H/D exchange reactions of benzene and different deuterium sources. The reactivities of those complexes were compared with former reported Cp*Ir(NHC) complexes. Besides benzene, the catalytic H/D exchange reactions of iso-propanol, diethyl ether, pyridine, et. al. have also been studied. The activation of dihydrogen and silane by $Cp^*Ir(NHC)(SO_4)$ have been observed and investigated.

A preliminary study of aerobic oxidation of HMF has been taken. Several Cp*Ir complexes have been applied in this reaction. Cp*Ir complexes with NHC ligand showed higher reactivity than complexes without NHC ligand. At one atmosphere of O_2 (14.5psi), 2,5-diformylfuran (DFF) was obtained in modest yield (about 50%) catalyzed by Cp*Ir(NHC) complexes. At higher pressure of O_2 (80-100psi), 2,5-furandicarboxylic acid (DFA) was achieved in a good yield (about 90%) catalyzed by Cp*Ir(NHC) complexes.

Iridium Complexes with Cp* Ligand: Synthesis, Characterization and Application in Catalysis

by
Bi Jiang

A dissertation submitted to the Graduate Faculty of
North Carolina State University
in partial fulfillment of the
requirements for the degree of
Master of Science

Chemistry

Raleigh, North Carolina

2010

APPROVED BY:

_____	_____
Dr. Elon Ison Chair of Advisory Committee	Dr. Mike Whangbo
_____	
Dr. Reza Ghiladi	

DEDICATION

To my great parents, my dear husband and my beloved children.

献给我的父母——

江小艇，蒋银兰，感谢他们的养育之恩，谆谆教导和无私的爱。

BIOGRAPHY

Bi Jiang was born in Wuhan, a beautiful city along Yangtze River in China. In 2002, she started her college life in Peking University, where she met her husband, Zhaoming Su. After four years, she graduated with a bachelor degree in chemistry and enrolled in North Carolina State University as a graduate student. She has worked with Dr. Elon Ison in the organometallic chemistry since 2007. In the same year, she gave birth to her lovely daughter, Helene. In 2010, besides her Master of Science degree, she also achieved her son, William.

ACKNOWLEDGMENTS

My first acknowledgement should go to my advisor Dr. Elon Ison. Without his expert guidance, stimulating advices, inspiration, and encouragement, this work would not be possible. His understanding and support helped me overcome the crisis of both my research and personal life. I would say that besides a professional scientist, he is a really generous and nice person. I am happy that I have worked in his group and learned a lot from him. I also want to give my thanks to my committee members, Dr. Mike Whangbo and Dr. Reza Ghiladi for reading my dissertation and giving me important advices.

I would like to give my appreciation to the entire Ison group, for the people who have worked here from couple of months to years. The wonderful time full of teamwork, joy and friendship is a precious memory of my life. I especially want to thank Dr. Yuee Feng. She has given me a lot of help, good advices and encouragement. She shared my worries, sorrow, and happiness as an elder sister that I never have.

I also want to give my deepest gratitude to my family. To my parents, thank you for raising me up, providing me good education and giving me unconditional love. My most heartfelt acknowledgement must go to my husband, Zhaoming. Having you stand beside me, I will fear nothing. Last but not least, I want to thank my beloved children, Helene and William, for giving me a lot of joy and teaching me to be strong.

TABLE OF CONTENTS

LIST OF TABLES

LIST OF CHARTS

LIST OF FIGURES

LIST OF SCHEMES

CHAPTER 1

1.1 Introduction

A wide variety of consumer goods, as well as thousands of applications in agriculture, manufacturing, construction, and service industries are made from chemicals. Major industrial products include rubber and plastic products, textiles, apparel, petroleum, pulp and paper, which are essential to our daily lives.[1] The chemical industry is a nearly $3 trillion global enterprise nowadays, and the EU and U.S. chemical companies are the world's largest producers. Probably 90% by weight of the organic chemicals the world uses comes from petroleum and natural gas.[2] A less important source of chemicals is coal. Coal was important historically, and the decline of coal correlates with the rise of petrochemicals. However, reserves of coal are much greater than those of oil. If petroleum becomes scarce, coal may loom again. Petroleum primarily consists of reduced hydrocarbons, and their selective oxidation remains one of the critical challenges in the chemistry industry. Traditionally, these oxidation reactions are performed with strong stoichiometric oxidants as salts of Mn(VII), Cr(VI), Os(VIII) and chlorine-based oxoanions.

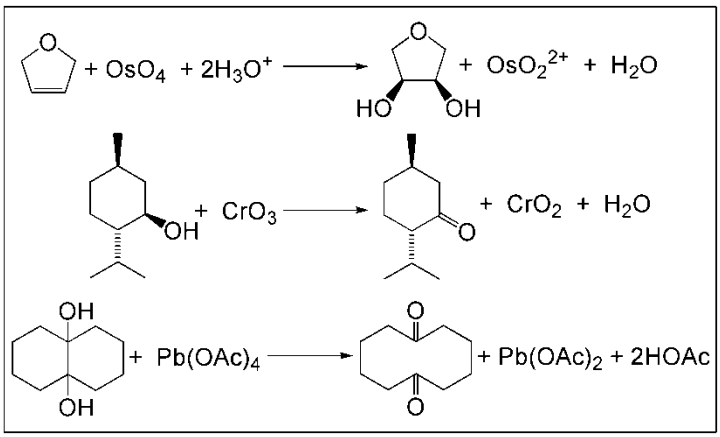

Scheme 1.1 Oxidation reactions using traditional oxidants

For scheme 1.1, OsO_4 oxidizes furan to (R, S)-3,4-furandiol, while it is reduced to OsO_2^{2+}. CrO_3 oxidizes secondary alcohol into ketone under acidic conditions, which is called Jone's reaction. Chromium residue Cr(VI) or Cr(IV) is very toxic and should be disposed properly. $Pb(OAc)_4$ oxidizes octahydro-naphthalene-4a,8a-diol into cyclodecane-1,6-dione while it is reduced to $Pb(OAc)_2$. These reagents, OsO_4, CrO_3, $Pb(OAc)_4$, in addition to their significant costs, lead to toxic by-products. The World Health Organization, (WHO), has determined that chromium(VI) is a human carcinogen, and chromium can strongly attach to the soil and only a small amount can dissolve in water and move deeper in the soil to underground water. Those oxidation reactions have high E-factors (environmental factor, kg waste / kg product) and low atom utilisation (molecular weight of the product divides the sum of molecular weight of all substances formed in a stoichiometric reaction). [3] For example, the E-factors and atom utilisations of stoichiometric (CrO_3) versus catalytic (O_2) oxidation of a secondary alcohol is depicted in scheme 1.2. From these two reactions, it is obvious that catalytic aerobic oxidation has better atom efficiency and lower or even no environmental effect. Therefore, a high efficient and "green" oxidant has been in demand in recent decades with the increasing emphasis on environmental protection.

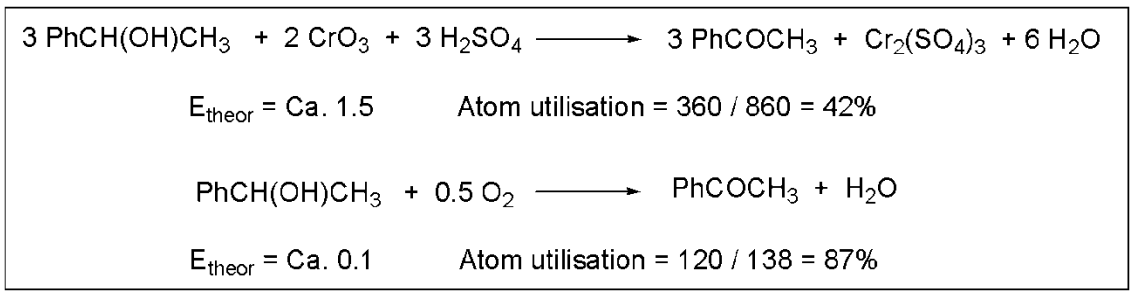

Scheme 1.2 E-factors and atom utilisations of stoichiometric vs catalytic oxidation[3]

The third source of organic chemicals is the group of naturally occurring, renewable materials, such as carbohydrates, triglycerides, sugar, et. al.. Biofuels are defined as solid, liquid or gas fuel derived from recently dead biological material and is distinguished from fossil fuels, which are derived from long dead biological material.[1] The carbon in petroleum and coal has been stored beneath the surface for millions of years. Using these sources of carbon increases the concentration of carbon dioxide in atmosphere. However, because biofuels are produced from photosynthetic plants which remove carbon dioxide from atmosphere, biofuels offer the possibility of producing energy without a net increase of carbon in the atmosphere. The use of biofuels reduces the dependence on petroleum and benefits us by sustainable development. Sustainable development is considered as development that "meets the needs of the present without compromising the ability of future generations to meet their own needs".[3]

The major component of biofuels is alcohol, and the selective oxidation of alcohol into aldehyde using environmentally benign oxidants is a promising new technology. For example, lignin, is an integral part of the secondary cell walls of plants, and the second most abundant organic polymer on earth, superseded only by cellulose. Lignin employs 30% of non-fossil carbon and constitutes from a quarter to a third of dry mass of wood. Lignin is a cross-linked racemic macromolecule with molecular masses in excess of 10,000.[4] There are three monolignol monomers of lignin, methoxylated to various degrees: *p*-coumaryl alcohol, coniferyl alcohol, and sinapyl alcohol.[4] Commercial lignin is currently produced as a co-product of the paper industry, separated from wood by a chemical pulping process.

Lignin can serve the following purposes: binder, dispersant, emulsifier, sequestrant.[4] The selective oxidation of lignin using cheap and benign oxidants is very attractive.

Molecular oxygen has both economic and environmental advantages as an oxidant. Oxygen is the third most abundant element in the universe by mass after hydrogen and helium. It is also the most abundant element by mass in the Earth's crust. Oxygen constitutes 88.8% of the mass of water and 20.9% of the volume of air.[5] The by-product of the oxidation reaction using molecular oxygen is either water or hydrogen peroxide which are both environmentally benign. Recently, oxidation using molecular oxygen has attracted researchers due to the advantages of O_2 mentioned above, however, aerobic oxidation reactions in industry often undergo radical autoxidation processes. For example, in the oxidation of terephthalic acid, a starting compound for the manufacture of polyester, used in clothing and to make plastic bottles.[6] These methods are limited to substrates that proceed via selective radical chemistry. An example of aerobic oxidations in industry by non-radical metal mediated process is the Wacker process which was developed more than 40 years ago.[6] It is the first organometallic or organopalladium reaction applied on industrial scale. However, it remains a rare example of a nonradical aerobic oxidation. In the Wacker process, ethylene is oxidized to acetaldehyde by oxygen in presence of palladium catalyst in water.

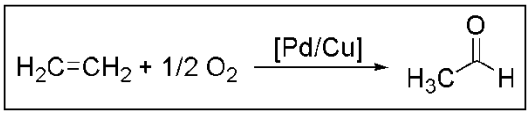

Equation 1.1 The Wacker-Process.[6]

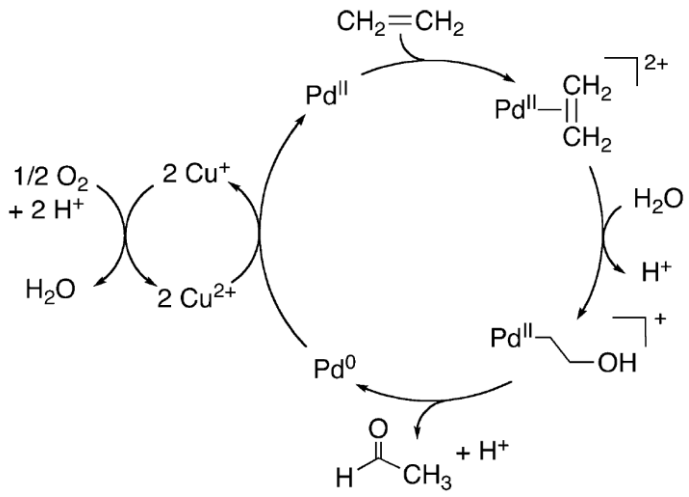

Scheme 1.3 Catalytic mechanism for the Wacker Process[6]

The mechanism of the Wacker-Process is shown in Scheme 1.3. The catalyst is regenerated, and only alkene and oxygen are consumed. Water supplies the oxygen atom in acetaldehyde, which is produced by β-hydride elimination. At the same time, a palladium-hydride intermediate is formed, and the oxidation state of palladium is reduced by two after reductive elimination. The palladium catalyst is regenerated by molecular oxygen through the intermediacy of a copper co-catalyst. The Wacker process is able to oxidize ethylene with molecular oxygen by catalytic amount of palladium catalyst, but copper co-catalyst is required for high yields.

Palladium is the most active and versatile transition metal employed in organic synthesis and has been studied for years.[6] However, a persistent problem in palladium catalysis is the decomposition of the homogeneous catalysts into inactive bulk metal. This decomposition pathway competes with the slow addition of dioxygen to Pd(0). Iridium complexes can alleviate this problem because the major oxidation states of iridium complexes are iridium(I),

iridium(III), iridium(V), all of which stay active in solution. Moreover, Oppenauer type oxidation reactions catalyzed by iridium complexes have been studied by Yamaguchi and coworkers.[40, 44] The high efficiencies of their iridium catalysts are apparent. Our preliminary investigations of applying iridium complexes in aerobic oxidation reactions shows promising results.

1.1.2 Transition metal-catalyzed aerobic alcohol oxidations

General challenges

Our research is focused on the development of new catalytic strategies through transition metal catalysis for the clean and efficient oxidation of hydrocarbons. The oxidation of an alcohol to the corresponding aldehyde or ketone is an important functional group transformation in synthetic organic chemistry. Common methods use toxic stoichiometric oxidants and produce environmental hazardous byproducts. The use of molecular oxygen as the stoichiometric oxidant is beneficial because it is inexpensive, readily available and produces environmentally benign byproducts such as H_2O. However, several challenges exist in the development of transition metal-catalyzed aerobic alcohol oxidations. This includes the use of mild temperature, low pressure of O_2 in flammable organic solvents, low catalyst loading, and use of low cost and non-toxic additives.[7] Functional group tolerance and ability to chemoselectively oxidize an alcohol in the presence of other functional groups are also common challenges. The subsequent sections describe some recent discoveries for different metal catalyzed aerobic oxidation of alcohols.

Cobalt

The first Cobalt catalyzed aerobic oxidation of alcohols was published in 1981 by Tovrog and co-workers.[8] Subsequently, several systems for Co-catalyzed aerobic alcohol oxidations have been investigated. Ishii and co-workers have shown that a variety of alcohols were successfully oxidized under aerobic conditions by Co(III) complexes that contain *N*-hydroxy-phthalimide(NHPI) ligand.[9] In their recent report, the optimized procedure utilized 0.5 mol % $Co(OAc)_2$, 10 mol % NHPI, and 5 mol % *m*-chlorobenzoic acid (MCBA) under oxygen at room temperature.[10] This method was successful for the oxidation of secondary aliphatic, allylic, and benzylic alcohols. Primary alcohols were oxidized to the corresponding carboxylic acids, and internal vicinal diols were converted to the corresponding diketones in modest yields. In addition to Ishii's report, Iqbal and Sain have reported similar examples of Co(II)-Schiff base catalyzed aerobic alcohol oxidations.[11-12] Their system successfully oxidized both secondary, aliphatic, and benzylic alcohols. In their method, *iso*-butanol was added to the catalytic system, which led to selective oxidation of benzyl alcohol to benzyl aldehyde and the oxidation of substrates containing olefins and alkynes without oxidation of the unsaturated bonds. Sain and coworkers have also showed a Co-phthalo-cyanine complex catalyzed aerobic oxidation of alcohols.[13-14] In their system, 5 mol % catalyst and 1 equivalent of KOH in xylenes were refluxed under O_2 atmosphere. Secondary benzylic, aliphatic, and propargylic alcohols were successfully oxidized. Limitations of Sain's system remain as primary alcohols are oxidized to carboxylic acid instead of corresponding aldehyde. Unfortunately, few mechanistic studies have been reported to explain the development of new catalyst systems.

Copper

The first practical Cu-catalyzed aerobic alcohol oxidation was reported by Semmelhack and coworkers in 1984.[15] In their catalytic system, 10 mol % CuCl and 10 mol % TEMPO (2, 2, 6, 6-tertramethyl-1-piperidinyloxy) were used to oxidize primary benzylic, allylic, and aliphatic alcohols in DMF under an O_2 atmosphere at room temperature.

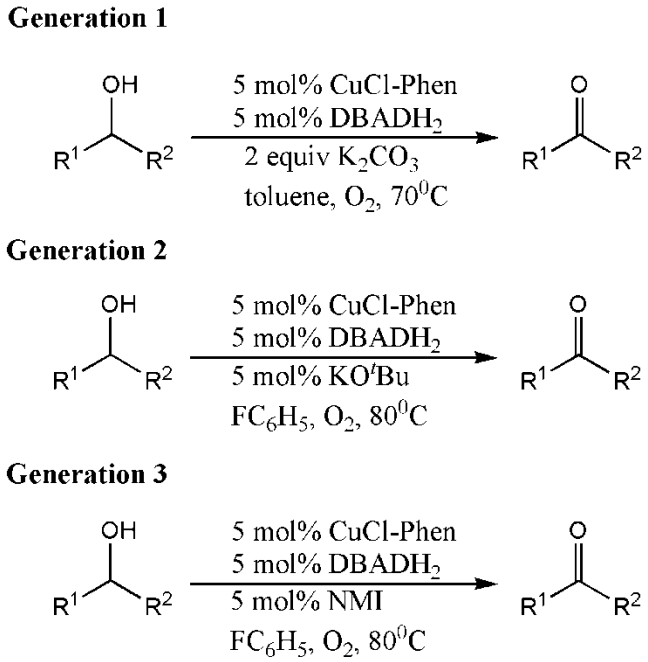

Scheme 1.4 Three generations of CuCl-Phenanthroline catalytic system[4]

Since Semmelhack's early work, much of the development has been pioneered by Markó and coworkers.[16-18] Three generations of catalyst systems have been developed. (Scheme 1.4) In their initial report, 5 mol % CuCl, 5 mol % phenanthroline, 5 mol % di-tert-butyl hydrazine-1,2-dicarboxylate ($DBADH_2$), and 2 equiv of K_2CO_3 were utilized to oxidize a series of alcohols(Generation 1). More recently, it was shown that changing the solvent from toluene to fluorobenzene allowed the use of catalytic K_2CO_3 and KO*t*-Bu instead of 2 equiv of strong base K_2CO_3(Generation 2). Further, they found that *N*-methylimidazole (NMI)

provided an efficient catalyst system for the oxidation of primary aliphatic alcohols (Generation 3). In addition to Markó's development, Sheldon and coworkers demonstrated that the use of 2, 2'-bypyridine as a ligand for $CuBr_2$ in combination with TEMPO resulted in oxidation of primary benzylic, allylic, and aliphatic alcohols to the corresponding aldehyde without any overoxidation products.[19-21] In their system, secondary alcohols were not oxidized when mixtures of primary and secondary alcohols were exposed to the reaction conditions. Punniyamurthy and coworkers recently reported a related catalytic system with a salen-type ligand on Cu that also selectively oxidized primary alcohols.[22] Both Sheldon and Punniyamurthy's systems require a pure oxygen atmosphere and high temperature (100 ^{0}C).

Gold

Organic transformations catalyzed by gold species have attracted considerable attention in the past few years. The first gold-catalyzed aerobic alcohol oxidation was reported by Tsukuda and coworkers in 2006. Colloidal gold nanoclusters (Au NCs) were used to catalyze the aerobic alcohol oxidations in water.[22] Later, Zhangjie Shi and coworkers reported the first homogeneous Au-catalyzed aerobic alcohol oxidation.[23] They utilized 5 mol % of AuCl and 6.3 mol % of 2, 6-diisopropylphenyl under a pure O_2 atmosphere in toluene. (Table 1.1) Their catalyst loading could be lowered to 1 mol % and the oxygen atmosphere could be replaced by an air atmosphere with extended reaction time. The limitation of this system was that primary aliphatic alcohols formed aldol products. Later, they reported homogeneous gold catalysts with neocuproine as a ligand for the oxidation of secondary and primary

benzyl and allylic alcohols to carbonyl compounds in air and water, but high pressure (50 atm) O_2 was utilized in the system.[24]

Table 1.1 Au-catalyzed aerobic alcohol oxidations.[4]

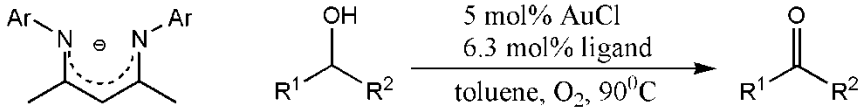

Ar = 2,6-di-*iso*-PrPhenyl

Entry	Substrate	Time (h)	Yield (%)
1		24	96
2	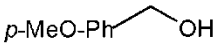	10	99
3	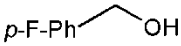	24	99
4	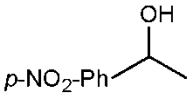	36	92
5	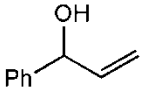	24	96
6	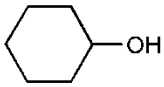	24	99
7	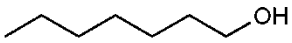	48	68

At the same time, Kobayashi and coworkers developed gold nanoclusters that are stabilized by multiple interactions with the benzene rings of polystyrene which catalyzed the aerobic oxidation of several alcohols efficiently at room temperature under atmospheric conditions.[25] From their O_2 up-take experiment, they were able to demonstrate that water was produced as a sole coproduct. The mechanism of Au-catalyzed aerobic alcohol oxidation reaction was investigated by Christensen and coworkers.[26] They used a series of parasubstituted benzyl alcohols. The competition experiments showed that the rate-

determining step of the reaction involves the generation of a partially positive charge in the benzylic position, which was substantiated by a significant kinetic isotope effect (k_H/k_D = 1.41).

Iron

Recently, iron has been employed as a catalyst for the aerobic alcohol oxidations. In 2002, Martin and Suárez reported the first Fe-catalyzed aerobic alcohol oxidation that used a combination of $Fe(NO_3)_3$ and $FeBr_3$ under 1 atm of air at room temperature.[27] The optimized conditions for this system employed 10 mol % $Fe(NO_3)_3$ and 5 mol % $FeBr_3$ in MeCN under 1 atm air at room temperature. The scope of this oxidation system includes primary and secondary aliphatic alcohols, but the reactions were performed under relative high catalyst loading. More recently, another Fe-catalyzed aerobic alcohol oxidation was reported by Liang and coworkers.[28] $NaNO_2$/TEMPO was utilized to oxidize a variety of alcohols. In their system, 5 mol % $FeCl_3$-$6H_2O$, 5 mol % $NaNO_2$ and 2 mol % TEMPO were employed in trifluorotoluene at room temperature under air.

Palladium

Palladium is one of the well studied transition metals applied in aerobic oxidation reactions. In the past 15 years, numerous effective palladium catalyst systems have been developed for aerobic oxidation reactions. A broad range of palladium catalyzed systems have been discussed in a review paper by Stahl, including primary, secondary, allylic and benzylic alcohol oxidations, intermolecular and intramolecular oxidation of alkenes and

oxidative C-C coupling reaction with non-alkene substrates, such as aryl nucleophiles.[6] Several catalytic systems of palladium-catalyzed alcohol oxidation that underwent dioxygen-coupled turnover have been discussed in this review.

The first significant breakthrough in palladium-catalyzed aerobic alcohol oxidation was reported by Peterson and Larock, who employed $Pd(OAc)_2$ (5%) / DMSO for the oxidation of a wide range of benzylic and allylic alcohols with O_2.[29] Anionic bases such as $NaHCO_3$ and K_2CO_3 enhanced the reaction rate and product yields for secondary alcohols. No H_2O_2 was detected which indicates that H_2O_2 underwent rapid disproportionation under this catalytic condition. At the same time, kinetic studies indicate that oxidation of Pd(0) to Pd(II) is the turnover-limiting step. Besides $Pd(OAc)_2$ (5%) / DMSO system, Uemura and co-workers reported $Pd(OAc)_2$ (5%) / pyridine (20%) / MS3A (3-Å molecular sieves) in toluene (80^0C).[30] The use of excess pyridine prevents precipitation of palladium metal. $Pd(OAc)_2$/Bathophenanthroline disulfonate catalyst system was reported by Sheldon and co-workers in 2000.[31] The optimized catalyst is [(PhenS*)$Pd(OAc)_2$], (Figure 1.1) and the reaction conditions are: catalyst (0.2-0.5mol%), NaOAc (10%), 30 bar air pressure at 100^0C. Their catalytic rates are up to 100 TOh^{-1} and their turn over numbers (200 - 400) are significantly higher than former reported studies.

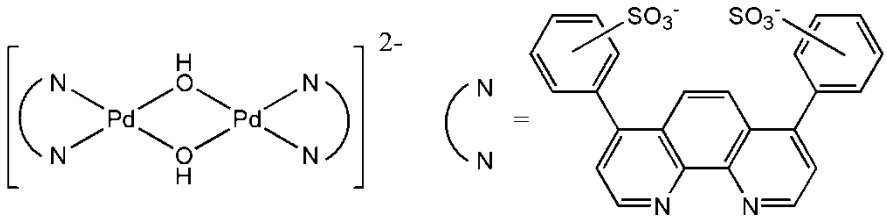

Figure 1.1 The structure of [(PhenS*)$Pd(OAc)_2$]

The catalyst systems above highlighted the ability of palladium to catalyze aerobic oxidation of alcohols, however, few enantioselective palladium-catalyzed oxidation reactions have been reported until Sigman and Stoltz applied sparteine as a ligand in these reactions. [((-)-sparteine)$PdCl_2$] (5%) was combined with an excess (-)-sparteine (20%) in toluene at 80^0C(Scheme 1.4). Mechanistic studies by Sigman and co-workers determined that excess (-)-sparteine serves as an exogenous base to promote the formation of the palladium alkoxide intermediate, which preceeded subsequent β-hydride elimination to yield the ketone product.

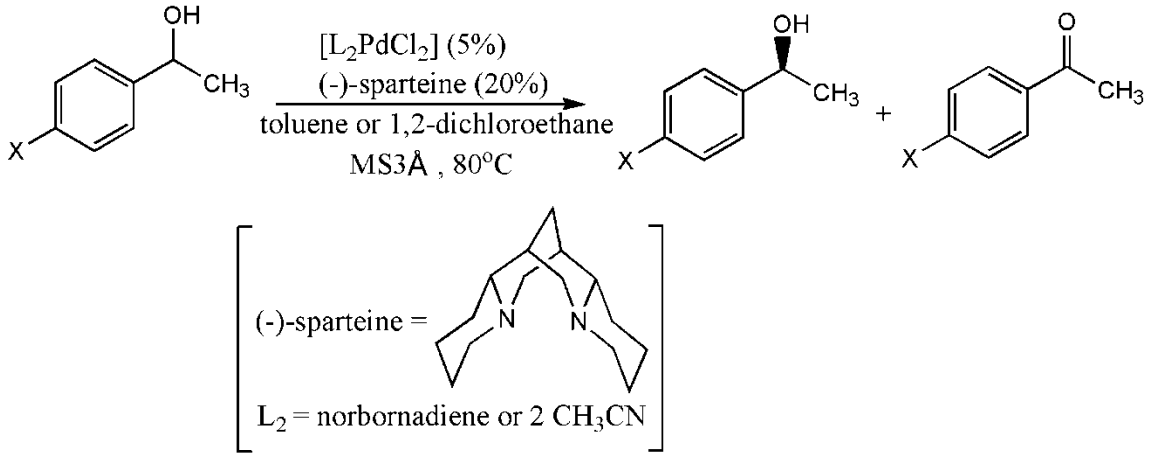

Scheme 1.5 The $PdCl_2$/(-)-sparteine catalyst system.

A number of new palladium-catalyzed aerobic alcohol oxidation systems have been reported in the past five years. Water is an ideal solvent from the view of green chemistry. A hydoxyapatite-supported palladium(0) catalyst was employed for the Suzuki coupling and aerobic oxidation of benzyl alcohols in water by Paul and coworkers.[32] Another water-soluble palladium(II) bathophenanthroline complex has been studied by Sheldon, Roger and coworkers[33] for the selective aerobic oxidation of a wide range of alcohols to aldehydes,

ketones, and carboxylic acids in a biphasic water-alcohol system. Heterogenous catalyst systems have also been studied. Supported palladium nanoparticles on silica-alumina were studied in the aerobic oxidation of alcohols in a solvent-free condition by Wan and coworkers.[34] The sizes of palladium nanoparticles was dependent on the ratio of Si/Al. Palladium was also utilized as heterogeneous catalyst in aerobic oxidation of alcohols by Karimi and coworker.[35] They combined organic ligands with ordered mesoporous channels resulting in a synergistic effect which led to enhanced activity and prevention of the agglomeration of the Pd nanoparticles. The mechanisms of palladium catalyzed aerobic oxidation have also been investigated by several research groups. The electronic, steric and temperature effects in the Pd(II)-biquinoline catalyzed aerobic oxidation of benzylic alcohols in water have been investigated by Verbeke and coworkers.[36] In their study, electron-donating substituents increase the reaction rate (ρ = −0.37), which suggests a partial reduction of the palladium center coupled with alcohol oxidation in the rate-limiting step. They also evaluated temperature dependence on 4-methoxybenzyl alcohol oxidation, providing activation parameters of $\Delta H^{\ddagger}$ = 7.4(4) kcal/mol and $\Delta S^{\ddagger}$ = −53(1) eu. Goddard and coworkers studied the mechanism of the aerobic oxidation of alcohols by N-heterocyclic carbene palladium complex by DFT.[37] Quantum mechanics (B3LYP density functional theory) and a solvation (Poisson-Boltzmann polarizable continuum solvent model) were used to investigate the mechanism. They found that "reductive β-hydride elimination", in which the β-hydrogen of a palladium-bound alkoxide is transferred directly to the free oxygen of the bound carboxylate, provides the lowest-energy route.

Mechanistic aspects of Pd-catalyzed aerobic alcohol oxidation

Metalloenzymes have a metal containing active site as part of its structure.[38] The studies of metalloenzymes which catalyze selective aerobic oxidation reactions provide important insight into the activation of molecular oxygen. Two distinct classes of such enzymes are oxygenases and oxidases. One example of oxygenases is the cytochrome P450 family, which is a superfamily of hemoproteins present in a wide variety of life-forms including animals, plants, fungi and microorganisms (Figure 1.2). Notable members of the P450 family are monooxygenases, which transfer one oxygen-atom to substrate (RH) while the other oxygen atom is reduced to water. One example of oxidase is cytochrome c oxidase, which is a large transmembrane protein complex found in bacteria and the mitochondrion (Figure 1.2). The enzyme transfers protons across the membrane, converting molecular oxygen into two molecules of water. Therefore, oxygenases transfers an oxygen-atom from dioxygen to substrate and oxidases use oxygen as electron/proton acceptor in oxidation reactions. This mechanistic distinction has great implications for the development of aerobic oxidation catalysts.

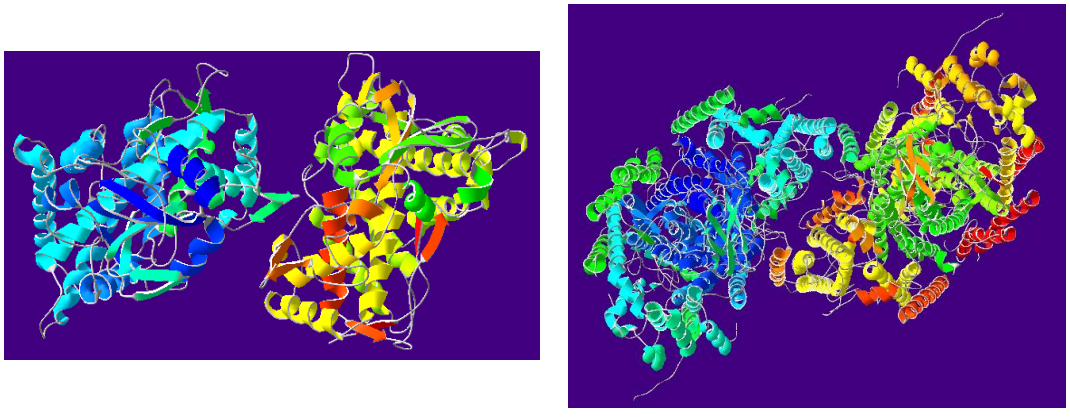

Figure 1.2 Crystal structure of cytochrome P450 and cytochrome c oxidase

Palladium catalyzed aerobic oxidation of alcohols utilize an oxidase strategy, which does not involve oxygen-atom transfer. Many Pd-catalyzed oxidations proceed via Pd(II)-hydride intermediates, which form during substrate oxidation via β-hydride elimination. Then, the Pd(II)-hydride undergoes reductive elimination of HX to yield Pd(0), and the catalyst is regenerated by molecular oxygen. However, several groups proposed that Pd(II)-hydride could react directly with O_2 to form Pd(II)-hydroperoxide intermediate, avoiding the formation of unstable Pd(0) during catalytic turnover. Stahl and coworkers used experimental and computational studies, providing the first direct evidence for the traditional Pd(II)/Pd(0) redox cycle proposed for Pd-catalyzed aerobic oxidation reactions.[31] In their study, the reductive elimination step is the rate-limiting step followed by rapid reaction of molecular oxygen with Pd(0) **C** to form a η^2-peroxo complex **D** and protonolysis of a Pd-O bond of **D** to for Pd-hydroperoxide complex **E**. (Scheme 1.5)

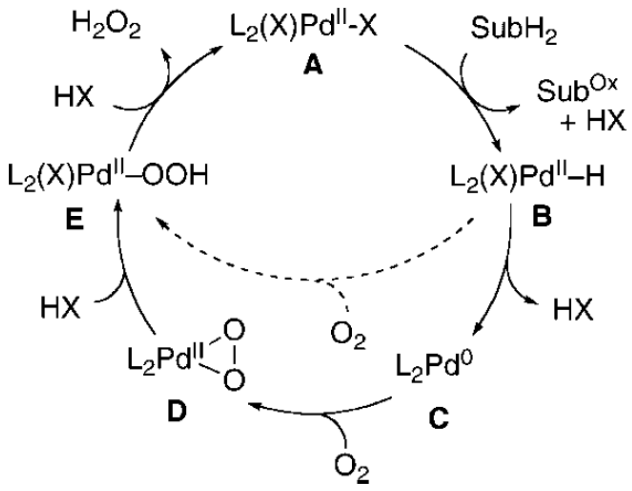

Scheme 1.6 The catalytic cycle for Pd-catalyzed aerobic oxidation

A persistent problem in palladium-catalyzed oxidation reactions is the aggregation of the catalyst into inactive bulk metal. In several early studies, this problem was addressed by conducting the reaction under high O_2 pressure (20-50 atm), which is not operationally appealing and also unsafe due to explosion hazards. One way to alleviate this problem is to rationally design catalytic systems that employ transition metals that readily activate dioxygen. Oxidative addition reactions of d^8 Ir(I) complexes are well known and the activation of O_2 by Ir(I) complexes have been reported.[39] Recently, Yamaguchi and coworkers have developed iridium-catalyzed complexes in Oppenauer-type oxidation of alcohols and achieved high turn-over numbers.[40] In the proposed mechanism for this reaction acetone inserts into an Ir(III) hydride to form an alkoxide ligand that subsequently undergoes alcohol exchange to yield isopropyl alcohol and regenerate the catalytically active iridium complex. We postulate that this strategy could be used in aerobic oxidations, where O_2 instead of acetone, serves as a hydrogen acceptor.

1.1.3 Iridium Catalyzed Aerobic Oxidations

Ir-catalyzed Oppenauer-type oxidation reactions

In 2001, Ajjou reported the first iridium catalyst for Oppenauer-type oxidation of alcohol is [Ir(COD)Cl_2] with 2,2'-biquinoline-4,4'-dicarboxylic acid dipotassium salt and sodium carbonate.[41] It is also the first example of a water-soluble transition-metal catalyst for Oppenauer-type oxidation of secondary alcohols. The catalyst oxidized a wide range of secondary alcohols with acetone under N_2 at 90^0C in water. Later, Hiroi and coworkers reported iridium-catalyzed Oppenauer oxidations of primary alcohols using acetone or 2-

butanone as oxidant.[42] In 2004, Yamaguchi and coworkers employed Cp*Ir complexes bearing N-heterocyclic carbene ligand for Oppenauer-type oxidation of alcohols.[40] With triethylamine was used as a base in toluene at 80^0C, high turn-over numbers up to 950 were achieved in the oxidation of secondary alcohols. Later they reported a dicationic Cp*Ir NHC complex which has extremely high catalytic activity (TON = 6640) in Oppenauer-type oxidation reactions.[43]

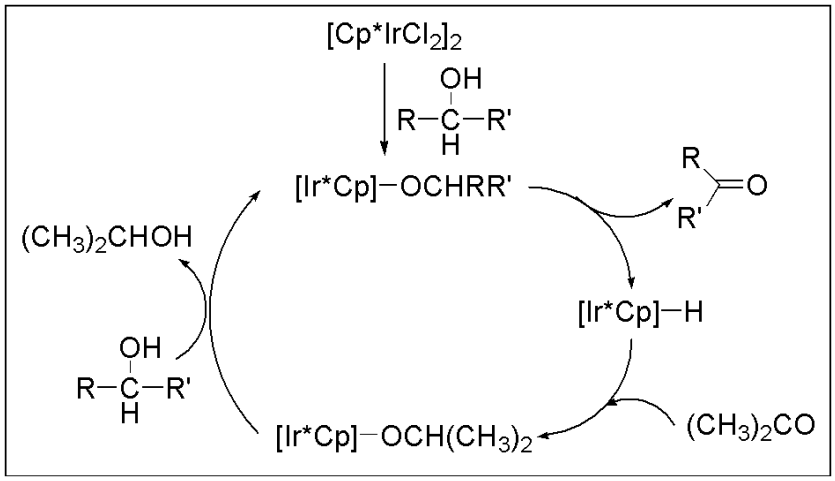

Scheme 1.7 Proposed mechanism of Oppenauer-type oxidation reactions.[40]

In this reaction, a secondary alcohol is oxidized to ketone, while acetone is sacrificially reduced. In the proposed mechanism for this reaction, acetone inserts into an Ir(III) hydride bond to form an alkoxide ligand that subsequently undergoes alcohol exchange to yield isopropyl alcohol and regenerate the iridium catalyst. (Scheme 1.6) Based on the studies above, iridium complexes serve as hydrogen-transfer catalysts and acetone is a good hydrogen acceptor, however, acetone is not as good as molecular oxygen from the view point

of green chemistry, so the application of iridium complexes in aerobic oxidations is promising.

Ir-catalyzed aerobic alcohol oxidation

Aerobic oxidations happen every day in our bodies, such as the aerobic oxidation of glucose which requires about 60 enzymatically catalyzed steps.[44] Exciting developments have been made in aerobic oxidation reactions by palladium catalysts, however, iridium catalyzed aerobic oxidation reactions are scarce.[45-56] Gabrielsson and coworkers reported the first examples of iridium based catalysts for the aerobic oxidation of alcohols with the highest turn-over number reported thus far of 70.[57] In their research, $[Cp^*Ir(H)(bpym)]^+$ (bpym=2,2'-bypyrimidine) and $[Cp^*Ir(H)(bpy)]^+$ (bpy=bi-pyridine) served as catalysts for the aerobic oxidation of alcohols. They propose that the catalytic cycle proceeds via acidic hydrides, while deprotonation of the hydride leads to a highly oxygen sensitive Ir(I) species which is oxidazed to Ir(III) species by dioxygen. Recently, Ikariya[58] and Rauchfuss[59] independently reported iridium complexes catalyze the oxidation of primary and secondary alcohols. In Ikariya's work, they found hydrogen transfer from the amine-hydrido complex to the oxygen and demonstrated the first example of aerobic kinetic resolution of racemic secondary alcohols. However, they were not able to improve the rate of the reaction and clarify the mechanism of hydrogen transfer to the oxygen. Rauchfuss and coworkers' work detailed potential transfer hydrogenation catalysts for aerobic oxidation. In their study, solutions of $Cp^*IrH(rac\text{-}TsDPEN)(TsDPEN)H_2NCHPhCHPhN(SO_2C_6H_4CH_3)^-$), (**IrsH(H)**), with O_2 generated Cp*Ir(TsDPEN-H), (**Irs**), and one equivalent of H_2O. (Scheme 1.7) The

kinetic analysis indicates the reaction is second order in (**IrsH(H)**) and first order in O_2. The deactivation of the catalyst with O_2 was traced to degradation of the Cp* ligand to a fulvene derivative. Iridium complexes can serve as transfer hydrogenation catalysts with molecular oxygen as a promising hydrogen acceptor, but the mechanism for the hydrogen transfer still needs to be clarified.

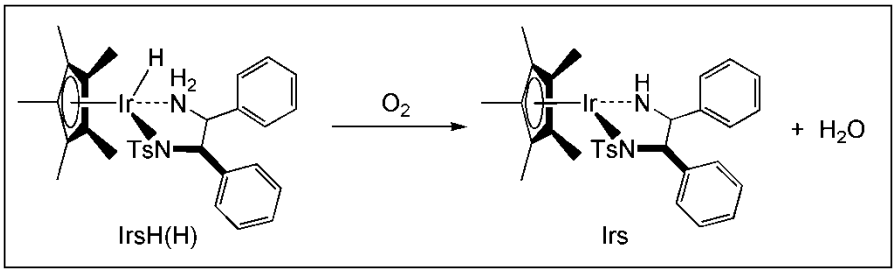

Scheme 1.8 Transfer hydrogenation of IrsH(H).[59]

1.2 Results and Discussion

1.2.1 Specific Research Objective

The specific goal of this research was to explore catalytic systems that employ transition metals that readily activate dioxygen, investigate iridium catalysts for the aerobic oxidation reactions of primary and secondary alcohols, and study the mechanism for this reaction. Several iridium complexes have been synthesized and their catalytic activity was compared. We also studied the mechanism of this reaction using kinetic methods. An iridium hydride intermediate was isolated and characterized and its presence in the catalytic cycle was established by a series of experiments.

1.2.2 Synthesis of Iridium Complexes

Several iridium(I) and iridium(III) complexes have been synthesized according to reported methods(see experimental section for detail).

Chart 1.1 Synthesized iridium complexes

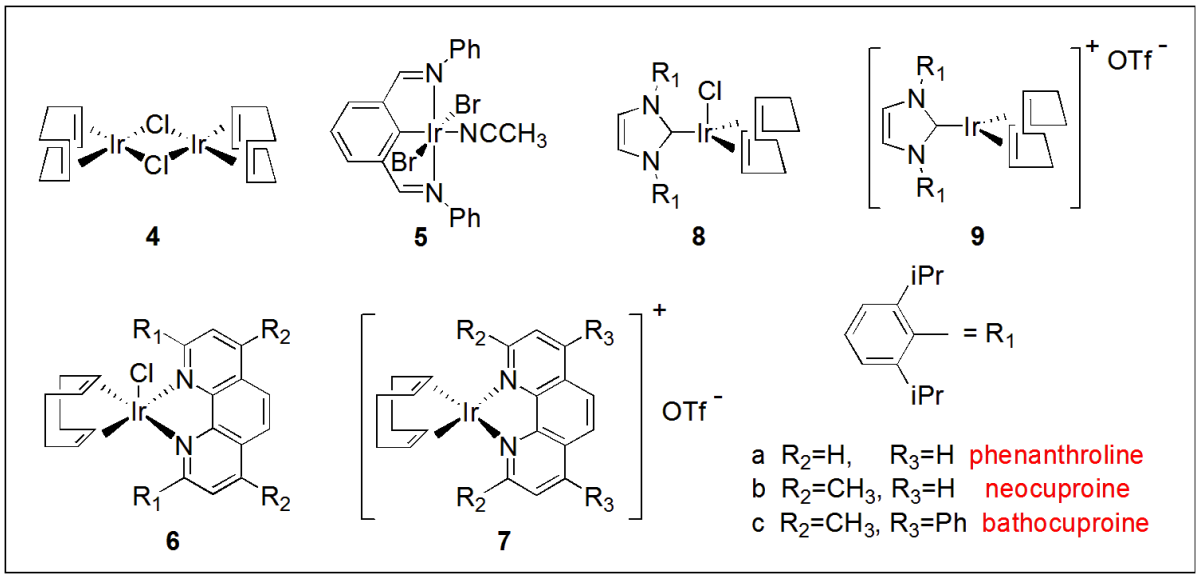

The reactivity of the above iridium complexes has been investigated for the oxidation of 4-methoxy benzyl alcohol in toluene under pure O_2 at 80^0C for 12 hours. The yield of benzyl aldehyde and the turn over number were used to compare the catalytic activities(Table 1.2).

Table 1.2 Catalytic reactivities of iridium complexes

Entry	Complex	Yield	TON
1	**7a**	88%	4.4
2	**6a**	40%	2.0
3	**7b**	64%	3.2
4	**6b**	50%	2.5
5	**7c**	25%	2.5
6	**6c**	5%	0.25
7	**4**	45%	2.25
8	**5**	50%	2.5
9	**8**	56%	2.8
10	**9**	66.6%	3.3
11	**1**	80.7%	32.3*

* (2.5 mol %) Ir, 14.5psi O_2, Triethyl amine, d-toluene, J Young Tube.

Based on the results above the following conclusions can be made. First, catalysts with more substituted phenanthroline ligands have corresponding lower catalytic activities. For example, the yield of **7a** is higher than **7b**, which is more substituted. This conclusion is also consistent to **7b** and **7c**. (Entry 1-6) Second, cationic species have higher catalytic activities than the corresponding neutral compounds. For example, **7a** is the cationic species of **6a**, and **7a** has higher catalytic activity than **6a**. This conclusion is also consistent to **7b**, **6b** and **7c**, **6c**. (Entry 1-6) The cationic species of the NHC complex is also more reactive than the

corresponding neutral one. (Entry 9-10). This may due to the open coordination site of the cationic species, which allow substrates to coordinate easily to the metal center. The cationic complexes are more electron deficient which makes binding of the nucleophilic benzyl alcohol. The di-imine complex **5** and NHC complex **8** and **9** did not show high efficiencies in this reaction. The NHC ligand contains a bulky iPr substituent, which may lead to the low catalytic activity. However, the commercially available $[Cp^*IrCl(\mu\text{-}Cl)]_2$ has the highest efficiency among the iridium complexes studied with a turn over number of 32.3. Good catalytic activity was reported for $[Cp^*IrCl(\mu\text{-}Cl)]_2$ in Oppenauer-type oxidation by Yamaguchi and coworkers.[43] Its derivatives, an iridium carbene complex, demonstrated extremely high reactivity with TON = 6640 in Oppenauer-type oxidation using acetone as oxidant. Our further investigations were based on using $[Cp^*IrCl(\mu\text{-}Cl)]_2$ to catalyze the aerobic oxidation of alcohols.

1.2.3 Aerobic Oxidation Reactions

We investigated the dependence of alcohol oxidation on O_2 with $[Cp^*IrCl(\mu\text{-}Cl)]_2$. We proposed that O_2 is needed for direct catalytic turn over. We tested this by examining the catalytic reaction of $[Cp^*IrCl(\mu\text{-}Cl)]_2$, **1** with 4-methoxybenzyl alcohol under three different conditions: (a) 1 atm of O_2, (b) 1 atm of air, (c) 1 atm of N_2, (Table 1.3). The data below clearly shows that O_2 is essential for catalytic turnover for these catalysts.

Table 1.3 Dependence of alcohol oxidation on O_2

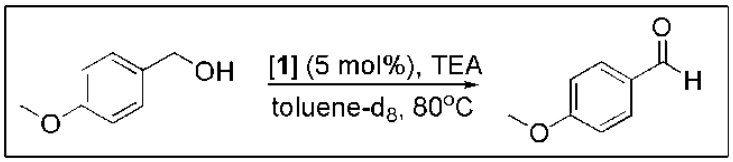

Reaction Condition	Conversion (%)	TON
O_2 (1 atm)	96	38
Air (1 atm)	24	9.6
N_2 (1 atm)	12	4.0

The scope of reactivity of $[Cp^*IrCl(\mu\text{-}Cl)]_2$ as a catalyst for the aerobic oxidation of different primary and secondary alcohols was then investigated (Table 1.4). A solution of alcohol (0.05 M), catalyst **1** (2.5 mM), Et_3N (0.018M) in toluene (10 ml) was purged with O_2 and stirred under constant O_2 (14.7 psig) at 80 ^oC for 12 hours. The products were analyzed by GC. Calibration curves for each substrate and product were made with octane as an internal standard. Conversions and yields were obtained based on the calibration curves.

Table 1.4 Aerobic Oxidations of Primary and Secondary Alcohols Catalyzed by **1**.

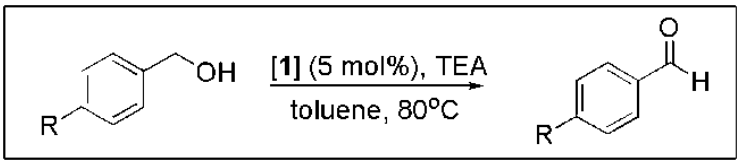

Entry	Substrate	Time (hrs)	Conv[b] (%)	Yield[c] (%)	TON[d]
1	4-methoxybenzyl alcohol	12	90(5)	82(8)	18
2	4-methylbenzyl alcohol	12	87(7)	81(5)	17
3	benzyl alcohol	12	82(4)	76(4)	16
4	4-chlorobenzyl alcohol	24	84(7)	79(6)	17
5	4-(methythio)benzyl alcohol	24	86(3)	81(4)	17
6	4-nitrobenzyl alcohol	12	46(2)	39(2)	9.2
7	Cyclohexanol	12	94(5)	86(3)	19
8	2-propanol	12	82(4)	74(4)	16

[a]Reaction Conditions: 5 mol % **1**, substrate (0.5-1M). [b]Conversion by GC with respect to alcohol. [c]Yield by GC with respect to aldehyde. [d]TON with respect to alcohol.

We successfully oxidized primary and secondary alcohols with $[Cp^*IrCl(\mu\text{-}Cl)]_2$ as a catalyst with good yields. There is a clear electronic dependence on the reactivity, demonstrating that the reaction favors electron-donating substituent (Entries 1-6).

1.2.4 Kinetic Studies

1.2.4.1 Kinetic Isotope Effect

Kinetic methods have been applied to study the mechanism of this reaction. The kinetic isotope effect of $[Cp^*IrCl(\mu\text{-}Cl)]_2$ catalyzed oxidation of benzyl alcohol was investigated by mixing benzyl alcohol ($\alpha,\alpha\text{-}d_2$) and benzyl alcohol in one reaction. Although we did not get the separation of benzaldehyde ($\alpha\text{-}d_1$) and benzaldehyde by GC-MS, we observed complete deuterium scrambling and the formation of benzyl alcohol ($\alpha\text{-}d_1$), as well as benzaldehyde ($\alpha\text{-}d_1$) and benzaldehyde (Figure 1.3). The isotopic labeling data strongly suggests the presence of an Ir-hydride as an intermediate in the catalytic cycle.

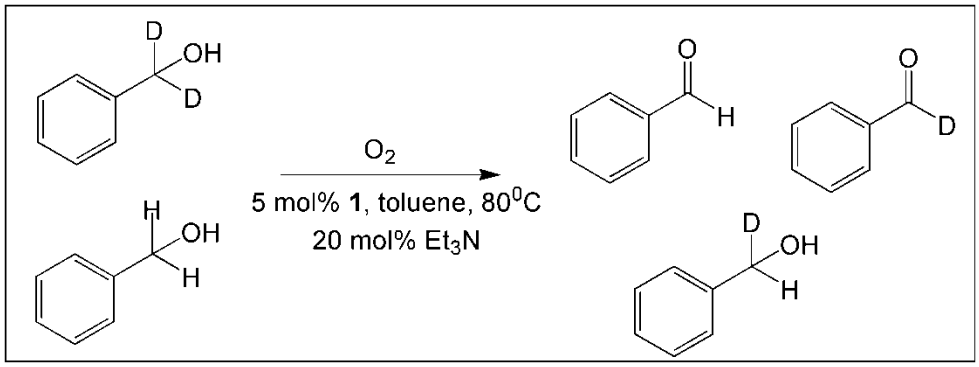

Figure 1.3 Isotopic experiment

In order to investigate the catalytic viability of this intermediate, we investigated the oxidation of 4-methoxybenzyl alcohol with $[Cp^*IrCl(\mu\text{-}Cl)]_2$ under nitrogen. Two new hydride species Ir-H (δ-13.5, δ-13.8ppm) in a ratio of 6:1 have been observed. The new species were assigned as the complexes $[(Cp^*IrCl)_2(\mu\text{-}H)(\mu\text{-}Cl)]$ **2** and $[Cp^*Ir(\mu\text{-}H)Cl]_2$ **3**. The ratio of $[Cp^*IrHCl]_2$ increased as the concentration of 4-methoxybenzyl alcohol is

increased. Also, in the presence of excess alcohol, $[(Cp^*IrCl)_2HCl]$ is slowly converted to $[Cp^*IrHCl]_2$. (Scheme 1.8) Complex **2** and **3** have been previously synthesized from **1** by Maitlis and co-workers using iso-propanol and KBH_4.[60] We examined the viability of these species as intermediates by examining their reactivity and their kinetic competency in the oxidation of benzyl alcohol. Treatment of **3** with Et_3NHCl and O_2 in C_7D_8 results in decomposition producing several unidentified species. Further, the aerobic oxidation of benzyl alcohol catalyzed by **3** resulted in a TON of 2 after twelve hours. In contrasts, the aerobic oxidation of benzyl alcohol catalyzed by **2** resulted in a similar TON (14) after twelve hours for the catalytic reaction.

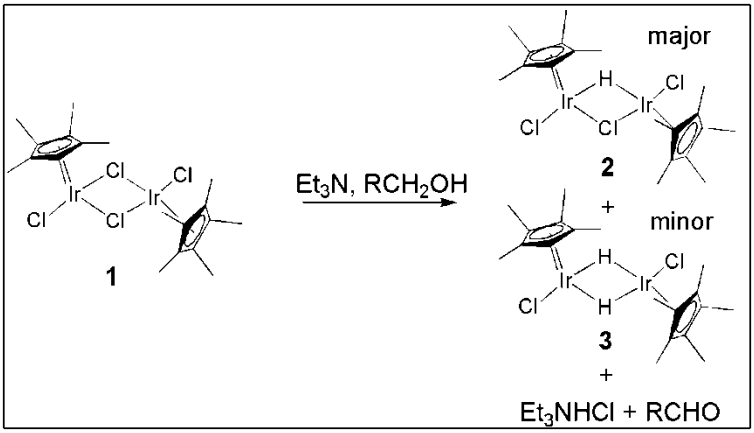

Scheme 1.9 Synthesis of iridium hydrides

1.2.5 Further evidence for iridium-hydride

The reactivity of $[(Cp^*IrCl)_2(\mu\text{-}H)(\mu\text{-}Cl)]$, **2** was investigated. Benzyl aldehyde and **2** were reacted in benzene (C_6D_6) with triethylamine under N_2. After two hours, the formation of benzyl alcohol and $[Cp^*IrCl(\mu\text{-}Cl)]_2$ **1** was observed. (Scheme 1.9) From the above result we conclude that the iridium hydride is a key intermediate in this reaction, the formation of iridium hydride does not need O_2, and the process of forming aldehyde is reversible.

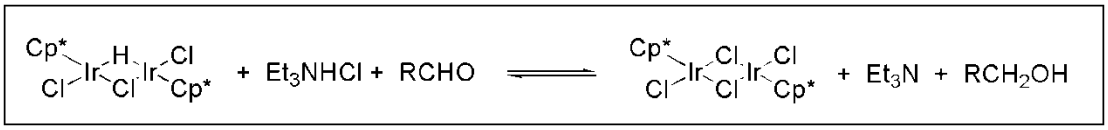

Scheme 1.10 The reverse reaction of aldehyde formation

We also tried to synthesize [(Cp*IrCl)$_2$(μ-D)(μ-Cl)] with KOD and isopropanol-d_8, but the reaction did not succeed, nor did the reaction with KBD_4 and isopropanol-d_8. (Scheme 1.10)

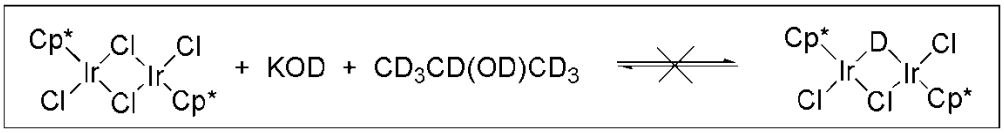

Scheme 1.11 Attempted synthesis of deuterated iridium hydride [(Cp*IrCl)$_2$(μ-D)(μ-Cl)], **4**

In our hypothesis, the oxidation state of iridium(III) does not change during the catalytic cycle, which is consistent with an Oppenauer-type mechanism. However, in the oxidase mechanism, the metal cycles between Ir(III)/Ir(I) process and an Ir(I) complex is a key intermediate. If Ir-hydride undergoes reductive elimination when it reacts with O_2, its oxidation state will be reduced to one. In the Oppenauer-type mechanism, we propose that iridium complexes stay as dimers during the catalytic cycle, but in oxidase mechanism, they react as monomers (Scheme 1.11). In order to prove the mechanism, the reactions of iridium-hydride with triethylamine hydrocholride under O_2 and N_2 were both conducted in C_6H_6 at 80^0C. Complex **2** decomposed under N_2, but formed an unidentified species under O_2. Further studies are currently underway with the Ir-hydride complex.

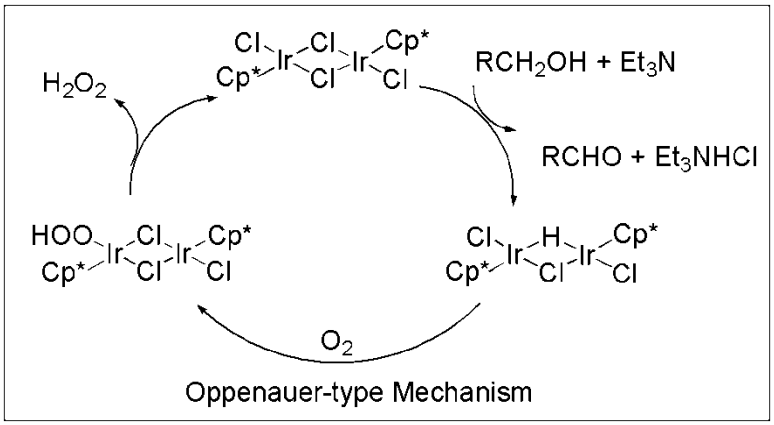

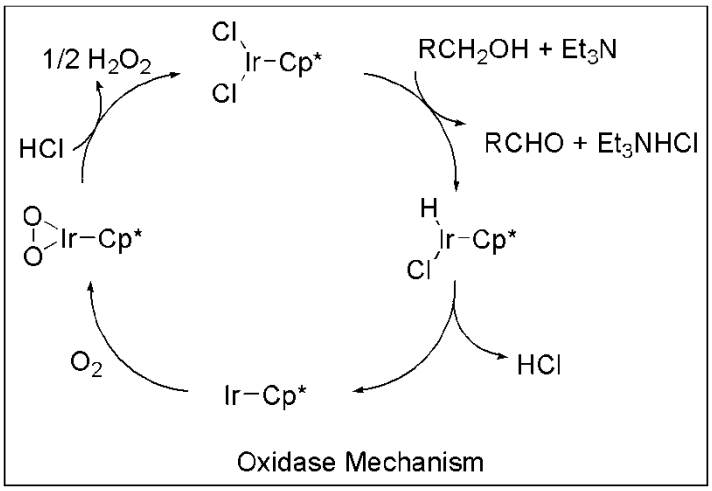

Scheme 1.12 Oppenauer-type mechanism and oxidase mechanism

1.2.6 O_2 up-take kinetic studies in Parr reactor

Kinetic studies were performed by monitoring the pressure of O_2 in a sealed, temperature-controlled Parr reaction vessel equipped with a high-accuracy pressure transducer in order to gather kinetic information about the catalytic reaction. The kinetic competency **2** is comparable to **1** under similar catalytic condition. (Figure 1.4, 1.5). For pseudo first order reaction, a large excess of alcohol was added so that its concentration did not change during the kinetic run. We observed that the reaction rates of O_2 in reactions catalyzed by both **1**

and **2** were fit to a single exponential decay curve, characteristic of a reaction that exhibits first order dependencies in the limiting reagent (O_2). The corresponding rate constants obtained by this method k_{obs}= 0.0128(2), (1) k_{obs}= 0.0199(2), (2) are comparable.

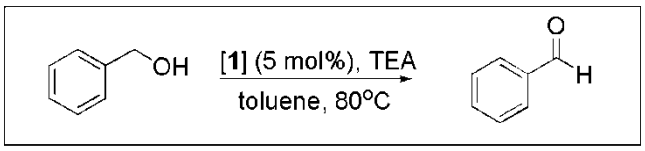

Scheme 1.13 Aerobic oxidation of benzyl alcohol

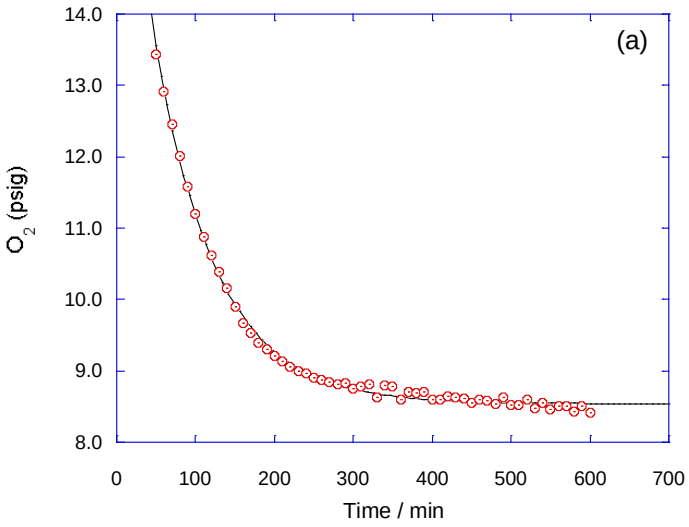

Figure 1.4 O_2 up-take experiment 1. Pressure of O_2 versus time profile for the oxidation of benzyl alcohol (1.0 M) with O_2 (14.7psig), Et_3N (0.018 M) and **1** (12.6 mM) in toluene at 353 K. The observed rate constant (k_{obs}) is 0.0128(2) / min^{-1}, R^2=0.997. The observed rate constants (k_{obs}) were obtained from nonlinear least squares fitting of P_t to: $[P_t] = \Delta P \exp(-k_{obs\Delta}t) + P_\infty$ where $\Delta P = P_0 - P_\infty$

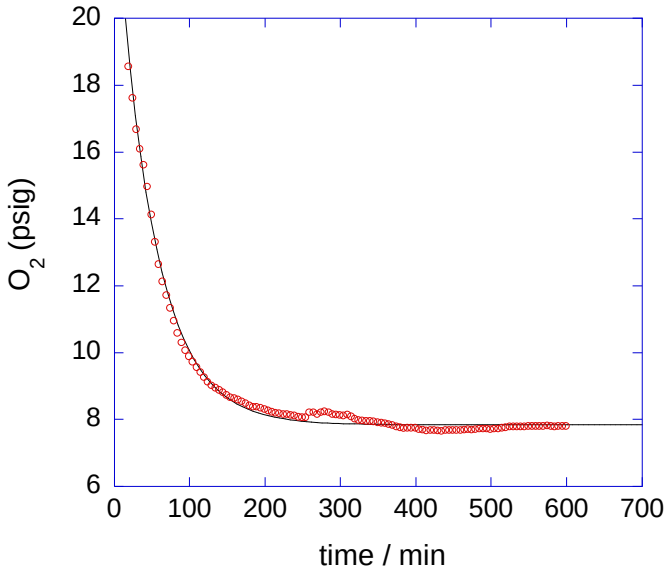

Figure 1.5 O_2 up-take experiment 2. Pressure of O_2 versus time profile for the oxidation of benzyl alcohol (1.0 M), with O_2 (14.7psig), Et_3N (0.018 M) and **2** (12.6 mM) in toluene at 353 K. The observed rate constant (k_{obs}) is 0.0199(2) / min^{-1}, R^2=0.994.

The dependencies of the primary components of the catalytic reaction, (catalyst, alcohol, triethyl amine) were determined. For alcohol, the concentration of benzyl alcohol was varied from 0.1M to 2.0M, and the corresponding rates were obtained. A plot of k_{obs} vs [benzyl alcohol] established that alcohol dependence exhibited saturation kinetics. (Figure 1.6).

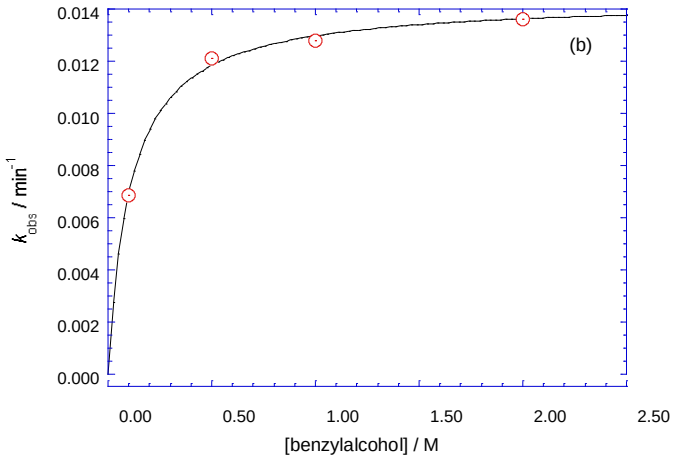

Figure 1.6 Plot of the k_{obs} versus [benzyl alcohol] with O_2 (14.7 psig), Et_3N (0.018 M) and **1** (12.6 mM). Rate measurements were carried out in toluene at 353 K.

Entry	Benzyl alcohol / M	k_{obs} / min^{-1}
1	0.10	0.00686
2	0.50	0.01210
3	1.00	0.01280
4	2.00	0.01360

A Similar procedure was used to determine the reaction order for catalyst. The concentration of catalyst was varied from 0.0070M to 0.0251M and corresponding rates were obtained concurrently. A first order dependence on catalyst was observed from a plot of k_{obs} vs [catalyst]. (Figure 1.7)

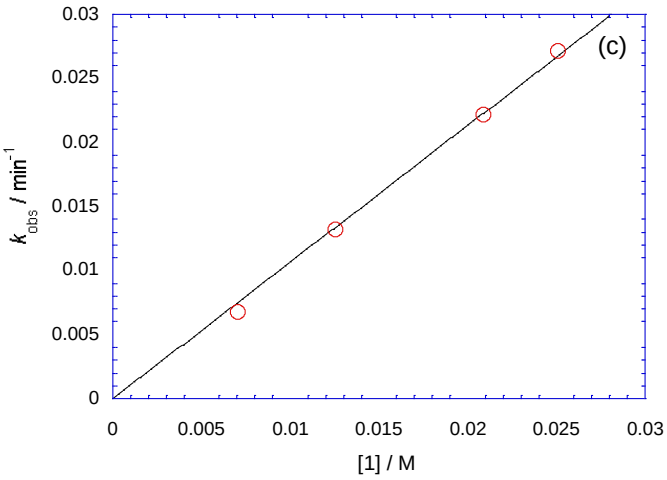

Figure 1.7 Plot of the k_{obs} versus catalyst [**1**] with benzyl alcohol (1M), O_2 (14.7 psig), Et_3N (0.018 M). Rate measurements were performed in toluene at 353 K.

Entry	Catalyst / M	k_{obs} / min^{-1}
1	0.00703	0.00681
2	0.0126	0.01320
3	0.0209	0.02215
4	0.0251	0.02719

The kinetic results for base (Et_3N) were different from alcohol and catalyst, although the same procedure was applied. The concentration of Et_3N was varied from 0.0179M to 0.144M, however, no dependence on Et_3N was observed. (Figure 1.8)

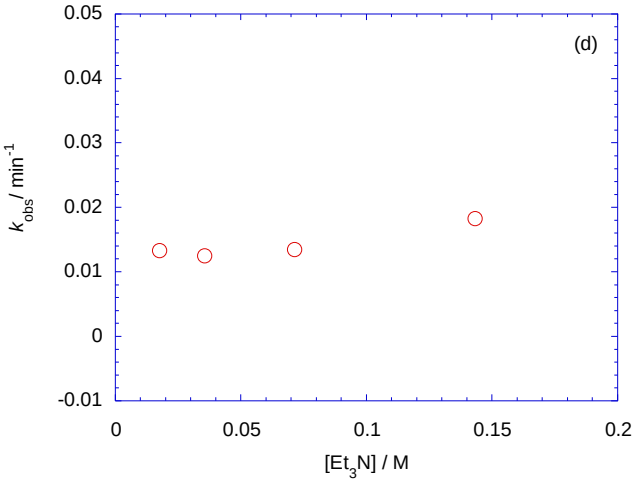

Figure 1.8 Plot of k_{obs} versus concentration of Et_3N with catalyst **1** (12.6 mM), benzyl alcohol (1M), O_2 (14.7 psig) in toluene at 353 K.

Entry	Et_3N/ M	k_{obs} / min^{-1}
1	0.0179	0.01322
2	0.0359	0.01238
3	0.0718	0.01334
4	0.1435	0.01810

1.2.7 Kinetic studies using UV-Vis

The formation of iridium hydride happens immediately after mixing of reactants. Complexes **1** and **2** have absorbance in UV region, so we used UV-Vis spectroscopy to study the kinetics of iridium hydride formation. We found that [Cp*IrCl(μ-Cl)]$_2$ **1** has a small peak around 350nm. When benzyl alcohol is added to it, the spectrum changed slightly due to absorbance of alcohol below 350nm. When Et_3N is added to the reactants, a large change occurred immediately, and the same absorbance pattern as iridium mono-hydride **2** was

observed. (Scheme 6) In order to determine the dependence on alcohol and Et_3N in this reaction, we varied their concentrations and monitored the absorbance change at 490nm, which is a typical absorbance of **2**. The change in absorbance of each concentration follows first order kinetics, so we plotted k_{obs} vs [concentration] to get saturation kinetics. (Figure 13) These results indicate that the formation of Ir-hydride is not a rate-determine step which is consistant with the result of the kinetic isotope effect of this reaction.

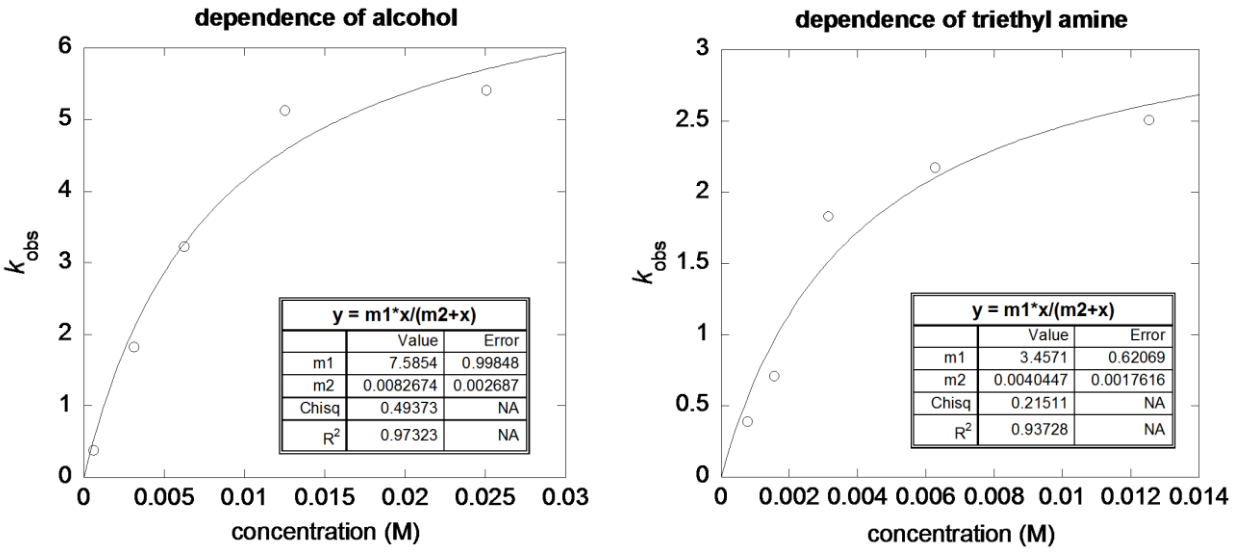

Figure 1.9 Dependence of Et_3N and benzyl alcohol.

The UV-Vis experiment was conducted at room temperature under air. The purpose of this experiment is to study the first two steps of this reaction based on our proposed mechanism. A rate law expression of the formation of iridium-hydride has been derived and it is consistent with our proposed mechanism.

Scheme 1.14 The rate law expression of iridium-hydride

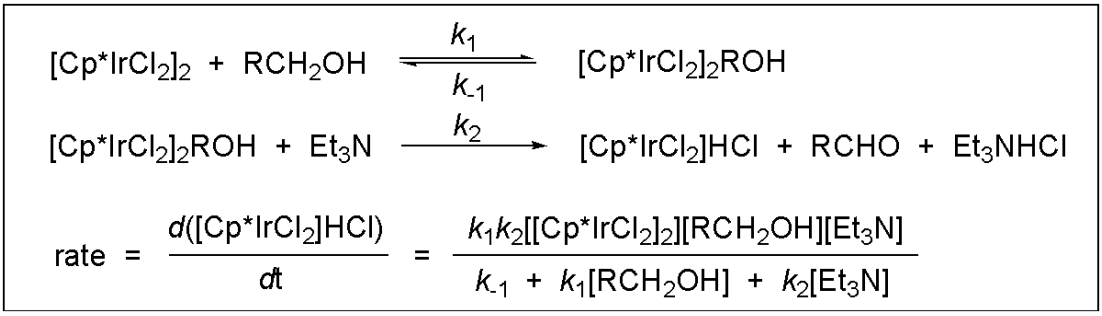

Since this reaction was conducted at room temperature, we assume the second step of this reaction is irreversable. The rate law expression shows saturation dependence on [RCH_2OH], which is consistent with our observation of UV-Vis experiment. (Figure 8)

1.2.8 Proposed Mechanism

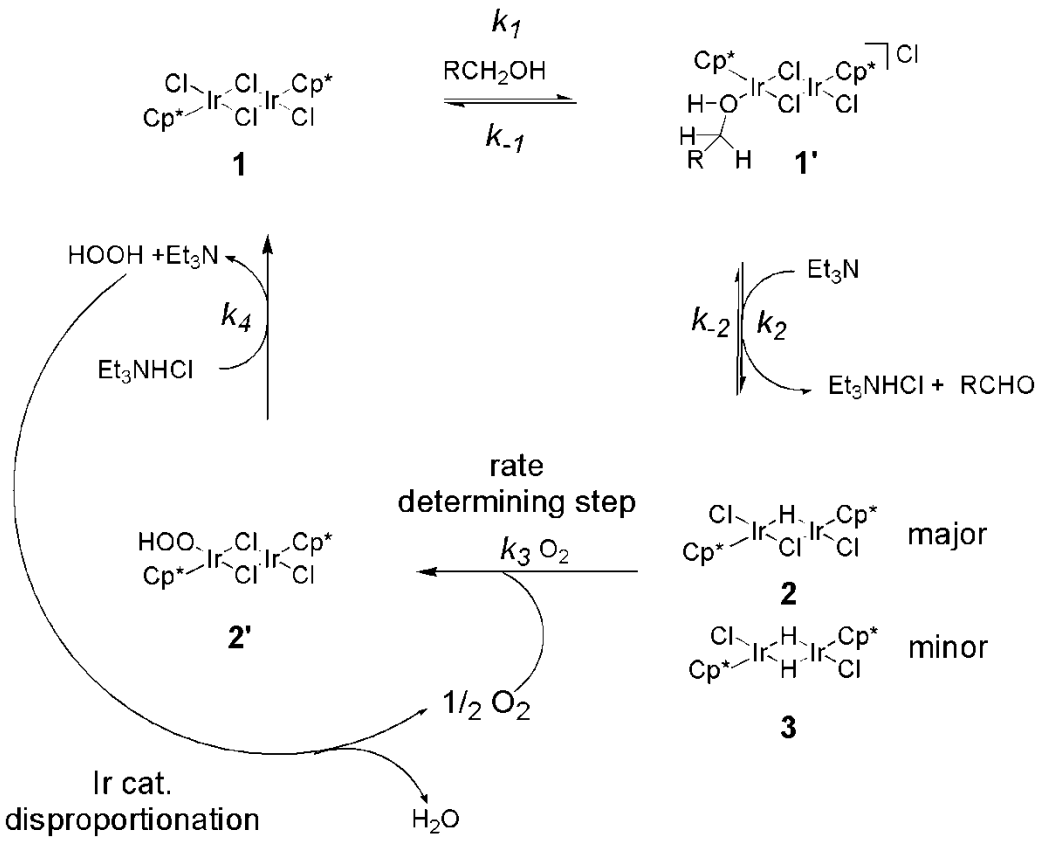

Scheme 1.15 Proposed mechanism of aerobic oxidation of benzyl alcohol

A mechanism for the oxidation of benzyl alcohol with Et_3N and pure oxygen catalyzed by $[Cp^*IrCl(\mu\text{-}Cl)]_2$ was proposed. (Scheme 14) In this mechanism, $[Cp^*IrCl(\mu\text{-}Cl)]_2$ reacts with benzyl alcohol to give complex **1'**. Triethyl amine deprotonates the alcohol and forms triethyl amine hydrochloride. Concurrently, β-hydride elimination results in the formation of one equivalent of benzyl aldehyde and intermediate **2**. This intermediate reacts with O_2 to give hydroperoxide intermediate **2'**, which then reacts with triethyl amine hydrocholoride formed from the second step to produce triethyl amine, the by-product hydrogen peroxide and regenerates $[Cp^*IrCl(\mu\text{-}Cl)]_2$. The hydrogen peroxide is catalyzed by the iridium catalyst

to form one equivalent of water and half an equivalent of oxygen. Since, this reaction consumes one equivalent of oxygen and forms half an equivalent oxygen at the end of the catalytic cycle, the actual stoichiometry of O_2 to alcohol is 1 : 2. Based on the proposed mechanism, we derived a rate expression for this reaction that is consistent with experimental observations.

1.2.9 Rate law derivations

The following mechanism accounts for the experiment observations.

$$[Cp^*IrCl_2]_2 + RCH_2OH \underset{k_{-1}}{\overset{k_1}{\rightleftharpoons}} [Cp^*IrCl_2]_2ROH$$

$$[Cp^*IrCl_2]_2ROH + Et_3N \underset{k_{-2}}{\overset{k_2}{\rightleftharpoons}} [Cp^*IrCl]_2HCl + RCHO + Et_3NHCl$$

$$[Cp^*IrCl]_2HCl + O_2 \xrightarrow{k_3} [Cp^*IrCl_2]HClO_2$$

$$[Cp^*IrCl_2]HClO_2 + Et_3NHCl \xrightarrow{k_4} [Cp^*IrCl_2]_2 + HOOH + Et_3N$$

$$RCH_2OH + O_2 \longrightarrow RCHO + HOOH$$

The rate of product formation is described by the following rate law.

$$\text{Rate} = \frac{-dP(O_2)}{dt} = k_3[[Cp^*IrCl]_2HCl][O_2] \quad (1)$$

According to the steady-state approximation,

$$k_2[[Cp^*IrCl_2]_2ROH][Et_3N] = k_{-2}[[Cp^*IrCl_2]_2HCl][RCHO][Et_3NHCl] + k_3[[Cp^*IrCl]_2HCl][O_2] \quad (2)$$

$$K_1 = (k_1/k_{-1}) = [IrROH] / [IrCl_2][RCH_2OH] \quad (3)$$

Substitute (2) in (3)

$K_1k_2[[Cp^*IrCl_2]_2][Et_3N][RCH_2OH] = k_{-2}[[Cp^*IrCl_2]_2HCl][RCHO][Et_3NHCl]$

$$+ k_3[[Cp^*IrCl]_2HCl][O_2] \quad (4)$$

According to mass balance for iridium,

$[[Cp^*IrCl_2]_2]_T = [Cp^*IrCl_2]_2 + [[Cp^*IrCl_2]_2ROH]$

$$+ [[Cp^*IrCl_2]_2HCl] + [[Cp^*IrCl]_2HClO_2] \quad (5)$$

We assume $[[Cp^*IrCl_2]_2ROH]$ and $[[Cp^*IrCl]_2HClO_2]$ are small,

$$[[Cp^*IrCl_2]_2]_T = [Cp^*IrCl_2]_2 + [[Cp^*IrCl_2]_2HCl] \quad (6)$$

Substitute (6) into (4),

$$[[Cp^*IrCl]_2HCl] = \frac{K_1k_2k_3[RCH_2OH][Et_3N][[Cp^*IrCl_2]_2]_T[O_2]}{k_{-2}[RCHO][Et_3NHCl] + k_3[O_2] + K_1k_2[RCH_2OH][Et_3N]} \quad (7)$$

Substitute (7) into (1),

$$\text{Rate} = \frac{-dP(O_2)}{dt} = \frac{K_1k_2k_3[RCH_2OH][Et_3N][[Cp^*IrCl_2]_2]_T[O_2]}{k_{-2}[RCHO][Et_3NHCl] + k_3[O_2] + K_1k_2[RCH_2OH][Et_3N]} \quad (8)$$

From the experimental data we observe that the reaction exhibits 1st order kinetics in $[O_2]$ (Figure 3),

Therefore $k_3[O_2] << k_{-2}[RCHO][Et_3NHCl] + K_1k_2[RCH_2OH][Et_3N]$

$$\text{Rate} = \frac{-dP(O_2)}{dt} = \frac{K_1k_2k_3[RCH_2OH][Et_3N][[Cp^*IrCl_2]_2]_T[O_2]}{k_{-2}[RCHO][Et_3NHCl] + K_1k_2[RCH_2OH][Et_3N]} \quad (9)$$

This expression is consistent with the experimental observations:

At high concentrations of RCH_2OH, $K_2k_2[RCH_2OH][Et_3N] >> k_{-2}[RCHO][Et_3NHCl]$

The rate law reduces to:

$$\text{Rate} = \frac{-dP(O_2)}{dt} = k_3[[Cp^*IrCl_2]_2]_T[O_2] \quad (10)$$

At low concentrations of RCH_2OH, $K_2k_2[RCH_2OH][Et_3N] << k_{-2}[RCHO][Et_3NHCl]$

The rate law reduces to:

$$\text{Rate} = \frac{-dP(O_2)}{dt} = \frac{K_1k_2k_3[RCH_2OH][Et_3N][[Cp^*IrCl_2]_2]_T[O_2]}{k_{-2}[RCHO][Et_3NHCl]} \qquad (11)$$

It is consistent to experimental observation of first order in $[Cp^*IrCl_2]_2$ (Figure 6).

1.3 Conclusions

We have investigated the iridium catalyzed aerobic oxidation of alcohol. The highlights of our system are the following: (1) it offers selective oxidation of primary and secondary alcohols, (2) the reaction illustrates a new role for catalysis by Ir complexes, (3) the reaction utilizes the environmentally benign O_2 as a stoichiometric oxidant. This last feature is very attractive because it limits the amount of organic waste typically generated by traditional organic oxidants and does not lead to environmentally hazardous by-products typically associated with stoichiometric transition metal oxidants.

Thus far, $[Cp^*IrCl(\mu\text{-}Cl)]_2$ (**1**) has the highest reactivity of all the catalysts studied. We optimized the catalytic system and also investigated the mechanism for these reactions. Based on our current understanding, iridium maintains its (+3) oxidation state throughout the entire catalytic cycle. The observation that iridium hydride complexes might play an important role in aerobic oxidations is a new and exciting development as it allows for the design of new catalytic systems that can avoid lower valent oxidation states altogether.

1.4 Experimental Section

1.4.1 Synthesis of Iridium Complexes

Materials and Methods. Reactions were performed open to the environment as stated or in a Nitrogen filled Glove-box as stated. Oxygen uptake experiments were performed in glass lined stainless steel Parr 4592 50 mL Micro Bench Top Reactor under O_2. Solvents were degassed, and purified with a Mbraun-SPS solvent purification system prior to use. $[Cp^*IrCl(\mu\text{-}Cl)]_2$ was purchased from Strem Chemicals and used as received. Substrates were purchased from VWR or Aldrich and used as received. Oxygen was purchased from Airgas, National Welders. The complexes μ-Chloro-μ-hydrido-bis[chloro(pentamethylcyclo-pentadienyl)-iridium, **2**, and Di-μ-hydrido-bis(pentamethylcyclopentadienyl)-iridium, **3**, were synthesized according to published procedures.[1] NMR spectra were recorded on Varian 300 instruments. Mass spectrometry was performed by the North Carolina State University Mass Spectrometry Center using an Agilent Technologies 6210LC-TOF mass spectrometer (GC/MS). GC was performed on Varian 3800 Gas Chromatograph with a Varian VF-53ms column.

Synthesis of $[Cp^*IrCl]_2HCl$, 2. $[Cp^*IrCl]_2HCl$ is synthesized according to published procedure. A solution of $[Cp^*IrCl(\mu\text{-}Cl)]_2$ (0.30g (0.377mmol)) and KBH_4 (0.05g (0.927mmol)) in isopropyl alcohol (10ml) was stirred at room temperature (20^{o}C) for 4 hours. The solvent was removed on a rotary evaporator to leave a red residual. It was extracted with toluene (30ml), filtered, and reduced to small volume. Hexanes was added and red-purple crystals of the hydrido-complex (**2**) were obtained. Yield (52 %).^{1}H NMR

(300MHz, Toluene-d_6): δ 1.62 (s, 30H), -13.85 (s, 1H); ^{13}C NMR (300MHz, Toluene-d_6): δ 10.15, 88.98.

Synthesis of [Cp*IrClH]$_2$, 3. [Cp*IrClH]$_2$ is synthesized by the same procedure above with the reaction time extended to 12 hours to give di-hydrido complex **3**. Yield (90%). ^{1}H NMR (300MHz, Toluene-d_6): δ 1.48 (s, 30H), -13.67(s, 2H); ^{13}C NMR (300MHz, Toluene-d_6): δ 10.15, 88.98.

Synthesis of [Ir(di-imine)(CH_3CN)Br_2], 5. A schlenk flask was charged with [IrCl(cod)]$_2$ (0.05g, 0.07mmol), di-imine ligand (0.0642g, 0.175mmol) and NaBr (0.1g, 14 molar equivalent with respect to iridium), degassed through three inert gas vacuum cycles. Degased methoxyethanol (10ml) then added to solid reactants the mixture was heated to 110^{0}C for 15 hours under an inert gas atmosphere. The resultant deep red solution was then filtered, the solvent evaperated to an external trap, and the red paste redissolved in acetonitrile (5ml). Water was added (10ml) and the solution left to stand overnight with precipitation of a deep red solid, which was recrystallized from DCM/hexane.

Synthesis of [Ir(cod)phenanthroline(OTf)], 6b. 50mg of phenanthroline was dissolved in 1ml of CH_2Cl_2. 67mg of [IrCl(cod)]$_2$ was dissolved in 3ml of CH_2Cl_2. Two solution was mixed together, reacted for half an hour under room temperature. Solvent was evaporated and the precipitate, **[Ir(cod)phenanthrolineCl] 6a** turned to green after 15 minutes. 1.2 equivalent of AgOTf was added to Ir(cod)phenanthrolineCl in 10ml of CH_2Cl_2, reacted for 2

hours under room temperature. The filtrate was evaporated and recrystallized from DCM/hexane.

Synthesis of [Ir(cod)neocuproine(OTf)], 7b and [Ir(cod)bathocuproine(OTf)], 8b. The same procedure as 6bwas applied to the synthesis of 7b and 8b.

Catalytic oxidation of 4-methoxyl benzyl alcohol under Oxygen, air and nitrogen atmosphere. In three J-Young NMR tubes, each was charged with $[Cp^*IrCl(\mu\text{-}Cl)]_2$ (3.6 mg, 4.52E-3mmol), 4-methoxyl benzyl alcohol (22 μL, 0.180mmol), triethylamine (22 μL,0.163mmol) and toluene-d_8 (1mL). Three NMR tubes were freeze-pump-thaw three times and back filled with A) oxygen; B) air and C) nitrogen. The NMR tubes were heated to 80oC in oil bath and NMR spectrum was monitored periodically. In all three tubes, the solution was red before heating, but 2 minutes after heating to boil, the solution turns to dark red clear solution without any precipitate, which is due to the formation of the intermediate [[Cp*IrCl]2HCl] (resonance at 1.62 ppm is observed, which is due to the CH_3 of Cp* ligand). After 12 hours, 95.65% of 4-methoxyl benzyl alcohol was converted to 4-methoxyl benzaldehyde in tube A (TON = 38.26) and conversion is 24.24% (TON = 9.6) for tube B and 11.5% (TON = 4.6) for tube C, respectively.

General Procedure for Kinetic Studies. All reactions were performed in a glass lined stainless steel Parr 4592 50 mL Micro Bench Top Reactor connected to a Cole-Palmer high-accuracy pressure transducer (0.15%) at 80^oC. The pressure of O_2 was monitored in ten

minute intervals with a Monarch Instrument paperless recorder. The reactor was filled with 10 mL of toluene, 1.0 mL (0.96 M) of benzyl alcohol, 25 L (0.018 M) of triethylamine and 100 mg of $[Cp^*IrCl(\mu\text{-}Cl)]_2$ (12.6 mM). The reactor was purged with O_2 and filled with 14.7 psi (1 atm) O_2. The data was analyzed using the Kaleidograph® software package. The observed rate constants k_{obs} were obtained from nonlinear least squares fitting of P_t to: $P_t = P \exp(-k_{obs}t) + P_\infty$ where $P = P_0 - P_\infty$.

Figure 1.10 Apparatus for oxygen uptake and kinetic studies

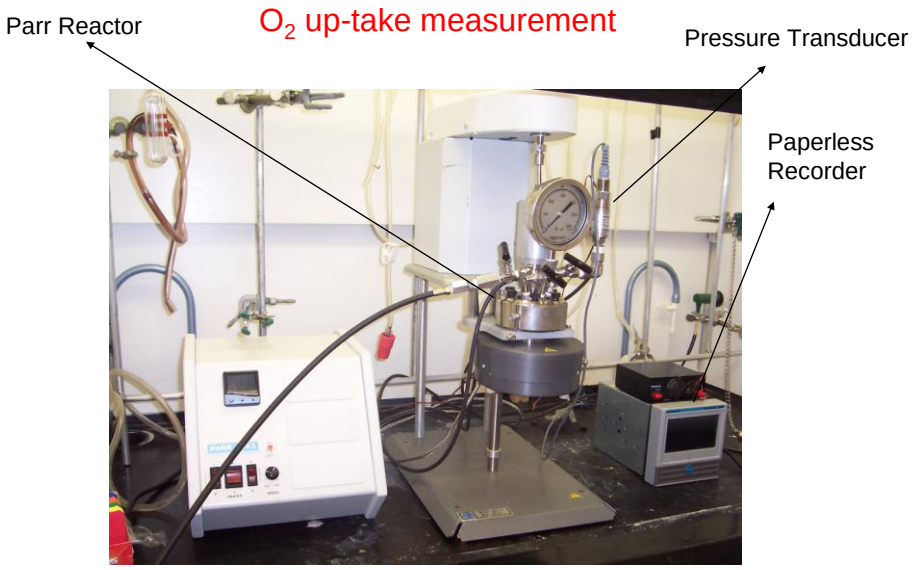

Measurement of Deuterium Kinetic Isotope Effect. k_{obs} of benzyl alcohol and benzyl alcohol-α,α-d_2 were obtained following procedures above. $k_H/k_D = k_{obs}$ (benzyl alcohol) / k_{obs} (benzyl alcohol-α,α-d_2) = 0.9(1).

[[Cp*IrCl]$_2$HCl] and Et$_3$NHCl in O$_2$ or N$_2$ at 80^{o}C. Two J-young NMR tubes were charges with [[Cp*IrCl]$_2$HCl] (5 mg, 6.56E-3 mmol) and Et$_3$NHCl (2.6 mg, 0.026 mmol) and toluene-d_8, respectively. Freeze-pump-thaw three times of both NMR tubes and tube A is back-filled with O_2, while tube B is back-filled with N_2. The two tubes were heated in a 80^{o}C oil bath and NMR spectrum were monitored periodically. For tube A, after 4 hours, a new resonance grew at 1.58 ppm, instead the resonance due to Cp* CH_3 of [[Cp*IrCl]$_2$HCl] decreased. After 16 hours, [[Cp*IrCl]$_2$HCl] was disappeared and only the unidentified new resonance was observed (see NMR spectrum shown below); for tube B, [[Cp*IrCl]$_2$HCl] resonances was observed even after 16 hours heating.

Oxygen atmosphere: 4 hours

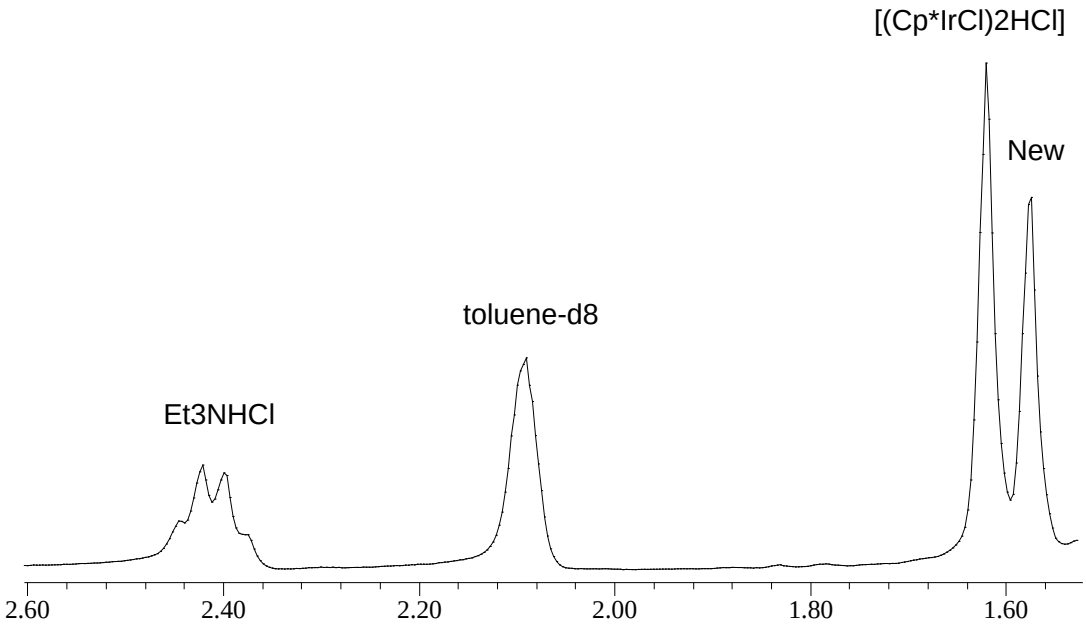

Figure 1.11 NMR spectrum of [[Cp*IrCl]$_2$HCl] and Et$_3$NHCl in O_2 after 4 hours.

Oxygen atmosphere: 16 hours

[Cp*IrCl)2HCl] at 1.62 ppm disappeared

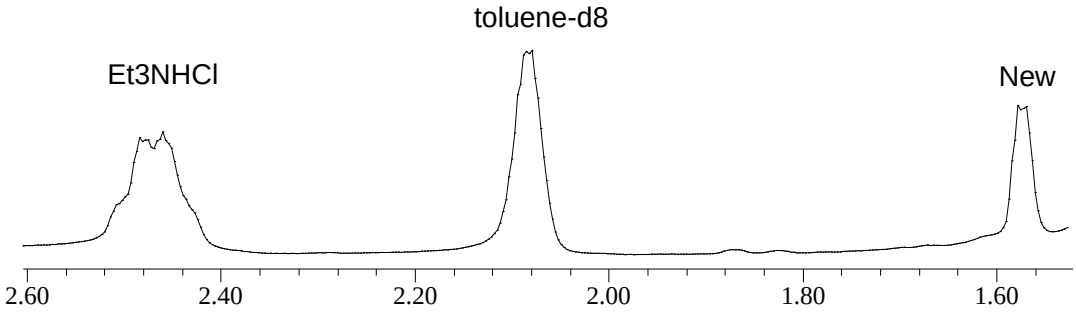

Figure 1.12 NMR spectrum of $[[Cp^*IrCl]_2HCl]$ and Et_3NHCl in O_2 after 16 hours.

Reaction of $[[Cp^*IrCl]_2HCl]$ and benzaldehyde: A J-young NMR tube was charged with $[[Cp^*IrCl]_2HCl]$ (5 mg, 6.56E-3 mmol), Et_3NHCl (3.61 mg, 0.026 mmol), benzaldehyde (13.6 uL, 0.131 mmol) and benzene-d_6 (0.5 mL). The NMR tube was freeze-pump-thaw three times and back-filled with N_2. The tube was heated to 80^{o}C in a oil bath and NMR spectrum was monitored. After 2 hours, the formation of benzyl alcohol was observed with the ratio of benzaldehyde : benzyl alcohol = 1.3 : 1. After 12 hours, the ratio of benzaldehyde : benzyl alcohol = 1:1.

Reaction of $[Cp^*IrCl(\mu\text{-}Cl)]_2$, benzyl alcohol and Et_3N in toluene-d_8 at room temperature. A regular NMR tube was charged with $[Cp^*IrCl_2]_2$ (5 mg, 6.28E-3 mmol), benzyl alcohol (13.0 uL, 0.125 mmol) and toluene-d_8 (0.5 mL), and NMR spectrum was monitored periodically. No reaction was observed after 12 hours at room temperature. Et_3N

(3.48 uL, 0.025 mmol) was added to the NMR tube and NMR spectrum was taken immediately, resonances (δ 9.60 (s, 1H, -C*H*O), 7.48 (d, 2H, *ortho*-phenyl), 7.09 (t, 1H, *para*-phenyl), 7.01 (t, 2H, *meta*-phenyl)) due to benzyl aldehyde (10% from NMR integration) and resonances [δ 1.62 (s, 30H, η^5-C_5Me_5), -13.85 (s, 1H, Ir-*H*)] due to [$(Cp^*IrCl)_2HCl$] were observed from NMR spectrum.

Reaction of $[Cp^*IrCl_2]_2$, benzyl alcohol and Et_3N at room temperature monitored by UV-Vis spectroscopy. Four methylene chloride solutions were prepared 1) $[Cp^*IrCl_2]_2$ (0.628 mM), 2) $[Cp^*IrCl_2]_2$ (0.628 mM) with benzyl alcohol (0.628 mM), 3) $[Cp^*IrCl_2]_2$ (0.628 mM) with benzyl alcohol (0.628 mM) and TEA (0.628 mM), 4) $[Cp^*IrCl_2]HCl$ (0.628 mM) and UV-Vis spectrum were taken of these four solutions. (Figure 11) There is no reaction of $[Cp^*IrCl]_2$ and benzyl alcohol (same UV absorption shown) and the reaction of $[Cp^*IrCl_2]_2$, benzyl alcohol and TEA forms [$[Cp^*IrCl_2]HCl$] immediately (same UV absorption, except different concentration).

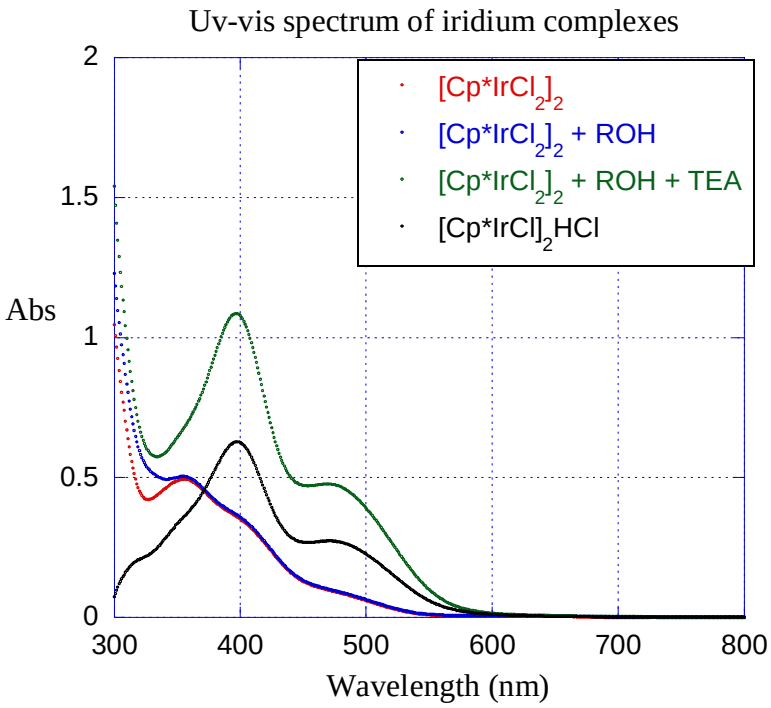

Figure 1.13 UV spectrum were taken in the order of $[Cp^*IrCl_2]_2$ (0.628 mM)(red line), $[Cp^*IrCl_2]_2$ (0.628 mM) with benzyl alcohol (0.628 mM)(blue line), $[Cp^*IrCl_2]_2$ (0.628 mM) with benzyl alcohol (0.628 mM) and TEA (0.628 mM)(green line), $[Cp^*IrCl_2]HCl$ (0.628 mM)(black line) (solvent: CH_2Cl_2).

Reaction of $[Cp^*IrCl(\mu\text{-}H)]_2$ and Et_3NHCl: A J-young NMR tube was charged with $[Cp^*IrCl(\mu\text{-}H)]_2$ (5 mg, 6.87E-3 mmol), Et_3NHCl (3.72 mg, 0.027 mmol) and benzene-d_6 (0.5 mL). The NMR tube was freeze-pump-thaw three times and back-filled with O_2. The tube was heated to 80^{o}C in a oil bath and NMR spectrum was monitored. After 12 hours, $[Cp^*IrClH]_2$ decomposed to several unidentified complexes.

Reaction of [Cp*IrCl(μ-H)]$_2$, benzyl alcohol and Et$_3$N: A J-young NMR tube was charged with [Cp*IrCl(μ-H)]$_2$ (5 mg, 6.87E-3 mmol), Et$_3$N (3.62 uL, 0.026 mmol), benzyl alcohol (14.2 uL, 0.137 mmol) and benzene-d_6 (0.5 mL). The NMR tube was freeze-pump-thaw three times and back-filled with O_2. The tube was heated to 80^{o}C in a oil bath and NMR spectrum was monitored. After 12 hours, 10% benzyl aldehyde was formed with TON=2.

Reaction of [Cp*IrCl(μ-Cl)]$_2$, 4-methoxy benzyl alcohol and Et$_3$N at room temperature under N$_2$: A J-young NMR tube was charged with [Cp*IrCl(μ-Cl)]$_2$ (5 mg, 6.28E-3 mmol), Et$_3$N (3.48 uL, 0.025 mmol), 4-methoxy benzyl alcohol (38.7 uL, 0.314 mmol) and toluene-d_8 (0.5 mL). The NMR tube was freeze-pump-thaw three times and back-filled with N_2. The tube was warmed to room temperature and NMR spectrum was monitored. After 2 hours, the formation of **2** and **3** were observed with the ratio of **2** : **3** = 6 : 1.

Reaction of [[Cp*IrCl]$_2$HCl], 4-methoxy benzyl alcohol and Et$_3$N at room temperature: A regular NMR tube was charged with **2** (5 mg, 6.56E-3 mmol), Et$_3$N (3.62 uL, 0.026 mmol), 4-methoxy benzyl alcohol (40.5 uL, 0.328 mmol) and toluene-d_8 (0.5 mL). After 1 hour, **3** was formed with a yield of 10%.

References

[1]. K.Weissermel, H.-J.A., *Industrial Organic Chemistry, 3rd ed.* **1997**.

[2]. *chemical industry.* www.basf.com.

[3]. Sheldon, R.A., Green Chemistry, **2007**. *9*(12): p. 1273-1283.

[4]. Wolfgang G. Glasser, *Lignin:Properties and Materials.***1989**

[5]. John Emsley, *Nature's Building Blocks*, **2003**

[6]. Stahl, S.S., *Angewandte Chemie-International Edition*, **2004**. *43*(26): p. 3400-3420.

[7]. Schultz, M.J. and M.S. Sigman, *Tetrahedron*, **2006**. *62*(35): p. 8227-8241.

[8]. Tovrog, B.S., et al., *J.Am.Chem.Soc*, **1981**. *103*(12): p. 3522-3526.

[9]. Iwahama, T., et al., *Tetrahedron Letters*, **1995**. *36*(38): p. 6923-6926.

[10]. Iwahama, T., et al., *Journal of Organic Chemistry*, **2000**. *65*(20): p. 6502-6507.

[11]. Sharma, V.B., S.L. Jain, and B. Sain, *Journal of Molecular Catalysis a-Chemical*, **2004**. *212*(1-2): p. 55-59.

[12]. Mandal, A.K. and J. Iqbal, *Tetrahedron*, **1997**. *53*(22): p. 7641-7648.

[13]. Sharma, V.B., S.L. Jain, and B. Sain, *Tetrahedron Letters*, **2003**. *44*(2): p. 383-386.

[14]. Jain, S.L. and B. Sain, *Journal of Molecular Catalysis a-Chemical*, **2001**. *176*(1-2): p. 101-104.

[15]. Semmelhack, M.F., et al., *Journal of the American Chemical Society*, **1984**. *106*(11): p. 3374-3376.

[16]. Marko, I.E., et al., *Science*, **1996**. *274*(5295): p. 2044-2046.

[17]. Marko, I.E., et al., *Angewandte Chemie-International Edition in English*, **1997**. *36*(20): p. 2208-2210.

[18]. Marko, I.E., et al., *Angewandte Chemie-International Edition*, **2004**. *43*(12): p. 1588-1591.

[19]. Gamez, P., et al., *Chemical Communications*, **2003**(19): p. 2414-2415.

[20]. Gamez, P., et al., *Advanced Synthesis & Catalysis*, **2004**. *346*(7): p. 805-811.

[21]. Velusamy, S., A. Srinivasan, and T. Punniyamurthy, *Tetrahedron Letters*, **2006**. *47*(6): p. 923-926.

[22]. Tsunoyama, H., H. Sakurai, and T. Tsukuda, *Chemical Physics Letters*, **2006**. *429*(4-6): p. 528-532.

[23]. Guan, B.T., et al., *Journal of the American Chemical Society*, **2005**. *127*(51): p. 18004-18005.

[24]. Li, H.R., et al., *Tetrahedron*, **2007**. *63*(35): p. 8430-8434.

[25]. Miyamura, H., et al., *Angewandte Chemie-International Edition*, **2007**. *46*(22): p. 4151-4154.

[26]. Fristrup, P., L.B. Johansen, and C.H. Christensen, *Catalysis Letters*, **2008**. *120*(3-4): p. 184-190.

[27]. Martin, S.E. and D.F. Suarez, *Tetrahedron Letters*, **2002**. *43*(25): p. 4475-4479.

[28]. Wang, N.W., et al., *Chemical Communications*, **2005**. (42): p. 5322-5324.

[29]. Peterson, K.P. and R.C. Larock, *Journal of Organic Chemistry*, **1998**. *63*(10): p. 3185-3189.

[30]. Nishimura, T., et al., *Journal of Organic Chemistry*, **1999**. *64*(18): p. 6750-6755.

[31]. ten Brink, G.J., et al., *Applied Catalysis a-General*, **2000**. *194*: p. 435-442.

[32]. Jamwal, N., M. Gupta, and S. Paul, *Green Chemistry*, **2008**. *10*(9): p. 999-1003.

[33]. ten Brink, G.J., I.W.C.E. Arends, and R.A. Sheldon, *Green, catalytic oxidation of alcohols in water*. Science, **2000**. *287*(5458): p. 1636-1639.

[34]. Chen, J., et al., *Advanced Synthesis & Catalysis*, **2008**. *350*(3): p. 453-464.

[35]. Karimi, B., et al., *Angewandte Chemie-International Edition*, **2006**. *45*(29): p. 4776-4779.

[36]. Buffin, B.P., N.L. Belitz, and S.L. Verbeke, *Journal of Molecular Catalysis a-Chemical*, **2008**. *284*(1-2): p. 149-154.

[37]. Nielsen, R.J. and W.A. Goddard, *Journal of the American Chemical Society*, **2006**. *128*(30): p. 9651-9660.

[38]. Stephen J. Lippard, *Principles of Bioinorganic Chemistry*, **1994**

[39]. Vaska, L. *Acc. Chem. Res*. **1976**, *9*, 175

[40]. Hanasaka, F., K.I. Fujita, and R. Yamaguchi, Organometallics, **2004**. *23*(7): p. 1490-1492.

[41]. Ajjou, A.N., *Tetrahedron Letters*, **2001**. *42*(1): p. 13-15.

[42]. Suzuki, T., et al., *Journal of Organic Chemistry*, **2002**. *68*(4): p. 1601-1602.

[43]. Tanabe, Y., et al., *Organometallics*, **2007**. *26*(18): p. 4618-4626.

[44]. Testa, C., et al., *J Magn Reson Imaging*, **2004**. *19*(3): p. 274-82.

[45]. Larock, R.C. and T.R. Hightower, *Journal of Organic Chemistry*, **1993**. *58*(20): p. 5298-5300.

[46]. Larock, R.C., et al., *Journal of Organic Chemistry*, **1996**. *61*(11): p. 3584-3585.

[47]. Larock, R.C., L.L. Wei, and T.R. Hightower, *Synlett*, **1998**(5): p. 522-+.

[48]. Larock, R.C., et al., *Journal of Organic Chemistry*, **1998**. *63*(7): p. 2154-2160.

[49]. Larock, R.C. and Q.P. Tian, *Journal of Organic Chemistry*, **1998**. *63*(6): p. 2002-2009.

[50]. Larock, R.C., C. Tu, and P. Pace, *Journal of Organic Chemistry*, **1998**. *63*(20): p. 6859-6866.

[51]. Toyota, M., M. Rudyanto, and M. Ihara, *Tetrahedron Letters*, **2000**. *41*(46): p. 8929-8932.

[52]. Toyota, M., et al., *Journal of the American Chemical Society*, **2000**. *122*(37): p. 9036-9037.

[53]. Toyota, M., V.J. Majo, and M. Ihara, *Tetrahedron Letters*, **2001**. *42*(8): p. 1555-1558.

[54]. Toyota, M. and M. Ihara, *Synlett*, **2002**(8): p. 1211-1222.

[55]. Toyota, M. and M. Ihara, *Journal of Synthetic Organic Chemistry Japan*, **1998**. *56*(10): p. 818-830.

[56]. Toyota, M., et al., *Journal of Organic Chemistry*, **1998**. *63*(17): p. 5895-5902.

[57]. Gabrielsson, A., P. van Leeuwen, and W. Kaim, *Chemical Communications*, **2006**(47): p. 4926-4927.

[58]. Arita, S., et al., *Angewandte Chemie-International Edition*, **2008**. *47*(13): p. 2447-2449.

[59]. Heiden, Z.M. and T.B. Rauchfuss, *Journal of the American Chemical Society*, **2007**. *129*(46): p. 14303-14310.

[60]. White, C., A.J. Oliver, and P.M. Maitlis, *Journal of the Chemical Society-Dalton Transactions*, **1973**(18): p. 1901-1907.

CHAPTER 2

2.1 Introduction

The use of aqueous/organic biphasic systems has many potential advantages such as the simple and complete separation of the product from the catalyst. It also alleviates the environmental problems associated with the use of organic solvents. For aerobic oxidation reactions, the use of aqueous solvents is also safer than organic solvents under pure oxygen conditions. In the last decade, water-soluble iridium complexes have been applied in many fields, such as the selective hydrogenation of C=O bonds,[1] the acceptorless dehydrogenation of alkanes,[2] transfer hydrogenations of carbonyl substrates,[3] and Markovnikov and Anti-Markovnikov hydration of phenylacetylene.[4] However, the iridium catalyzed aerobic oxidation reactions of alcohol in aqueous solution have not been studied intensively. Here, a series of water-soluble iridium complexes have been synthesized by straightforward procedures and their catalytic reactivities in aerobic oxidations of primary and secondary alcohols have been investigated.

Recently, the aerobic oxidations of primary and secondary alcohols catalyzed by homogenous Ir(III) complexes in organic solvent have been investigated by our group.[5] We became interested in applying these reactions in aqueous solutions. Thus, a series of water-soluble iridium (III) catalysts bearing Cp*(1,2,3,4,5-pentamethylcyclopentadiene) as an efficient ancillary ligand have been synthesized and characterized. $[Cp^*Ir(H_2O)_3]^{2+}$ (**1**, **2**) is a catalyst precursor in transfer hydrogenation of water-soluble carbonyl compounds in water.[6] $Cp^*Ir(H_2O)(CF_3COO)_2$ (**3**) was reported by White and Maitlis in 1971 as a reagent in the

preparation of Ir-arene complexes, however, its crystal structure and elemental analysis have not been reported yet.[7] Here, we report the full characterization of this complex. Cp*Ir(η^2-NO_3)(η^1-NO_3) (**4**) was synthesized by Ogo and coworkers in 2007.[8] One of the nitrate ligands is monodentate and the other one is bidentate. $[Cp^*Ir^{III}(H_2O)_3]^{2+}$ is reversibly deprotonated, producing the hydroxo complex $[(Cp^*Ir^{III})_2(\mu\text{-}OH)_3]^+$ (**5**) around pH 2.8.[9]

2.2 Results and Discussion

Synthesis and characterization of 3. Reaction of $[(Cp^*IrCl)_2(\mu\text{-}Cl)_2]$ with 4 equivalents of $Ag(CF_3COO)$ in wet methylene chloride results in the formation of a yellow solid $Cp^*Ir(H_2O)(CF_3COO)_2$, **3**. (Scheme 1) Complex **3** is soluble in water and polar solvents such as CH_3OH and CH_2Cl_2, but insoluble in non-polar solvents such as Et_2O and hexanes. Complex **3** is stable in both solution and solid-state. The IR spectrum (KBr) of complex **3** has several absorption bands at 1685, 1437, 1209, 1134 cm^{-1}.

Scheme 2.1 Synthesis of $Cp^*Ir(H_2O)(CF_3COO)_2$

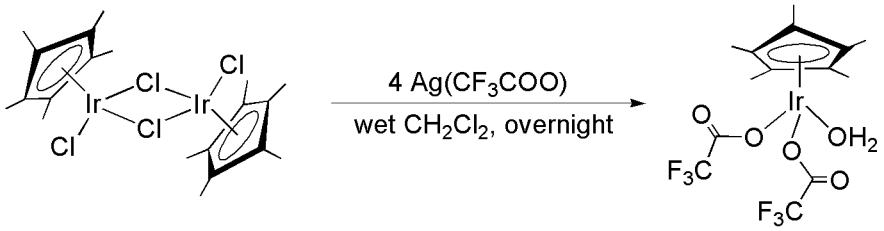

X-ray crystal structure of 3. Crystals suitable for X-ray diffraction were obtained by slow diffusion of pentane into a concentrated CH_2Cl_2 solution at room temperature. The unit cell consisted of two chemically equivalent but crystallographically independent molecules.

The Ir-O5 bond (2.1533(19) Å) indicates that the water molecule is bonded to the iridium center through inner-sphere coordination.

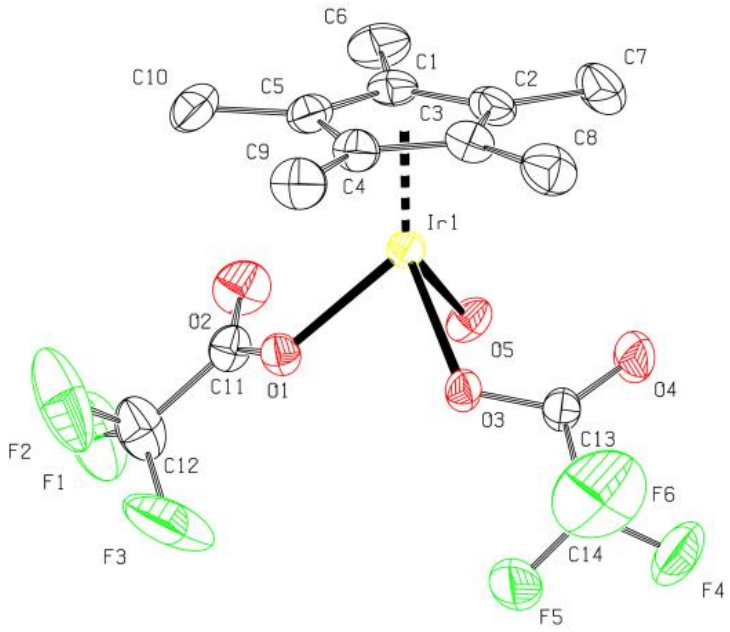

Figure 2.1 The X-ray crystal structure of **3**. Hydrogen atoms have been omitted for clarity. Selected bond lengths (Å) and angles (^{0}). Ir1-O1 2.1124(18), Ir1-O3 2.1172(18), Ir1-O5 2.1533(19), Ir1-C1 2.126(3), O1-C11 1.268(3), O2-C11 1.215(3), O3-C13 1.265(3), O4-C13 1.212(3), C11-O1-Ir1 120.69(17), C13-O3-Ir1 120.29(17), O1-Ir1-O5 81.49(7), C1-Ir1-O5 101.91(9).

Synthesis and characterization of 6. The reaction of $[(Cp^*IrCl)_2(\mu\text{-}Cl)_2]$ with 2 equivalents of $Ag(CF_3COO)$ in methylene chloride results in the formation of an orange solid $[Cp^*IrCl(CF_3COO)]_2$, that is soluble in water and polar solvents such as CH_2Cl_2 but insoluble in non-polar solvents such as Et_2O, and hexanes. Complex **6** is stable in both solution and solid-state. ^{1}H NMR resonance at 1.46 is assigned to the Cp* ligand. In

addition, several absorption bands were observed in the IR spectrum (KBr) in the region (1685, 1457, 1208, 1137 cm^{-1}), indicative of covalently bound trifluoroacetate ligands.

Scheme 2.2 $[Cp^*IrCl(CF_3COO)]_2$

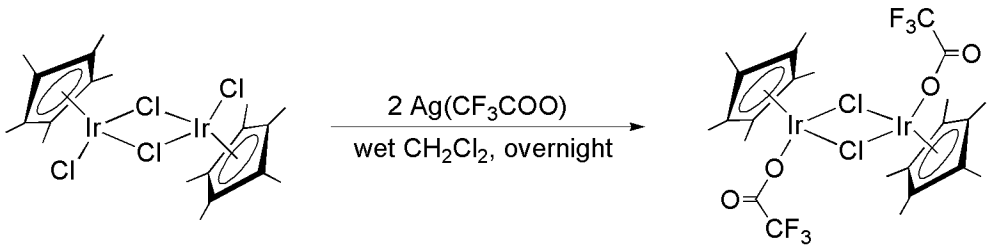

X-ray crystal structure of 6. Crystals suitable for X-ray diffraction were obtained by slow diffusion of pentane into a concentrated CH_2Cl_2 solution at room temperature. The unit cell consisted of two chemically equivalent but crystallographically independent molecules. The Ir-O bond (2.1075(14) Å) is comparable to known $Cp^*Ir(H_2O)(CF_3COO)_2$.

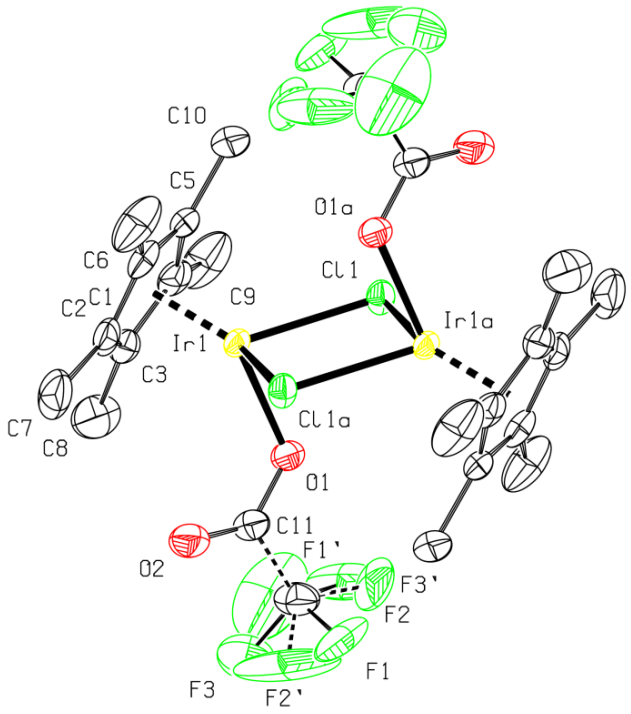

Figure 2.2 The X-ray crystal structure of **6**. Hydrogen atoms have been omitted for clarity. Selected bond lengths (Å) and angles (^{0}). Ir1-O1 2.1075(14), Ir1-Cl1 2.4415(5), C11-O2 1.217(3), O1-Ir1-Cl1 82.34(4), O1-Ir1-C1 157.24(8), O2-C11-O1 130.3(2).

Synthesis and characterization of 7. The complex $[Cp^*Ir(NCMe)_3](OTf)_2$, 7, was prepared by stirring $[(Cp^*IrCl)_2(\mu\text{-}Cl)_2]$ with two equivalent of AgOTf in acetonitrile overnight at room temperature. The solution was filter through celite after completion and the crystal was obtained by slow diffusion of pentane into a concentrated CH_2Cl_2 solution at room temperature. Complex **7** is soluble in polar solvent as acetonitrile, methanol and methylene chloride et. al. The complex is stable indefinitely, both in solution and solid state.

Scheme 2.3 The synthesis of $[Cp^*Ir(NCMe)_3](OTf)_2$

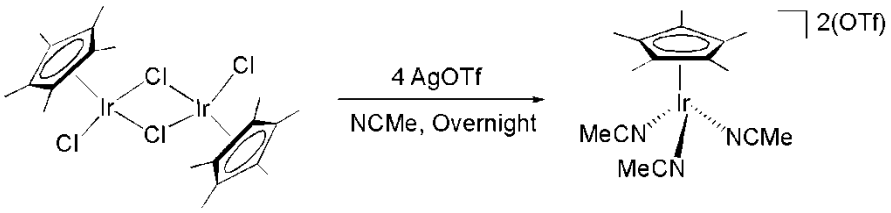

X-ray crystal structure of 7. Crystals suitable for X-ray diffraction were obtained by slow diffusion of pentane into a concentrated CH_2Cl_2 solution at room temperature. The unit cell consisted of two chemically equivalent but crystallographically independent molecules.

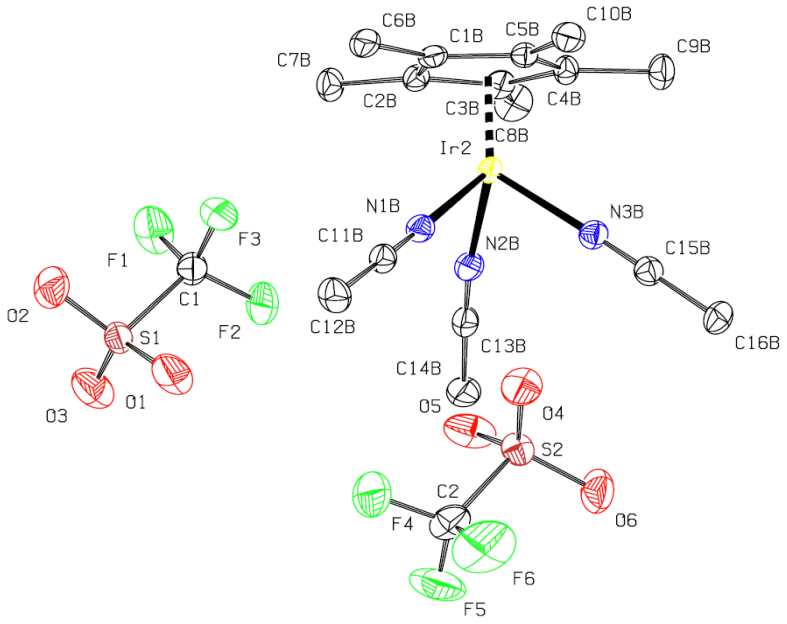

Figure 2.3 The X-ray crystal structure of **7**. Thermal ellipsoid plot of the cation $[(Cp^*Ir)_2Cl_3]BF_4$. Thermal ellipsoids are 50%. Hydrogen atoms have been omitted for clarity. Selected bond length (Å) and angles (^{0}). Ir1-N1A 2.066(2), Ir1-N2A 2.078(2), Ir1-N3A 2.072(2), Ir1-C1A 2.176(2), N1A-C11A 1.136(3), N2A-C13A 1.133(3), N3A-C15A 1.125(4) C11A-C12A 1.438(4), C13A-C14A 1.453(4), C15A-C16A 1.459(4), C11A-N1A-Ir1

178.2(2), C13A-N2A-Ir1 170.5(2), C15A-N3A-Ir1 174.0(3), N1A-C11A-C12A 178.8(3), N2A-C13A-C14A 178.4(3), N3A-C15A-C16A 179.2(4).

Syntheses and characterization of 8. The complex $[(Cp^*Ir)_2(\mu\text{-}Cl)_3](BF_4)$, **8**, was prepared by stirring $[(Cp^*IrCl)_2(\mu\text{-}Cl)_2]$ with one equivalent of $AgBF_4$ in methylene chloride overnight at room temperature. Complex **8** was obtained as a yellow solid, which is soluble in polar solvents such as H_2O, CH_3OH and CH_2Cl_2, but is insoluble in non-polar solvents such as hexanes and Et_2O. The complex is stable in solution and solid state.

Scheme 2.4 The synthesis of $[(Cp^*Ir)_2(\mu\text{-}Cl)_3](BF_4)$

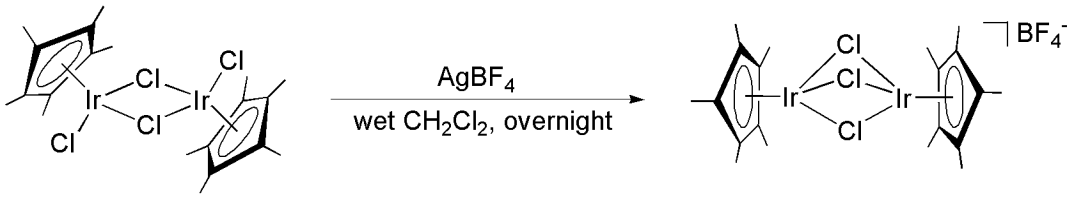

X-ray crystal structure of 8. Crystals suitable for X-ray diffraction were obtained by slow diffusion of pentane into a concentrated CH_2Cl_2 solution at room temperature. The unit cell consisted of two chemically equivalent but crystallographically independent Ir dications, BF_4 anions, and two water molecules. The structure of the cation is comparable to known $[(Cp^*Ir)_2(\mu\text{-}OH)_3](OAc)$ complex.

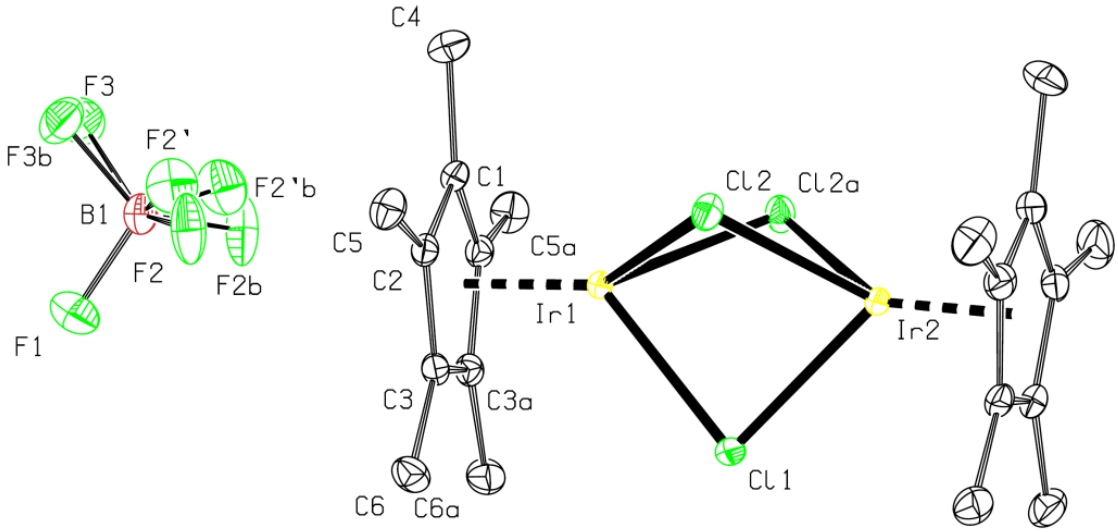

Figure 2.4 The X-ray crystal structure of **8**. Thermal ellipsoid plot of the cation $[(Cp^*Ir)_2Cl_3]BF_4$. Thermal ellipsoids are 50%. Hydrogen atoms have been omitted for clarity. Selected bond length (Å) and angles (^{0}). Ir1-Cl1 2.4655(5), Ir1-C1 2.1344(19), B1-F1 1.379(3), Cl1-Ir1-Cl2 79.678(12), C1-Ir1-Cl1 165.00(6), F1-B1-F2 104.2(2).

Syntheses and characterization of 9. $[Cp^*Ir(DMSO)][SO_4]$, **9**, was prepared by stirring $[Cp^*Ir(H_2O)_3]SO_4$ with one equivalent of DMSO in methylene chloride overnight at room temperature. Complex **9** was isolated as an orange solid which is soluble in polar solvents and insoluble in non-polar solvents. The complex is stable, both in solution and solid state.

Scheme 2.5 The synthesis of complex **9**

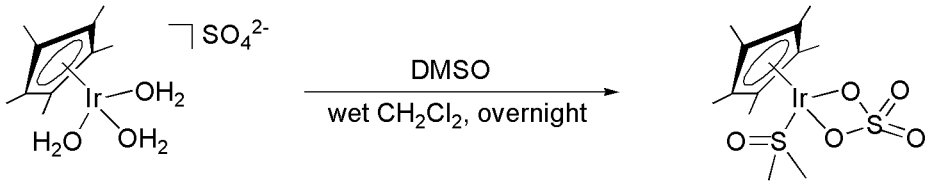

X-ray crystal structure of 9. Crystals suitable for X-ray diffraction were obtained by slow diffusion of pentane into a concentrated CH_2Cl_2 solution at room temperature. The unit cell consisted of two chemically equivalent but crystallographically independent molecules. The Ir-O bond lengths are 2.1421(9) Å and 2.1232(9) Å which are comparable to the bond lengths of other reported Ir-SO_4 complexes.[10] The bond length of Ir-S2 2.3037(3) Å, S2-O5 1.4752(10) Å, S2-C11 1.7764(13) Å indicate the coordination of SO_4 to the metal center through S-Ir bond.

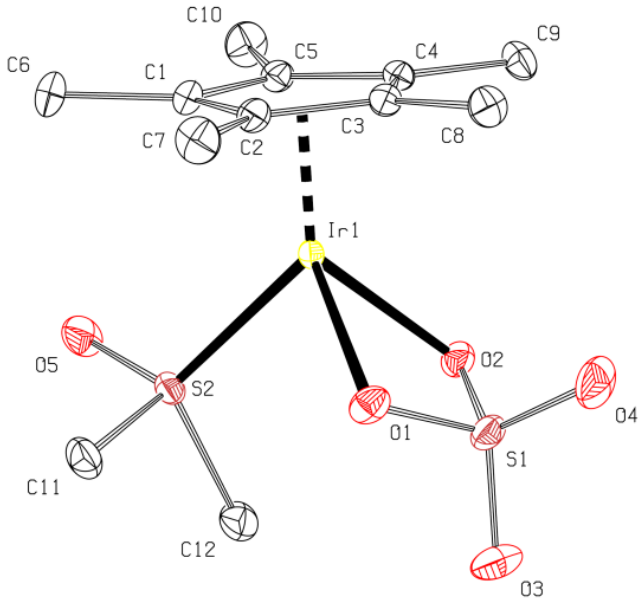

Figure 2.5 The X-ray crystal structure of **9**. Ellipsoids are at the 50% probability level and hydrogen atoms were omitted for clarity. Selected bond length (Å) and angles (^{0}). Ir1-O1 2.1421(9), Ir1-O2 2.1232(9), Ir1-S1 2.7492(3), Ir1-S2 2.3037(3), S1-O1 1.5376(10), S1-O3 1.4404(11), S2-O5 1.4752(10), S2-C11 1.7764(13), O5-S2-C11 108.68(6), C11-S2-C12 100.05(7), O2-Ir1-S2 89.56(3), O2-Ir1-O1 66.34(4), O2-S1-O1 98.98(5), O4-S1-O3 114.29(7), O3-S1-O1 110.45(6), O1-Ir1-S2 86.82(3).

Aerobic Oxidation. The reactivities of these complexes have been examined in the aerobic oxidation of benzyl alcohol and cyclopentanol in aqueous solution under ambient oxygen (Table 1). Complex **2**-**8** exhibited low reactivities in the aerobic oxidation reactions of benzyl alcohol; however, complex **1** and **9** had higher yield for this reaction. Complex **3**, **4**, **5**, and **8** had higher turn-over-numbers for the aerobic oxidation reactions of cyclopentanol. This difference in reactivity can be attributed to the different solubility of benzyl alcohol and cyclopentanol. Although the different solubilities of benzyl alcohol and benzyl aldehyde made the separation easy, it also reduced the yield.

Table 2.1 Aerobic oxidations of benzyl alcohol and cyclopentanol in water.

Entry	Catalyst	Benzyl alcohol[a]		Cyclopentanol[a]	
		Yield	TON	Yield	TON
1	$[Cp^*Ir(H_2O)_3]SO_4$	52.0%	10.4(2)		
2	$[Cp^*Ir(H_2O)_3](OTf)_2$	12.3%	3.0(5)		
3	$Cp^*Ir(H_2O)(CF_3COO)_2$	7.4%	1.5(5)	33.3%	6.6
4	$[Cp^*IrCl(CF_3COO)]_2$	6.5%	1.3(6)	40.0%	8.0
5	$[(Cp^*Ir)_2(\mu\text{–}Cl)_3]BF_4$	6.5%	1.3(5)	68.0%	13.6
6	$Cp^*Ir(DMSO)(SO_4)$	4.8%	1.0(4)		
7	$[Cp^*Ir(MeCN)_3](OTf)_2$	12.1%	3.0(5)		
8	$[(Cp^*Ir)_2(\mu\text{–}OH)_3]OAc$	6.6%	1.3(2)	84.6%	12.9
9	$Cp^*Ir(\eta_1\text{–}NO_3)(\eta_2\text{–}NO_3)$	56.0%	11.2(4)		

[a] 5% catalyst, 20% Et_3N, 0.25 M NaOAc, in water reflux 24 hours.

pH-Dependent Aerobic Oxidation. The pH-dependence of complex **1** in the hydrogenation of water-soluble carbonyl compounds has been studied by Watanabe and coworkers.[9] The pH-dependence of complexes **5** and **8** in the aerobic oxidation of

cyclopentanol in NaOH solution was investigated. The turn-over-number of this reaction has a pH-dependence which shows a maximum at pH 13 for both complex **5** and **8**. (Figure 2.5)

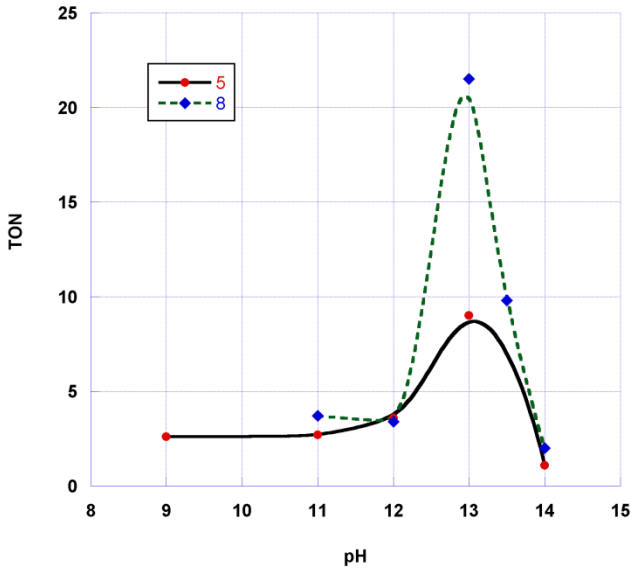

Figure 2.6 Typical pH-dependent profile of the aerobic oxidation of cyclopentanol.

The acetate peak of complex **8** shifted up-field in the ^{1}H NMR spectrum as pH value was varied from 9 to 14. When pH was 14, Cp* peak was no longer present, which might due to the decomposition of the complex.

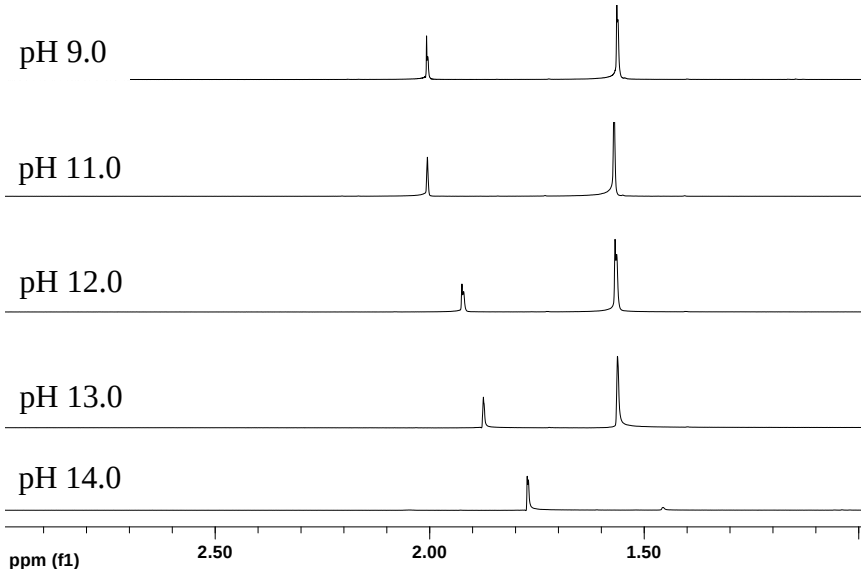

Figure 2.7 pH-Dependent ^{1}H NMR spectra of **5** in D_2O solution.

Ir-hydride. The formation of an Ir-hydride was observed after heating a solution of **8**, cyclopentanol, Et_3N and NaOAc, the color of the solution changes from light yellow to intense red. A singlet at -12.20 ppm was observed in the ^{1}H-NMR spectrum and the integration of the hydride relative to the Cp* resonance was about 1:30.(Figure 2.7)

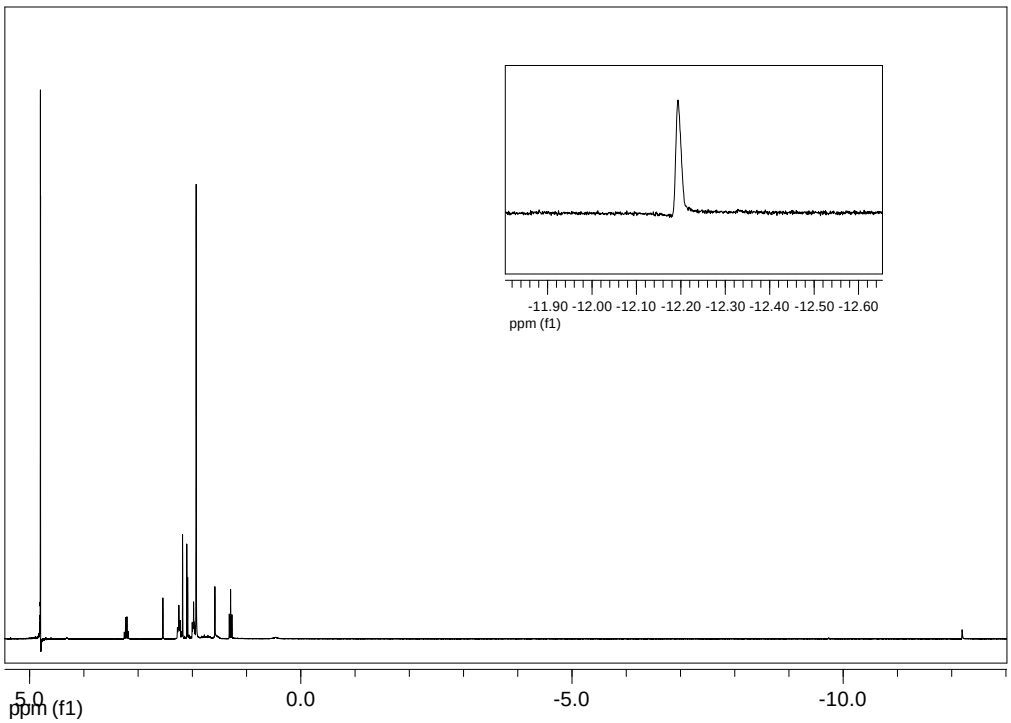

Figure 2.8 ^{1}H NMR spectrum of Ir-H intermediate.

Mechanism for the Aerobic Oxidation. We propose a mechanism for the aerobic oxidation as follows (Scheme 4). The substrate binds to a metal center of the dinuclear catalyst, producing one equivalent of hydrochloride and intermediate (**A**), which undergoes β -hydride elimination resulting in formation of the product and Ir-H intermediate (**B**). Then, (**B**) reacts with O_2 to generate the hydro-peroxide complex (**C**), which reacts with HCl to regenerate the catalyst **8**. At the same time, an equivalent of H_2O_2 is produced, which rapidly disproportionats into O_2 and H_2O.

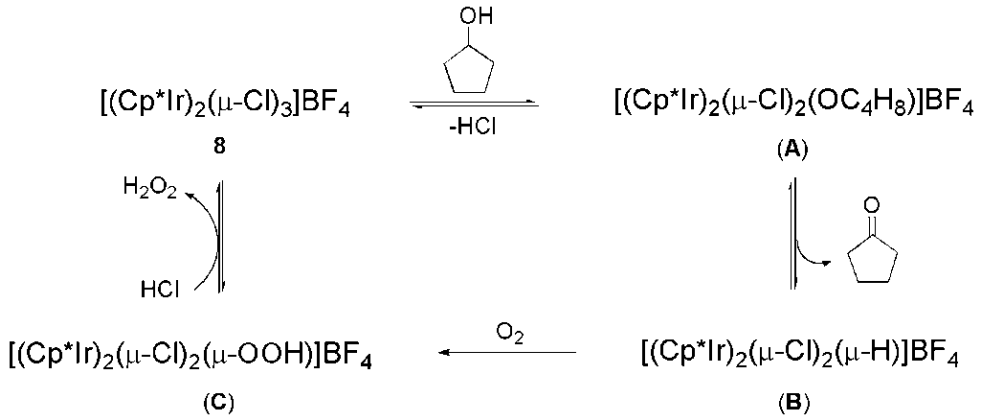

Scheme 2.6 Proposed mechanism of the aerobic oxidation of cyclopentanol

2.3 Conclusion

We have synthesized a series of water-soluble iridium (III) complexes bearing Cp*(1, 2, 3, 4, 5-pentamethylcyclopentadiene) as an efficient ancillary ligand. They are effective catalysts for the aerobic oxidation of primary and secondary alcohols in aqueous solution. The turn over number shows a sharp maximum at pH 13. An Ir-H intermediate was generated during the reaction. Studies of the reaction between Ir-H and O_2 are currently underway.

2.4 Experimental Section

Reagents and instrumentation. $[Cp^*Ir(H_2O)_3]SO_4$, $[Cp^*Ir(H_2O)_3](OTf)_2$, $Cp^*Ir(\eta^2\text{-}NO_3)(\eta^1\text{-}NO_3)$ (Cp^* = η^5-pentametylcyclopentadienyl) were prepared as previously reported. Other reagents were purchased from commercial sources and used as received. Solvents were degassed and purified with a solvent purification system (Mbraun Inc.) prior to use. ^1H and ^{13}C NMR spectra were recorded on a Varian Mercury 300 MHz or a Varian Mercury 400 MHz spectrometer. All ^1H and ^{13}C NMR spectra were referenced against tetramethylsilane

or using resonances due to the residual protons in the deuterated solvents or the ^{13}C resonances of the deuterated solvents. Elemental analyses were performed by Atlantic Microlabs, Inc. X-ray crystallography was performed at the X-ray Structural Facility of North Carolina State University.

$[Cp^*Ir(H_2O)_3]SO_4$ (1) was synthesized by $[(Cp^*Ir^{III}Cl)_2(\mu\text{-}Cl)_2]$ (200mg, 0.25mmol) and Ag_2SO_4 (156mg, 0.50mmol) in DI water (5 ml) under nitrogen atmosphere for 12 hours, and the precipitating AgCl was removed by filtration. The solvent was evaporated in vacuo and pure yellow product was achieved (205mg, 86% yield). ^1H NMR (DMSO-d_6): δ 1.68 (s; Cp*), 3.31(br; H_2O). ^{13}C NMR (D_2O): δ 11.09 (s; η^5–$C_5(CH_3)_5$), 86.94 (s; η^5-$C_5(CH_3)_5$).[6]

$[Cp^*Ir(H_2O)_3](OTf)_2$ (2) was synthesized by $[(Cp^*Ir^{III}Cl)_2(\mu\text{-}Cl)_2]$ (200mg, 0.25 mmol) and Ag(OTf) (257mg, 1.0 mmol) in DI water (5 ml). The solution was stirred for 12 hours under nitrogen atmosphere at room temperature, and AgCl was removed by filtration. The solvent was evaporated and dried under vacuum to yield the product (298mg, 87% yield). ^1H NMR (DMSO-d_6): δ 1.68 (s; Cp*), 3.31(br; H_2O). ^{13}C NMR (D_2O): δ 11.09 (s; η^5-$C_5(CH_3)_5$), 86.94 (s; η^5-$C_5(CH_3)_5$).[6]

$Cp^*Ir(H_2O)(CF_3COO)_2$ (3) A 50 ml round bottom flask was charged with $[(Cp^*Ir^{III}Cl)_2(\mu\text{-}Cl)_2]$ (79.7 mg, 0.1 mmol), $Ag(CF_3COO)$ (88.4 mg, 0.4 mmol) and CH_2Cl_2 (10 ml). The mixture was allowed to stir overnight at room temperature. The resulting mixture was filtered

through a pad of Celite, and the solvent was reduced in vacuo. Hexane was added to form 95mg product (83% yield). ^{1}H NMR (CD_2Cl_2): δ 1.52 (s, Cp*), 6.58 (s, H_2O). ^{13}C NMR (CD_2Cl_2): δ166.1 (s, O*C*OCF$_3$), 165.8 (s, O*C*OCF$_3$), 83.9 (s, *C*$_5$Me$_5$), 8.7 (s, C$_5$*Me*$_5$). Crystals was obtained by slow diffusion of pentane into a concentrated CH_2Cl_2 solution at room temperature. Anal. Calcd for $C_{14}H_{17}IrF_6O_5$: C, 29.42; H, 3.00. Found: C, 29.57; H, 2.90.

Cp*Ir(η^2-NO$_3$)(η^1-NO$_3$) (4) was prepared by reacting [(Cp*Ir^{III}Cl)$_2$(μ-Cl)$_2$] (200mg, 0.25mmol) and $AgNO_3$ (170mg, 1.0mmol) in acetone (5 ml) for 1 hour. The filtrate was separated, and the volume was reduced to half under vacuum. Addition of diethyl ether provided an orange microcrystalline material, which was isolated and dried under vacuum (173mg, 76% yield). ^{1}H NMR ($CDCl_3$): δ 1.69 (s, 15H, Cp*). ^{13}C NMR (CD_3Cl): δ 84.73 [s, C$_5$-(CH$_3$)$_5$, -C=C-], 9.79 [C$_5$(CH$_3$)$_5$, -CH$_3$].[8]

[(Cp*Ir)$_2$(OH)$_3$]OAc (5) A suspension of [(Cp*Ir^{III}Cl)$_2$(μ-Cl)$_2$] (200 mg, 0.25 mmol) and AgOAc (166 mg, 1.0 mmol) in wet toluene (10 ml) was refluxed under nitrogen with stirring for 12 hours. The mixture was cooled and filtered. The filtrate was evaporated to dryness under vacuo and the residue was extracted with diethyl ether. On removal of the ether an orange solid remained which was crystallized from ether-hexane to give 160mg (83% yield) of pure product. ^{1}H NMR (*d*$_6$-DMSO): δ1.59 (s, 15H, Cp*), 1.86 (s, 6H, CH_3COO). ^{13}C NMR (*d*$_6$-DMSO): δ 174.6 (s, CH$_3$*C*OO), 89.2 (s, *C*$_5$Me$_5$), 23.9 (s, *C*H$_3$COO), 9.1 (s, C$_5$*Me*$_5$). Crystals was obtained by slow diffusion of hexane into a concentrated diethyl ether solution at room temperature.

[Cp*IrCl(CF_3COO)]$_2$ (6) A 50 ml round bottom flask was charged with [(Cp*$Ir^{III}Cl)_2(\mu$-$Cl)_2$] (79.7 mg, 0.1 mmol), Ag(CF_3COO) (44.2 mg, 0.2 mmol) and CH_2Cl_2 (10 ml). The mixture was allowed to stir overnight at room temperature. The resulting mixture was filtered through a pad of Celite, and the solvent was reduced in vacuo. Hexane was added to form 87mg product (91% yield). ^{1}H NMR (CD_2Cl_2): δ 1.46 (s, Cp*). ^{13}C NMR (CD_2Cl_2): δ 161.6 (s, O*C*OCF_3), 86.5 (s, *C*$_5$Me$_5$), 9.5 (s, C$_5$*Me*$_5$). Crystals was obtained by slow diffusion of pentane into a concentrated CH_2Cl_2 solution at room temperature. Anal. Calcd for $C_{24}H_{30}F_6Cl_2IrO_4$: C, 30.28; H, 3.18. Found: C, 30.32; H, 3.11.

[Cp*Ir($NCMe)_3$]($OTf)_2$ (7) A 50 ml round bottom flask was charged with [(Cp*$Ir^{III}Cl)_2(\mu$-$Cl)_2$] (79.7 mg, 0.1 mmol), AgOTf (56.1 mg, 0.4 mmol) and CH_3CN (10 ml). The mixture was allowed to stir overnight at room temperature. The resulting mixture was filtered through a pad of Celite, and the solvent was reduced in vacuo. Hexane was added to form 106mg product (71% yield). ^{1}H NMR (CD_2Cl_2): δ 1.76 (s, Cp*), 2.66 (s, $NCCH_3$). Crystals was obtained by slow diffusion of pentane into a concentrated CH_2Cl_2 solution at room temperature.

[(Cp*IrCl)$_2$Cl]BF_4 (8) A 50 ml round bottom flask was charged with [(Cp*$Ir^{III}Cl)_2(\mu$-$Cl)_2$] (79.7 mg, 0.1 mmol), $AgBF_4$ (19.5 mg, 0.1 mmol) and CH_2Cl_2 (10 ml). The mixture was allowed to stir overnight at room temperature. The resulting mixture was filtered through a pad of Celite, and the solvent was reduced in vacuo. Hexane was added to form 80mg product (94% yield). ^{1}H NMR (CD_2Cl_2): δ 1.68 (s, Cp*). ^{13}C NMR (CD_2Cl_2): δ 88.7 (s,

C_5Me_5), 9.9 (s, $C_5\mathit{Me}_5$). Crystals was obtained by slow diffusion of pentane into a concentrated CH_2Cl_2 solution at room temperature. Anal. Calcd for $C_{14}H_{21}IrO_4$: C, 28.33; H, 3.57. Found: C, 28.49; H, 3.50.

Cp*Ir(DMSO)(SO_4) (9) A 100 ml round bottom flask was charged with Cp*Ir(H_2O)$_3$(SO_4) (0.61 g, 1.0 mmol), DMSO (0.071 ml, 1.0 mmol) and CH_2Cl_2 (20 ml). The mixture was allowed to stir overnight at room temperature. The resulting mixture was filtered through a pad of Celite, and the solvent was reduced in vacuo. Hexane was added to form 0.47g product (94% yield). ^{1}H NMR (CD_2Cl_2): δ 1.75 (s, Cp*), 3.09 (br, CH_3SOCH_3). Crystals was obtained by slow diffusion of pentane into a concentrated CH_2Cl_2 solution at room temperature. Anal. Calcd for $C_{12}H_{21}IrS_2O_5$: C, 28.73; H, 4.22. Found: C, 28.70; H, 4.22.

General procedure for aerobic oxidation experiments. In a typical reaction, a storage tube was charged with catalyst (0.1 mmol), 20 eq substrate (2.0 mmol), 4 eq Et_3N (0.4 mmol) and 0.25M NaOAc in 5 ml DI water solution. The storage tube was freeze-pump-thaw and refilled with O_2 three times. The reaction mixture was heated to 150^{o}C for 24 hours. Upon completion, the reaction was cooled to room temperature and the resulting solution was extracted by Et_2O (5 ml) and filtered through a silicon column. The resulting solution was then analyzed by GC-MS.

General procedure for pH-dependent aerobic oxidation experiments. In a typical reaction, a storage tube was charged with catalyst (0.1 mmol) and 20 eq substrate (2.0 mmol)

in NaOH solution. The pH value was measured by Oakton pH-meter 510 series. The pH-meter was calibrated by buffer solutions from Fisher. The storage tube was freeze-pump-thaw and refilled with O_2 three times. The reaction mixture was heated to 150^{o}C for 24 hours. Upon completion, the reaction was cooled to room temperature and the resulting solution was extracted by Et_2O (5 ml) and filtered through a silicon column. The resulting solution was then analyzed by GC-MS.

X-ray structure determination. The samples were mounted on a nylon loop with a small amount of Paratone N oil. All X-ray measurement was made on a Bruker-Nonius Kappa Axis X8 Apex2 diffractometer at a temperature of 110K. The structure was solved by direct methods using the SIR97 program. Most non-hydrogen atoms were obtained from the initial solution and the remaining atomic positions were obtained from a subsequent difference Fourier map. The hydrogen atoms were introduced at idealized positions and were allowed to ride on the parent atom. The structure model was fit to the data using full matrix least-squares based on F^2. The calculated structure factors included corrections for anomalous dispersion from the usual tabulation. The structure was refined using the XL program suite. Additional information and other relevant literature references can be found in the reference section of the Facility's web page (http://www.xray.ncsu.edu)

Table 2.2 Summary of crystal data, data collection parameters, and structure refinement for **3**, **6**, **8**, and **9**

	3	**6**	**8**	**9**
empirical formula	$C_{14}H_{17}F_6IrO_5$	$C_{24}H_{30}Cl_2F_6Ir_2O_4$	$C_{20}H_{36}BCl_3F_4Ir_2O_3$	$C_{12}H_{21}IrO_5S_2$
FW	571.48	951.78	902.05	501.61
crystal system	monoclinic	Monoclinic	monoclinic	monoclinic
space group	C 2/c	P 2_1/n	P 2_1/m	P 2_1/n
a, Å	21.9814(6)	8.8475(3)	8.6409(2)	9.7878(4)
b, Å	9.8448(3)	12.1879(3)	11.4698(3)	13.5315(4)
c, Å	18.2302(5)	13.7625(4)	14.5294(4)	12.0198(4)
V ($Å^3$)	3615.64(18)	1416.57(7)	1390.71(6)	1577.02(10)
Z	8	2	2	4
ρ (*g/cm*)	2.100	2.231	2.154	2.113
crystal size (mm)	0.26 × 0.15 × 0.08	0.12 × 0.10 × 0.09	0.24 × 0.17 × 0.12	0.22 × 0.20 × 0.15
R1	0.0314	0.0285	0.0236	0.0158
wR2 tic	0.0609	0.0532	0.0447	0.0304
GOF	1.026	1.016	1.088	1.030

$R_1 = \Sigma(|F_o| - |F_c|) / \Sigma F_o$. $wR_2 = [\Sigma(w(F_o^2 - F_c^2)^2) / \Sigma(w F_o^4)]^{½}$. GOF = [$\Sigma(w(F_o^2 - F_c^2)^2$) / (No. of reflns. - No. of params.)]^{½}

References

[1]. Fukuoka, Atsushi *Chem. Commun.* **1999**, 489.

[2]. Krogh-Jespersen *J. of Molecular Catalysis A: Chemical* **2002**, 189(1), 95

[3]. Seiji Ogo *J. Am. Chem. Soc.*, **2003**, 125 (14), 4149

[4]. Seiji Ogo *J. Am. Chem. Soc.*, **2004**, 126 (50), 16520

[5]. Elon Ison *J. Am. Chem. Soc.*, **2008**, *130* (44), 14462

[6]. Yoshihito Watanabe *Organometallics*, **1999**, 18(26), 5470

[7]. Peter M. Maitlis *J. Chem. Soc. A***, 1971**, 3322

[8]. Seiji Ogo *Chemistry Letters*, **2007**, 36(12), 1468

[9]. Yoshihito Watanabe *Organometallics*, **2001**, 20(23), 4903

[10]. Feng, Y.; Jiang, B.; Ison, E. A. *Organometallics* **2010**, 29(13), 2857.

CHAPTER 3

3.1 Introduction

Alkanes or saturated hydrocarbons are major constituents of petroleum and natural gas, which are the primary feedstocks of chemical industry. The constituent atoms of alkanes are held together by strong and localized C-C and C-H bonds, so that the molecules have no empty orbital of low energy or filled orbitals of high energy that could readily participate in a chemical reaction.[1] Therefore, there are few practical processes for converting them directly to more valuable chemicals. One challenge of C-H activation is the slow rate of reaction, as only adequate rate of the reaction will be practical and useful. Another challenge is selectivity. The selectivity of C-H activation is hard to control because of two reasons. First, the desired product cannot have a functional group that reacts more readily with the metal center than the alkane starting material. The second reason arises from the relative reactivity of different C-H bonds in the same molecule. Although C-H activation has a lot of challenges, the potential of metal-mediated C-H activation will allow us to use Earth's alkane resources more efficiently and cleanly. In the past few decades, C-H bond activation at transition-metal centers has been studied intensively in both academia and industry. In a review paper by Bercaw et al., metal-mediated C-H activation could be classified into five categories: oxidative addition, σ-bond metathesis, metalloradical activation, electrophilic activation and 1, 2-addition. [1]

3.1.1 Oxidative addition

Anionic ligands, A and B of an A-B molecule, are added to complex M and form M(A)(B) complex. The A-B bond is broken and an M-A and an M-B bond are formed during the

reaction. Since A and B are X-type ligands, the oxidation state, electron count, and coordination site number of complex M all increase by two units. Oxidative additions proceed by several mechanisms, like concerted additions, S_N2 reactions, radical mechanisms and ionic mechanisms. However, the fact that the electron count increases by two means that a vacant 2e site is always required on the metal. [2] An one example of oxidative addition achieved by C-H activation is shown in Figure 3.1. Bergman and coworkers found that under irradiation, $Cp^*Ir(H)_2(PPh)_3$ released one equivalent of H_2 and activated the hydrocarbon solvent. [3] A 16-e precursor was generated in situ by photochemical decomposition of $Cp^*Ir(H)_2(PPh)_3$, however, this unsaturated complex is not observed due to rapid reaction with the solvent.

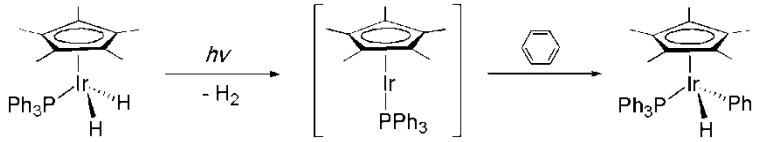

Figure 3.1 Oxidative addition of benzene to $Cp^*Ir(H)_2(PPh)_3$ under irradiation.

Oxidative addition reactions are typical for electron-rich, low-valent complexes. C-H bond activation proceeds by the C-H bond electrons overlapping with an unfilled metal orbital, and the metal back-bonding to C-H σ* anti-bonding orbital through its dπ orbital. (Figure 3.2)

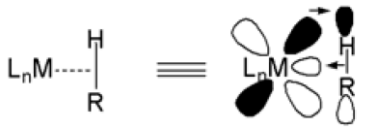

Figure 3.2 Interaction between the metal center and the hydrocarbons.

3.1.2 σ-bond metathesis

σ-bond metathesis can be achieved by an oxidative addition followed by reductively elimination. Early transition metals with d^0 electronic configuration, lanthanides and actinides most commonly undergo σ-bond metathesis reaction.

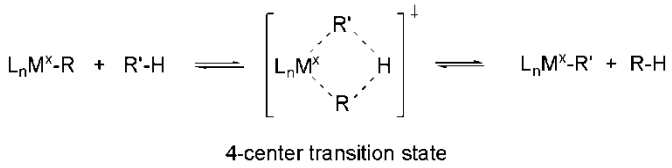

Figure 3.3 Mechanism of σ-bond metathesis

One example of σ-bond metathesis in C-H activation is from the work of Hartwig and coworkers in 2010. Transition-metal-boryl compounds have been reported that selectively functionalize primary C-H bonds in alkanes in high yield. This process was investigated with one of the well-defined systems that reacted under photochemical conditions. Both density functional theory calculations and pico- through microsecond time-resolved IR spectroscopy have been used in the study. The spectroscopic data imply that the resulting complex, *cis*-$Cp^*W(CO)_2(Bpin)(pentane)$, (pin = 1,2-$O_2C_2$-$(CH_3)_4$) undergoes C-H bond activation by a *σ*-bond metathesis mechanisms in 16 μs, the terminal hydrogen on pentane appears to migrate to the Bpin ligand to form a *σ*-borane complex, $Cp^*W(CO)_2(H\text{-}Bpin)(C_5H_{11})$. [4] (Figure 3.4)

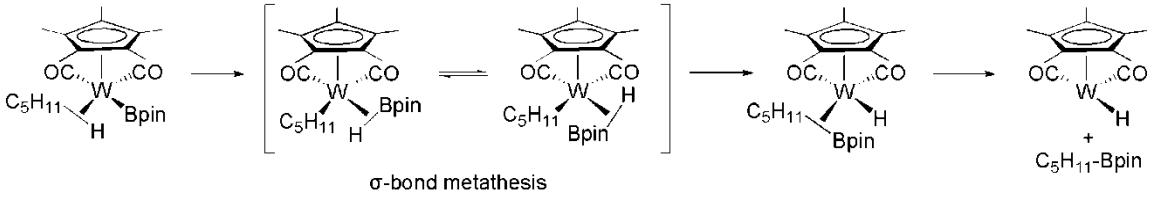

Figure 3.4 The *σ*-bond metathesis mechanism for the C-H activation of C_5H_{12}.

3.1.3 Metalloradical activation

Another important C-H activation mechanism is the unique porphyrin-based metal radical system. (Tetramesitylporphyrinato)rhodium(II) dimer was observed to react with methane and formed Rh-CH_3 and Rh-H by a metalloradical mechanism by Wayland and coworkers in 1990. [5] Rate laws, activation parameters, and deuterium isotope effects suggest that a four-centered liner transition state (Rh-CH_3-H-Rh) provides a relatively low activation enthalpy route for methane reacting with two metalloradicals. [6] (Figure 3.5)

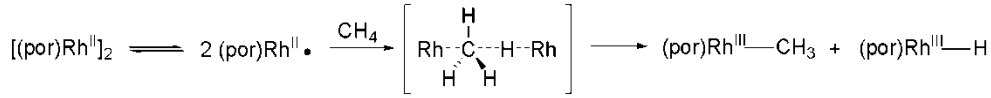

Figure 3.5 C-H activation of methane by metalloradical mechanism

The low Rh-H bond strength, 60 kcal mol^{-1} compared to the normal 105 kcal mol^{-1}, suggests that C-H bond activation of methane would be endothermic, in agreement the experimental observations.

3.1.4 1,2-additon

1,2-addition reactions involve the addition of an alkane to a metal-nonmetal double bond, like M = N or M = C double bonds. Wolczanski and coworkers found that (*t*-$Bu_3SiNH)_2Zr$=NSi-*t*-Bu_3 could activate the C-H bond of methane and benzene under mild conditions. [7] (Figure 3.6)

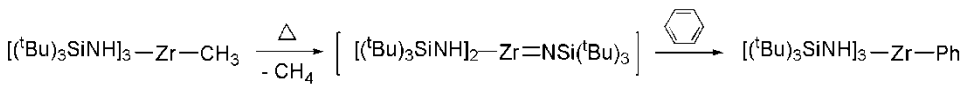

Figure 3.6 C-H activation of benzene through 1,2-addition pathway

Bergman's group successfully generated imidozirconocene complexes, which readily activated the C-H bond of benzene. [8] (Figure 3.7)

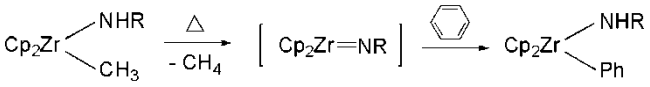

Figure 3.7 C-H activation by imidozirconocene complex

Similar to the σ-bond metathesis pathway, the activation of C-H bond by metal imido species is believed to occur through a four-centered transition state, but the C-H bond adds across the metal-nitrogen double bond to generate an alkyl amido metal center. (Figure 3.8)

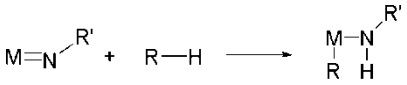

Figure 3.8 The 1,2-addition mechanism

3.1.5 Electrophilic activation

Rather than forming organometallic species, reactions that lead directly to functionalized alkanes have been classified as electrophilic activation reactions. C-H activation reactions through electrophilic activation pathway usually involve late transition metals, like Pd^{2+}, Pt^{2+}, Pt^{4+}, Hg^{2+}, Tl^{3+} and a strongly polar medium such as water or an anhydrous strong acid. [1] The electrophilic metal center coordinates the hydrocarbon, generating a proton and an ionic ligand at the same time. The resulting intermediate leads to a functional organic product by various pathways, like reductive elimination. (Figure 3.9)

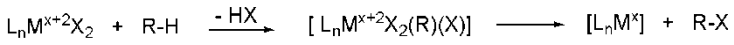

Figure 3.9 The electrophilic activation mechanism

One example of electrophilic activation is Shilov system, which was first investigated by Shilov and coworkers in 1969. [9] This system illustrates the C-H activation of alkanes with chloroplatinum salts in aqueous solution and a mechanism was proposed. [10] (Figure 3.10)

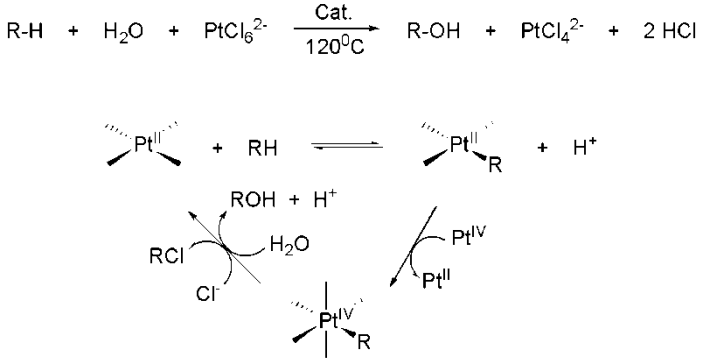

Figure 3.10 The Shilov system of C-H activation of alkane

There are three steps in the Shilov system. First, an alkylplatinum(II) intermediate is generated by electrophilic substitution of the alkane. Second, oxidation of the alkylplatinum(II) intermediate by a Pt(IV) oxidant occurs to produce an alkylplatinum(IV) species. The final step is a reductive elimination of ROH and regeneration of the Pt(II) catalysts.

3.2 Results and Discussion

Water-soluble iridium complexes bearing the Cp* (1,2,3,4,5-pentamethylcyclopentadiene) ligand which catalyze the aerobic oxidation reactions were discussed in Chapter 2. However, the utilization of those complexes in catalytic H/D exchange reactions has not been thoroughly studied. Iridium complexes that contain the Cp*Ir(phosphine) fragment have been shown to efficiently catalyze H/D exchange between various organic substrates and

deuterium sources.[11-15] Recently, a series of Cp*Ir(NHC) complexes $[Cp^*Ir(NHC)(L)_2][OTf]_2$ (NHC=1,3,4,5-tetramethylimidazol-2-ylidene; X=Cl^-, NO^{3-}, -$OC(O)CF_3$(=TFA), n=2; X=SO_4^{2-}, n=1; L=H_2O, CH_3CN; OTf=trifluoromethanesulfonato) have been synthesized and utilized for catalytic H/D exchange reactions between benzene and various deuterium sources by our group. [16] The reactivity of these complexes in catalytic H/D exchange reactions was assessed by GC/MS using a quantitative assay reported by Sanford et al. [17]

3.2.1 H/D exchange

A standard assay for Pt-catalyzed H/D exchange between C_6H_6 and various deuterium sources was recently reported.[17] We employed this assay under the same reaction conditions for catalytic H/D exchange reactions between C_6H_6 and various deuterium sources using the Cp*Ir complexes $[Cp^*Ir(H_2O)_3][SO_4]$, $[Cp^*Ir(H_2O)_3][OTf]_2$, $[Cp^*Ir(H_2O)_3][PF_6]_2$, $Cp^*Ir(DMSO)(SO_4)$, $(Cp^*Ir)_2(OH)_3$, $[Cp^*Ir(NCMe)_3][OTf]_2$, and $Cp^*Ir(\eta^1\text{-}NO_3)(\eta^2\text{-}NO_3)$. This method allowed us to rapidly compare the ability of these catalysts to perform C-H activation reactions by comparing turnover numbers (TONs) after a defined period of time (24 h). All the complexes examined catalyzed H/D exchange between C_6H_6, CD_3OD, CF_3COOD and CD_3OCD_3 (Table 3.1).

Table 3.1 Catalytic H/D exchange between C_6H_6 and various deuterium solvents catalyzed by various water-soluble Cp*Ir complexes (Numbers are reported as TON, and with 2mol% catalyst load, maximum TON = 300)

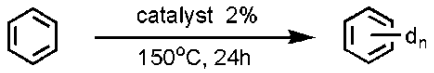

Entry	Catalysts	CD_3OD		CF_3COOD		CD_3OCD_3	
		TOF	TON	TOF	TON	TOF	TON
1	$Cp^*Ir(H_2O)_3(SO_4)$	4.6E-5	3(1)	3.1E-5	2(1)	5.2E-5	3(1)
2	$Cp^*Ir(H_2O)_3(OTf)_2$	2.3E-4	19(3)	9.4E-4	66(4)	7E-6	0.5(4)
3	$Cp^*Ir(H_2O)_3(PF_6)_2$	2.5E-4	16(2)	6.4E-5	4(1)	5.2E-5	3(1)
4	$Cp^*Ir(DMSO)SO_4$	4.0E-5	3(1)	7.7E-5	5(2)	5.2E-5	3(1)
5	$(Cp^*Ir)_2(OH)_3$	1.6E-4	12(2)	5.1E-5	3(1)	1.3E-4	8(2)
6	$Cp^*Ir(MeCN)_3(OTf)_2$	2.8E-5	2(1)	3.8E-5	3(1)	8E-6	0.5(3)
7	$Cp^*Ir(NO_3)_2$	2.9E-5	2(1)	4.6E-5	3(2)	2.6E-5	2(1)

The complex $[Cp^*Ir(H_2O)_3][OTf]_2$ exhibited better reactivity in CD_3OD and CF_3COOD. Compare to $Cp^*Ir(DMSO)(SO_4)$, $(Cp^*Ir)_2(OH)_3$, and $Cp^*Ir(NO_3)_2$, the ligands of $[Cp^*Ir(H_2O)_3][OTf]_2$ are easier to dissociate from the metal center, which might attribute to the higher turnover numbers. For complexes $Cp^*Ir(H_2O)_3(SO_4)$, $[Cp^*Ir(H_2O)_3][OTf]_2$, and $Cp^*Ir(H_2O)_3(PF_6)_2$, they all have the same cationic fragment $Cp^*Ir(H_2O)_3^{2+}$. The difference of the counteranion might attribute to the different reactivities. Our group have reported a series of Cp*Ir(NHC) complexes catalyzed H/D exchange reactions under the same conditions (table 3.2). Complexes 1-Cl, 1-OH_2, 1-SO_4, 1-NO_3, and 1-TFA exhibited modest reactivity toward catalytic H/D exchange reactions (TONs between 15 and 62); however, the complex 1-NCMe exhibited better reactivity under the same reaction conditions (TON157±33). This difference in reactivity can be attributed to the ability of the ancillary

ligand to dissociate from the metal center. Acetonitrile is more labile than Cl^-, OH_2, SO_4^{2-}, NO^{3-}, or TFA; thus, the NCMe ligand readily dissociates to form a 16-electron iridium metal fragment with an open coordination site. These results imply that the dissociation of a ligand to form an open coordination site is likely an important step prior to C-H bond activation for the catalytic H/D exchange reaction between benzene and CD_3OD.

Table 3.2 Catalytic H/D exchange between C_6H_6 and various deuterium solvents catalyzed by various Cp*Ir(NHC) complexes (Numbers are reported as TON, and with 2mol% catalyst load, maximum TON = 300)

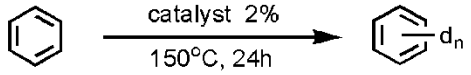

Entry	Catalysts	CD_3OD	CF_3COOD	CD_3OCD_3	D_2O
1	$Cp^*Ir(NHC)Cl_2$(1-Cl)	62(8)	8	0	0
2	$[Cp^*Ir(NHC)(NCMe)_2][OTf]_2$ (1-NCMe)	156(23)	7	0	2
3	$[Cp^*Ir(NHC)(OH_2)_2][OTf]_2$ (1-OH_2)	57(15)	8	0	3
4	$Cp^*Ir(NHC)(SO_4)$ (1-SO_4)	50(2)	1	0	3
5	$[(Cp^*Ir(NHC)Cl)_2][OTf]_2$ and $Cp^*Ir(NHC)(Cl)(OTf)$ (2)	100(20)	6	2	0

In general, Cp*Ir complexes contain NHC ligand show better reactivities than the Cp*Ir complexes without NHC ligand in the H/D exchange reactions of benzene with CD_3OD as deuterium source. NHC ligands are strong σ-donor ligands, which make the metal center less electrophilic, reducing the Lewis base inhibition. In order to understand the effect of NHC ligand on H/D exchange reactivity, the Cp*Ir aqua complex $[Cp^*Ir(H_2O)_3][OTf]_2$ was

compared with the complex $[Cp^*Ir(NHC)(OH_2)_2][OTf]_2$ (Table 3.3). For these reactions, two deuterium sources, CD_3OD and CF_3COOD, were utilized. For $[Cp^*Ir(NHC)(OH_2)_2][OTf]_2$, methanol-$d_4$ (TON = 57 ± 21) was the more effective deuterium source compared to CF_3COOD (TON = 8 ± 1). In contrast, for complex $[Cp^*Ir(H_2O)_3][OTf]_2$ higher TONs were observed in CF_3COOD (TON = 66 ± 4) than in CD_3OD (TON = 19 ± 3). These results are an illustration of the effect of the ancillary ligands on the mechanism of C-H activation. Since H/D exchange would require an open coordination site for benzene to bind to the metal center, the carbene ligand in $[Cp^*Ir(NHC)(OH_2)_2][OTf]_2$, being a strong σ-donor, would make the metal center less electrophilic and consequently labilize the aqua ligand. In contrast, the aqua ligand in $[Cp^*Ir(H_2O)_3][OTf]_2$ is a much poorer σ-donor and , as a result, the metal center in this environment is more electrophilic. Acidic conditions are therefore required for the dissociation of an aqua ligand to form an open coordination site.

Table 3.3 Reactiviy comparison between $[Cp^*Ir(NHC)(OH_2)_2][OTf]_2$, $[Cp^*Ir(H_2O)_3][OTf]_2$

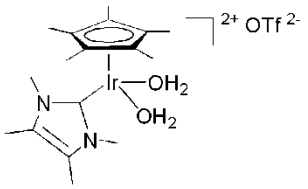

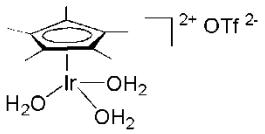

		TON	
entry	D source	1-OH_2	$[Cp^*Ir(H_2O)_3][OTf]_2$
1	CD_3OD	57(15)	19(3)
2	CF_3COOD	8(1)	66(4)

In order to find the best deuterium sources for the H/D exchange reaction of benzene, seven different deuterium sources have been studied (Table 3.4). 2 mol % of $Cp^*Ir(H_2O)_3(OTf)_2$, benzene and 20 equivalent of deuterium source, relative to benzene, were mixed and heated

in 150^0C oil bath for 24 hours. The reactions with CD_3OD and CF_3COOD as deuterium source had good TONs (entry 6-7), but the reactions with other deuterium sources did not show reactivity in H/D exchange with benzene (entry 1-5).

Table 3.4 H/D exchange reactions between benzene and different deuterium sources

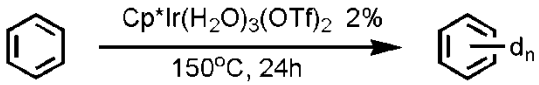

Entry	Deuterated Solvent	TOF	TON
1	CF_3CD_2OD	3.2E-5	2.1
2	CD_3CN	0	0
3	D_2O	0	0
4	cyclohexane-d_{12}	0	0
5	pyridine-d_{12}	0	0
6	CD_3OD	2.3E-4	19
7	CF_3COOD	9.4E-4	66

The H/D exchange between deuterium source and substrates other than benzene have also been studied (Table 3.5). 5 mol % of $[Cp^*Ir(H_2O)_3][OTf]_2$, D_2O/CD_3OD (1:1) and substrate were mixed and heated in a screw-cap NMR tube at 150^0C for 24 hours. The results were determined by ^{1}H NMR. The terminal methyl group of isopropanol had a conversion of 44.8% and the conversion of the methylene protons was 48.1% (entry 1). The conversions of diethyl ether were 61.8% for methyl group and 62.15 for the methylene group (entry 2). For THF, protons in the 1,4 positions had a conversion of 43.6% and protons in the 2,3 positions had relatively higher conversion, 58.9%. The acidic proton of benzoic acid was completely converted and the conversion for para, meta, ortho position were 39.9%, 45.7% and 90%.

Table 3.5 Catalytic H/D exchange catalyzed by $[Cp^*Ir(H_2O)_3][OTf]_2$

entry	substrates/selectivity	% D_{total}
1	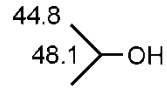	45.3
2	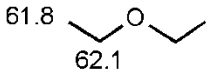	61.9
3	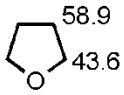	51.3
4	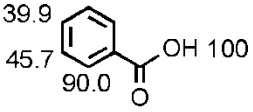	68.6

An iridium complex bearing both Cp* and N-heterocyclic carbene ligands was also tested for H/D exchange between different substrates and D_2O/CD_3OD (1:1). 5 mol % of $[Cp^*Ir(NHC)(H_2O)_2][OTf]_2$ and substrate were mixed in a screw-cap NMR tube and heated at 150^0C for 24 hours (Table 3.6). 93.8% of the protons of isopropanol were converted to deuterium (entry 1) and 69.5% of the protons of diethyl ether were converted (entry 2). However, 5.93% H/D exchange for THF was observed (entry 3) and protons on 3, 4 positions of THF did not have any H/D exchange. THF is not as flexible as iso-propanol and diethyl ether, the bond tension pushes the protons on 3,4 position far away from the metal center, which make the H/D exchange harder.

Table 3.6 Catalytic H/D exchange catalyzed by $[Cp^*Ir(NHC)(H_2O)_2][OTf]_2$

entry	substrates/selectivity	% D_{total}
1	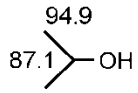	93.8
2	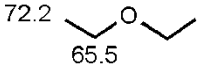	69.5
3	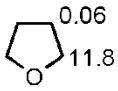	5.93

3.2.2 The reaction with H_2 and silane

Activation of dihydrogen by transition metals has been an active field in recent years, since these studies will provide sights into the hydrogenation and dehydrogenation catalysts. Before 1984, the binding of H_2 to a transition metal was regarded to proceed via oxidative addition to form transition metal di- or polyhydrides. [19] Kubas and coworkers demonstrated that in certain cases H_2 is capable of coordinating to a metal without breaking the H-H bond. [20] Bergman *et al.* reported an example of dihydrogen activation by $[Cp^*Ir(NPh)]_2$(Figure 3.11). [21]

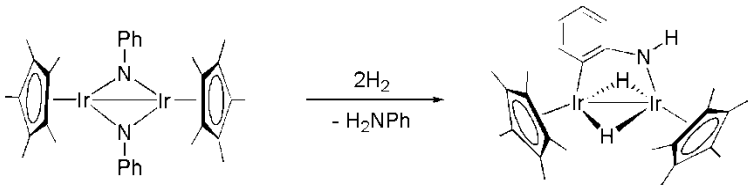

Figure 3.11 Activation of H_2 by $[Cp^*Ir(NPh)]_2$

An iridium hydride complex, $[(Cp^*IrCl)_2(\mu\text{-}H)(\mu\text{-}Cl)]$, was observed as an intermediate of the aerobic oxidation reactions catalyzed by $[Cp^*Ir(\mu\text{-}Cl)Cl]_2$. [19] This complex was independently synthesized by reacting with KBH_4 in iso-propanol. However, $[Cp^*Ir(\mu\text{-}Cl)Cl]_2$ did not react with H_2 in toluene at 80^0C. When mixed $Cp^*Ir(NHC)(SO_4)$ with H_2 in

methanol at 80^0C, an intensive red iridium complex, $[Cp^*Ir(NHC)(\mu\text{-}H)]_2$ was formed immediately. This complex was first synthesized by Dr. Yamaguchi and his group in 2005 by reacting $Cp^*Ir(NHC)Cl_2$ with $Cp^*Ir(NHC)H_2$. [18] The product was identified by ^{1}H NMR and ^{13}C NMR. ^{1}H NMR (CD_3OD): δ 3.68 (s, 12H, NMe), 2.39 (s, 12H, C=CMe), 1.45 (s, 30H, Cp*), -17.48 (s, 2H, μ-H). ^{13}C NMR (CD_3OD): δ 162.5 (s, Ir-C), 129.2 (s, C=C), 97.9 (s, C_5Me_5), 36.7 (s, NMe), 10.1 (s, C_5Me_5), 9.2 (s, C=C*Me*). The reaction of $Cp^*Ir(NHC)(SO_4)$ with diphenylmethylsilane also gave the same product under the same reaction conditions. (Figure 3.12)

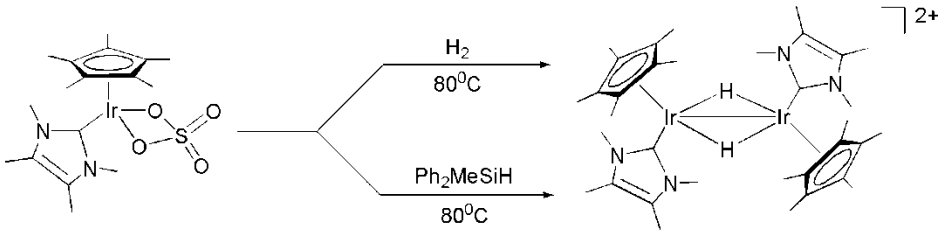

Figure 3.12 The reaction of $Cp^*Ir(NHC)(SO_4)$ with H_2 and silane

3.3 Conclusion

A series of water-soluble iridium complexes which contain the Cp* ligand were utilized in the H/D exchange reactions of benzene and different deuterium sources. The reactivities of those complexes were compared with former reported Cp*Ir(NHC) complexes. Except for benzene, the H/D exchange reactions of other substrates have also been studied. The activation of dihydrogen and silane by $Cp^*Ir(NHC)(SO_4)$ are under investigation.

3.4 Experimental section

Reagents and instrumentation. The preparations of $[Cp^*Ir(H_2O)_3][SO_4]$, $[Cp^*Ir(H_2O)_3][OTf]_2$, $[Cp^*Ir(H_2O)_3][PF_6]_2$, $Cp^*Ir(DMSO)(SO_4)$, $(Cp^*Ir)_2(OH)_3$, $[Cp^*Ir(NCMe)_3][OTf]_2$, and $Cp^*Ir(\eta^2\text{-}NO_3)$ $(\eta^1\text{-}NO_3)$ ($Cp^* = \eta^5$-pentametylcyclopentadienyl) were discussed in the last chapter. $[Cp^*Ir(NHC)(H_2O)_2][OTf]_2$ and $Cp^*Ir(NHC)(SO_4)$ were prepared as previously reported.[16] Other reagents were purchased from commercial sources and used as received. Solvents were degassed and purified with a solvent purification system (Mbraun Inc.) prior to use. ^1H and ^{13}C NMR spectra were recorded on a Varian Mercury 300 MHz or a Varian Mercury 400 MHz spectrometer. All ^1H and ^{13}C NMR spectra were referenced against tetramethylsilane using resonances due to the residual protons in the deuterated solvents or the ^{13}C resonances of the deuterated solvents. Elemental analyses were performed by Atlantic Microlabs, Inc. X-ray crystallography was performed at the X-ray Structural Facility of North Carolina State University.

General procedure for catalytic H/D exchange experiments between C_6H_6 and deuterium solvents (CF_3CD_2OD, CD_3CN, D_2O, cyclohexane-d_{12}, pyridine-d_{12}, CD_3OD, acetone-d_6). In a typical reaction, a screw cap NMR tube or a storage tube was charged with catalyst, 20 eq benzene and 1000 eq deuterium solvent. The tube was sealed and the reaction mixture was heated to 150^0C. Upon completion of the reaction, the reaction was cooled to room temperature. The resulting solution was filtered through Celite, and the Celite plug was washed with methylene chloride. The organic layer was then separated and analyzed by

GC-MS. The percent deuterium incorporation was defined as the percent of C-H bonds converted to C-D bonds.

General procedure for catalytic H/D exchange experiments between C_6H_6 and trifluroacidic acid-d_1. In a typical reaction, a screw cap NMR tube or a storage tube was charged with catalyst, 20 eq benzene, and 1000 eq trifluroacidic acid-d_1. The tube was sealed and the reaction mixture was heated to 150^{o} C. Upon completion of the reaction, the reaction was cooled to room temperature. Aqueous K_2CO_3 was added slowly to quench trifluroacidic acid-d_1. The resulting solution was filtered through Celite, and the Celite plug was washed with methylene chloride. The organic layer was then separated and analyzed by GC-MS. The percent deuterium incorporation was defined as the percent of C-H bonds converted to C-D bonds.

General procedure for catalytic H/D exchange experiments between organic compounds and CD_3OD/D_2O. In a typical reaction, a screw cap NMR tube or a storage tube was charged with catalyst, 20 eq of certain organic compound, 500 eq CD_3OD, and 500 eq D_2O. The tube was sealed and the reaction mixture was heated to 150^{o} C. Upon completion of the reaction, the reaction was cooled to room temperature. The results were analyzed by ^{1}H NMR.

References

[1] Labinger, J. A.; Bercaw, J. E. *Nature* **2002**, 417, 507.

[2] Rober H. Crabtree, *The Organometallic Chemistry of the Transition Metals*, fifth edition

[3] Janowicz, A. H.; Bergman, R. G. *J. Am. Chem. Soc.* **1982,** 104, (1), 352-354.

[4] John. Hartwig, *J. Am. Chem. Soc.* **2010,** 132, 1848-1859

[5] Sherry, A. E.; Wayland, B. B. *J. Am. Chem. Soc.* **1990,** 112, 1259-1261.

[6] Wayland, B. B.; Sherry, A. E. *J. Am. Chem. Soc.* **1991,** 113, (14), 5305-5311.

[7] Cummins, C. C.; Wolczanski, P. T. *J. Am. Chem. Soc.* **1988,** 110, 8731-8733.

[8] Walsh, P. J.; Bergman, R. G. *J. Am. Chem. Soc.* **1988,** 110, 8729-8731.

[9] Goldshle.N.F.; Shilov, A. E. *Zh. Fiz. Khim. (Engl.Transl.)* **1969,** 43, (8), 1222-1223.

[10] Labinger, J. A. & Bercaw, J. E. *J. Organometall. Chem.* **1995**, 504, 75–91.

[11] Skaddan, M. B.; Yung, C. M.; Bergman, R. G. *Org. Lett.* **2004**, 6, 11.

[12] Klei, S. R.; Golden, J. T.; Bergman, R. G. *J. Mol. Catal. A: Chem.* **2002**, 189, 79.

[13] Klei, S. R.; Tilley, T. D.; Bergman, R. G. *Organometallics* **2002**, 21, 4905.

[14] Golden, J. T.; Andersen, R. A.; Bergman, R. G. *J. Am. Chem. Soc.* **2001**, 123, 5837.

[15] Yung, C. M.; Bergman,R.G. *J. Am. Chem. Soc.* **2004**, 126, 13033.

[16] Feng, Y.; Jiang, B.; Ison, E. A. *Organometallics* **2010**, 29(13), 2857.

[17] Hickman, A. J.; Villalobos, J. M.; Sanford, M. S. *Organometallics* **2009**, 28, 5316.

[18] Hanasaka, F.; Yamaguchi, R.; *Organometallics* **2005**, 24, 3422.

[19] Heinekey, D.; Brookhart, M.; *J. Am. Chem. Soc.* **2006**, *128*, 17114.

[20] Kubas, G. J.; Vergamini, P. J.; Wasserman, H. J. *J. Am. Chem. Soc.* **1984**, *106*, 451.

[21] Dobbs, D.; Bergman R. *J. Am. Chem. Soc.* **1993**, *115*, 3836.

CHAPTER 4

4.1 Introduction

It's estimated that at the current rate of consumption, the oil supply of the earth will last for less than four decades.[1] Therefore, the alternative feedstocks for the chemical industry in the future have raised serious consideration in both academia and industry. The use of renewable resources like carbohydrates and plant oil products would lead to sustainable development. Biomass generated from CO_2 and H_2O by photosynthesis are renewable resources which can participate in the ecological biodegradation and regeneration cycles. There are three primary products formed from this process: C_6- and C_5- sugars which form cellulose by polymerization of glucose, hemicelluloses by polymerization of glucose and xylose, and lignin. The third component is lignin, which is a highly cross-linked polymer built of substituted phenols. Lignin fills the spaces in the cell wall between cellulose, hemicelluloses, and pectin components to give strength to plants.

Nature produces about 170 billion metric tons of biomass per year by photosynthesis and about three quarters of them can be assigned to the class of carbohydrates.[2] However, only 3-4% of these compounds are used by humans for food and non-food purpose.[3] As the most abundant renewable resources, carbohydrates viewed as a feedstock for "Green Chemistry". Petroleum feedstocks usually have a low extent of functionality which makes them suitable for direct use as fuels after appropriate refinery process. Functional groups have to be added to petroleum feeds to produce commercial chemical products. In contrast, biomass-derived

carbohydrates contain excess functionality for use as fuels and chemicals, so the challenge of using biomass-derived carbohydrates is to reduce their functionality.

5-Hydroxymethylfurfural (HMF) is a good platform compound which leads to several of 2,5-disubstituted furan derivatives, and those derivatives are monomers for furan-containing polymers and materials with special properties.[4] They are good substitutes of important petroleum-based building block. HMF can be converted into many types of compounds now obtained from petroleum sources.[5] HMF is one of the few individual organic compounds that can be prepared directly from fructose and glucose by straightforward procedures. It's identified by the US Department of Energy as one of 12 priority chemicals for establishing the "green" chemistry industry of the future.

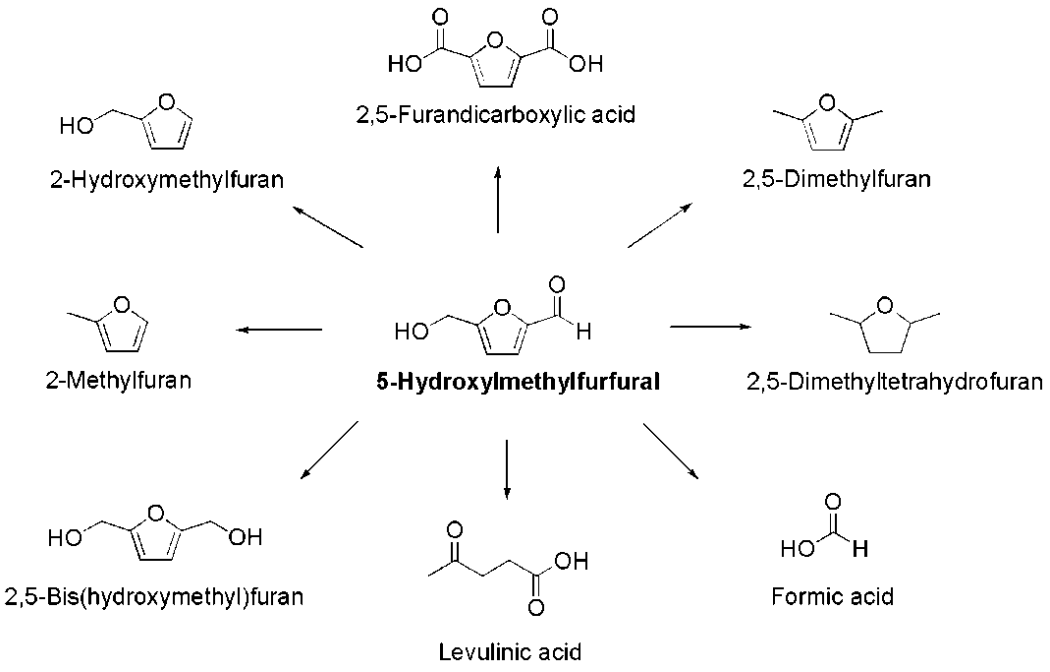

Figure 4.1 Products that can be converted from HMF.[5]

Hydrolysis is one of the major processing reactions degrading polysaccharides in which glycosidic bonds between sugar unites are cleaved to form glucose, fructose, and xylose. Hydrolysis reactions are typically carried out using acid and base catalysts at mild temperatures in aqueous solution. [5] HMF can be obtained from D-fructose by acidic elimination of three moles of water. It can also be made from meso-galactaric acid with hydrobromic acid or from 2,5-diketo adipic acid through acidification. Recently, Dr. Z. Conrad Zhang's team at Pacific Northwest National Laboratory demonstrated a one-step procedure for converting cellulose to HMF under mild conditions. [6] Currently HMF is made from fructose and glucose, and the synthesis of HMF directly from raw nature cellulose removes a major obstacle of the development of a sustainable HMF platform. A pair of metal chlorides ($CuCl_2$ and $CrCl_2$) dissolved in 1-ethyl-3-methylimidazolium chloride at temperature of 80-120^{0}C convert cellulose to HMF with a 55.4% yield of pure HMF.

Selective oxidation of HMF to 2,5-diformylfuran and 2,5-furandicarboxylic acid are quite attractive since both of them are monomers for furan-containing polymers. However, traditional oxidation methods use stoichiometric amounts of inorganic oxidants like MnO_2, CrO_3, and NaClO course environmental pollution and they are not economic for industry scale too.[7] The application of Schiff bases Mn complexes as catalysts, and NaClO as an oxidant yields 89% of HMF, but this method has a very low atom economy and generates large amounts of by-products.[8] Catalytic oxidations of HMF with environmentally benign oxygen or air have been considered as the most promising process, because of high atom economy, convenient separation, low pollution, low cost and so on. HMF has been oxidized

with O_2 to 2,5-furandicarboxylic acid in the presence of Pt catalysts with stoichiometric amount of alkali.[9] It could also be oxidized to 2,5-diformylfuran with TEMPO radicals, inorganic vanadium oxide complexes and nitrite.[10] In 2000, W. Partenheimer and coworkers oxidized HMF by dioxygen and metal/bromide catalysts [Co/Mn/Br, Co/Mn/Zr/Br, Co/Mn = Br/ (Co+Mn) = 0.1 mol/mol] to form 2,5-diformylfuran in 57% isolated yield, which can also be oxidized to 2, 5- furandicarboxylic acid in 60% yield.[11]

4.2 Results and discussion

The aerobic oxidation of HMF by iridium catalysts has not been thoroughly investigated. Autoxidation of HMF generates a series of 2, 5-disubstituted furan derivatives (Figure 4.2), therefore, control of the selectivity and minimization of the by-product through different catalytic systems and reaction conditions become the main challenges of the oxidation of HMF.

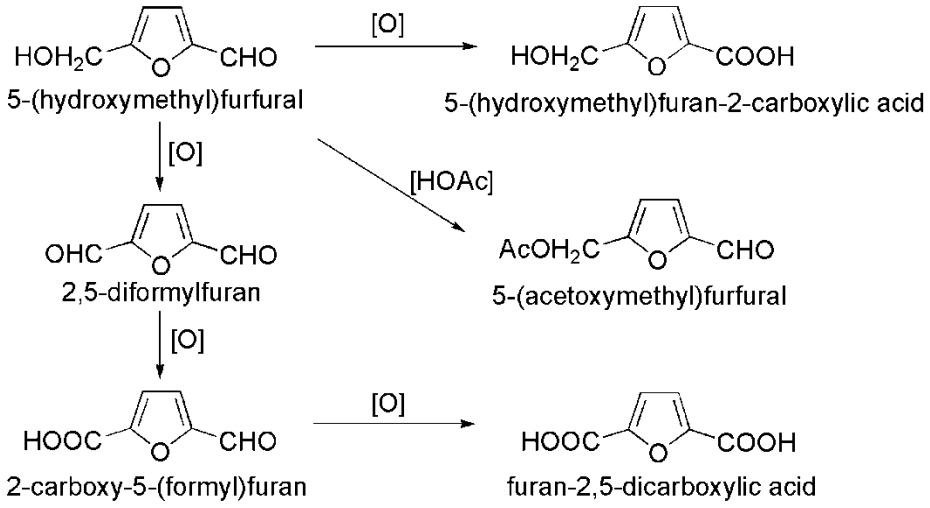

Figure 4.2 Products from the Autoxidation of HMF. [11]

Recently, iridium catalysts in the aerobic oxidation of primary and secondary alcohols,[12] catalytic H/D-exchange reactions[13] by iridium complexes contain NHC (N-heterocyclic carbene) ligand have been studied by our group. Iridium complexes bearing Cp* and NHC ligands showed good reactivities in the aerobic oxidation reactions of primary and secondary alcohols, so a variety of iridium complexes have been utilized in the aerobic oxidation of HMF. Biomass-derived carbohydrate feeds are usually treated at mild temperatures, and most of these processes are carried out in the liquid phase.[14] Using water as solvent alleviates the environmental problems associated with organic solvent and reduces the cost. HMF is highly soluble in water, so water was used as solvent in our catalytic system. The aerobic oxidations of HMF in water under atmospheric pressure of pure oxygen formed 2, 5-diformylfuran (DFF) in good yields.(Table 4.1) These reactions were catalyzed by three different iridium carbene complexes at 150^0C for 12 hours. Triethyl amine was used as a base in this system. The products were identified by ^{1}H NMR and ^{13}C NMR spectroscopy in $CDCl_3$. ^{1}H NMR ($CDCl_3$): δ = 7.4 (s, 2H, furan H), 9.8 (s, 2H, CHO); ^{13}C NMR (CD_2Cl_2): δ = 120.4 (s, CH), 154.8 (s, qC), 179.7 (s, CHO). The aerobic oxidation of HMF catalyzed by water-soluble iridium catalyst $(Cp^*Ir)_2(\mu\text{-}OH)_3$ was carried out in TEA/NaOAc solution at 150^0C for 12 hours. However, no product was observed by ^{1}H NMR. Three other water-soluble iridium catalysts $[(Cp^*IrCl)_2(\mu\text{-}Cl)_2]$, $Cp^*Ir(NO_3)_2$ and $Cp^*Ir(DMSO)(SO_4)$ have also been applied in the aerobic oxidation of HMF with TEA as base, but none of them showed catalytic reactivity either. In conclusion, Cp*Ir complexes contain NHC ligand show much higher reactivity in this reaction than Cp*Ir complexes without NHC ligand. The reason for this result has not been clarified yet.

Table 4.1 Oxidation of HMF to DFF at 1 atm oxygen

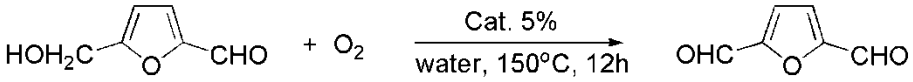

entry	catalyst	additives	yield	TON
1	$Cp^*Ir(NHC)Cl_2$	TEA	53.8%	10.8
2	$Cp^*Ir(NHC)SO_4$	TEA	58.8%	11.8
3	$Cp^*Ir(NHC)(NCMe)_2(OTf)_2$	TEA	59.7%	11.9
4	$(Cp^*Ir)_2(OH)_3$	TEA/NaOAc	0	0
5	$(Cp^*IrCl_2)_2$	NaOAc	0	0
6	$Cp^*(DMSO)SO_4$	NaOAc	0	0
7	$Cp^*Ir(NO_3)_2$	NaOAc	0	0

Another water-soluble iridium carbene complex $[Cp^*Ir(NHC)(H_2O)_2][OTf]_2$ has been studied in three different conditions for the aerobic oxidation of HMF.(Table 4.2) Entry 1 was performed in 3% $HOAc/H_2O$ solution under one atmospheric O_2 at 150^0C for 12 hours. After the reaction, all the HMF had been converted, but no 2, 5-furandicarboxylic acid was formed. Entry 2 was performed in water with triethyl amine as base, but no product was observed either. Entry 3 was also carried in 0.4M NaOH solution. After 12 hours, the products were worked up with HCl to pH below 1. About 33% of 2, 5-furandicarboxylic acid was formed based on ^{1}H NMR results. ^{1}H NMR (DMSO): δ = 7.3 (s, 2H, furan CH); ^{13}C NMR (DMSO): δ = 118.5 (s, CH), 148.1 (s, C), 158.8 (s, COOH). The results are comparable to the reported characterization of FDA. [11]

Table 4.2 Oxidation of HMF to FDA at 1 atm oxygen

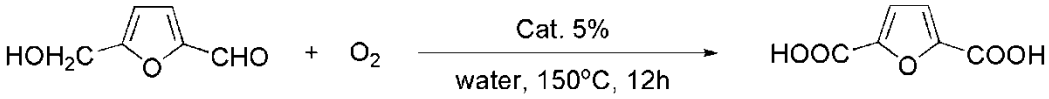

entry	catalyst	additives	yield	TON
1	$Cp^*Ir(NHC)(H_2O)_2(OTf)_2$	CH_3COOH (3%)	0	0
2	$Cp^*Ir(NHC)(H_2O)_2(OTf)_2$	Et_3N	0	0
3	$Cp^*Ir(NHC)(H_2O)_2(OTf)_2$	NaOH (0.4M)	33%	6.6

Benzoic acid was observed as a major product when benzyl alcohol was oxidized under high pressure of dioxygen (80 psi). High pressure of O_2 might also increase the portion of FDA in the products of HMF oxidation, so three different catalytic systems have been investigated for the aerobic oxidation of HMF under higher pressure of dioxygen in a Parr reactor. Under 80 psi O_2, 60.5% of FDA was obtained from $[Cp^*Ir(NHC)(H_2O)_2][OTf]_2$ catalyzed aerobic oxidation of HMF (entry 1). When the pressure of O_2 increased to 100 psi, the yield of FDA increased to 72.4% under the same condition (entry 2). 90.5% FDA was achieved using $Cp^*Ir(NHC)Cl_2$ and two equivalents of AgOTf as catalyst under 80psi (entry 3). No starting material was observed by ^1H NMR after the reactions, which means the total conversion of HMF, but the by-products have not been identified yet. Stoichiometric amount of base (NaOH) is needed, which is the biggest challenge in this catalytic system. Acid has to be used to neutralize the base after the reaction, which generates stoichiometric amount of salts as byproducts and reduces the atom economy of this system. The stability and selectivity of the iridium catalysts under high pressure need to be improved too.

Table 4.3 Oxidation of HMF to FDA at different pressures

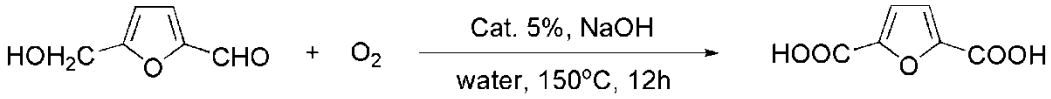

entry	catalyst	O_2 psi	yield	TON
1	$[Cp^*Ir(NHC)(H_2O)_2][OTf]_2$	80	60.5%	12.1
2	$[Cp^*Ir(NHC)(H_2O)_2][OTf]_2$	100	72.4%	14.5
3	$Cp^*Ir(NHC)Cl_2$ + 2AgOTf	80	90.5%	18.1

4.3 Conclusion

A preliminary study of aerobic oxidation of HMF has been performed. Several Cp*Ir complexes have been studied. Cp*Ir complexes with NHC ligand showed higher reactivity than other complexes. At one atmosphere of O_2 (14.5 psi), 2,5-diformylfuran (DFF) was obtained in modest yield (about 50%) catalyzed by Cp*Ir(NHC) complexes. At higher pressure of O_2 (80-100 psi), 2,5-furandicarboxylic acid (DFA) was achieved in good yield (about 90%) catalyzed by Cp*Ir(NHC) complexes.

4.4 Experimental section

Reagents and instrumentation. The reagents were purchased from commercial sources and used as received. Solvents were degassed and purified with a solvent purification system (Mbraun Inc.) prior to use. ^1H and ^{13}C NMR spectra were recorded on a Varian Mercury 300 MHz or a Varian Mercury 400 MHz spectrometer. All ^1H and ^{13}C NMR spectra were referenced against tetramethylsilane using resonances due to the residual protons in the

deuterated solvents or the ^{13}C resonances of the deuterated solvents. Oxygen was purchased from Airgas, National Welders. High pressure experiments were performed in glass lined stainless steel Parr 4592 50ml Micro Bench Top Reactor under O_2.

General procedure for aerobic oxidation experiments at one atm dioxygen. In a typical reaction, a storage tube was charged with catalyst (0.1 mmol), 20 eq substrate (2.0 mmol), 0.4M NaOAc in 5 ml DI water solution. The storage tube was freeze-pump-thaw and refilled with O_2 three times. The reaction mixture was heated to 150^0C for 12 hours. Upon completion, the reaction was cooled to room temperature and the resulting solution was extracted by Et_2O (5 ml) and filtered through a silicon column. The organic solvent was then evaporated and the product was identified by NMR.

General procedure for aerobic oxidation experiments in the Parr reactor. In a typical reaction, a glass vial of the Parr reactor was charged with catalyst (0.1 mmol), 20 eq substrate (2.0 mmol), 0.4M NaOH in 5 ml DI water solution. The Parr reactor was sealed and filled with certain pressure of O_2. The reaction mixture was then heated to 150^0C for 12 hours. Upon completion, the reaction was cooled to room temperature. The products were work up with HCl to pH below 1. The resulting solution was extracted by DMSO (5 ml) and filtered through a silicon column. The organic solvent was then evaporated under vacuum and the product was identified by NMR.

References

[1] "BP Statistical Review of Energy **2006**"

[2] Roper, H. *Starch-Starke* **2002**, 54, 89.

[3] Chemical Reviews, **2007**, Vol. 107, No. 6

[4] A. Gandini, N. M. Belgacem, *Polym. Int.* **1998**, 47, 267

[5] M. Jacoby, *C&EN*, **2009**, July 6, 26

[6] Y. Su *Applied Catalysis A: General* 361 (**2009**) 117-122

[7] *Acc. Chem. Res.* **2002**, 35, 728-737

[8] *Catalysis Communications*, **2008**, 9, 286-288

[9] E. I. Leupold, *Ger. Offen.* DE 3826073,**1990**.

[10] J. Xu, *Int. Cl.* C07D 307/46, **2006**.

[11] W. Partenheimer *Adv. Synth. Catal.* **2001**, 343

[12] E. A. Ison, *J. Am. Chem. Soc.* **2008**, 130, 14462

[13] E. A. Ison, *Organometallics*, **2010**,

[14] J. A. Dumesic, *Angew. Chem. Int. Ed.* **2007**, 46, 7164